Centrum voor Wiskunde en Informatica
REPORT*RAPPORT*

Front propagation into unstable states: Universal algebraic convergence towards uniformly translating pulled fronts

Ute Ebert and Wim van Saarloos

Modelling, Analysis and Simulation (MAS)

MAS-R9908 April 30, 1999

Report MAS-R9908
ISSN 1386-3703

CWI
P.O. Box 94079
1090 GB Amsterdam
The Netherlands

Front Propagation Into Unstable States: Universal Algebraic Convergence Towards Uniformly Translating Pulled Fronts

Ute Ebert[1,2] and Wim van Saarloos[2]

[1] *CWI, Postbus 94079, 1090 GB Amsterdam, The Netherlands*
[2] *Instituut–Lorentz, Universiteit Leiden, Postbus 9506, 2300 RA Leiden, The Netherlands*

Depending on the nonlinear equation of motion and on the initial conditions, different regions of a front may dominate the propagation mechanism. The most familiar case is the so-called pushed front, whose speed is determined by the nonlinearities in the front region itself. Pushed dynamics is always found for fronts invading a linearly stable state. A pushed front relaxes exponentially in time towards its asymptotic shape and velocity, as can be derived by linear stability analysis. To calculate its response to perturbations, solvability analysis can be used. We discuss, why these methods and results in general do not apply to fronts, whose dynamics is dominated by the leading edge of the front. This can happen, if the invaded state is unstable. Leading edge dominated dynamics can occur in two cases: The first possibility is that the initial conditions are "flat", i.e., decaying slower in space than $e^{-\lambda^* x}$ for $x \to \infty$ with λ^* defined below. The second and more important case is the one in which the initial conditions are "steep", i.e., decay faster then $e^{-\lambda^* x}$. In this case, which is known as "pulling" or "linear marginal stability", it is as if the spreading leading edge is pulling the front along. In the central part of this paper, we analyze the convergence towards uniformly translating pulled fronts. We show, that when such fronts evolve from steep initial conditions, they have a universal relaxation behavior as time $t \to \infty$, which can be viewed as a general center manifold result for pulled front propagation. In particular, the velocity of a pulled front always relaxes algebraically like $v(t) = v^* - 3/(2\lambda^* t)\ \left(1 - \sqrt{\pi/\left((\lambda^*)^2 D t\right)}\right) + O(1/t^2)$, where the parameters v^*, λ^*, and D are determined through a saddle point analysis from the equation of motion linearized about the unstable invaded state. This front velocity is independent of the precise value of the amplitude which one tracks to measure the front velocity. The interior of the front is essentially slaved to the leading edge, and develops universally as $\phi(x,t) = \Phi_{v(t)}\left(x - \int^t d\tau\ v(\tau)\right) + O(1/t^2)$, where $\Phi_v(x - vt)$ is a uniformly translating front solution with velocity v. We first derive our results in detail for the well known nonlinear diffusion equation of type $\partial_t \phi = \partial_x^2 \phi + \phi - \phi^3$, where the invaded unstable state is $\phi = 0$, and then generalize our results to more general (sets of) partial differential equations with higher spatial or temporal derivatives, to *p.d.e.*'s with memory kernels, and also to difference equations occuring, e.g., in numerical finite difference codes. Our *universal* result for pulled fronts thus also implies independence of the precise nonlinearities, independence of the precise form of the dynamical equation, and independence of the precise initial conditions, as long as they are sufficiently steep. The only remainders of the explicit form of the dynamical equation are the nonlinear solutions Φ_v and the three saddle point parameters v^*, λ^*, and D of the linearized equation. As our simulations confirm all our analytical predictions in every detail, it can be concluded that we have a complete analytical understanding of the propagation mechanism and relaxation behavior of pulled fronts, if they are uniformly translating for $t \to \infty$. An immediate consequence of the slow algebraic relaxation is that the standard moving boundary approximation breaks down for weakly curved pulled fronts in two or three dimensions.

Physics and Astronomy Classification Scheme (PACS) numbers:
02.30.Jr, 47.54.+r, 47.20.Ky, 03.40.Kf.

1991 Mathematics Subject Classification:
35B20, 35B40, 35K22, 35K57, 35L25, 39A10, 45K05, 35-02, 35B32, 35B35.

Keywords and Phrases: Pulled fronts, linear marginal stability, algebraic relaxation, Fisher-KPP-equation, general (sets of) *p.d.e.*'s, finite difference equations, integro-differential equations.

Note: The work was carried out at Instituut-Lorentz, University of Leiden, and under CWI-project MAS 1.3 *Partial differential equations in porous media research.* It was financially supported by the EU-TMR-network *Patterns, Noise and Chaos* and by the priority program *Nonlinear Systems* of the Dutch Science Foundation NWO. The paper was submitted to Physica D on March 31, 1999.

Contents

I. INTRODUCTION

A. Outline of the problem

In this paper we address the rate of convergence or "relaxation" of the velocity and profile of a front that propagates into an unstable state. The particular fronts we analyze separate two nonequilibrium homogeneous states, one of which is stable and one of which is unstable, and are such that the asymptotic front solution is a uniformly translating one. We assume that the unstable state is initially completely unperturbed in a large part of space, and that thermal and other noise are negligible. Examples of such situations arise in one form or another in physics [1–29], chemistry [29–35], and biology [30,32,36]. If the unstable state domain is not perturbed by imperfect initial conditions or thermal noise, it can only disappear through invasion by the stable state domain. We analyze the propagation of fronts formed in this process, in particular the temporal convergence towards an asymptotic front shape and velocity, and show, that it is characterized by a universal power law behavior in the so-called pulled regime. We concentrate on planar fronts, which thus can be represented in one spatial dimension, but our results for these and for the dynamical mechanism have important implications [37] for the derivation of moving boundary approximations [38,39] for weakly curved fronts in higher dimensions, as well as for the evaluation of the effects of noise on fronts [40–45], especially the effect of multiplicative noise [46].

The problem of front propagation into an unstable state has a long history, which dates back [47] to the pioneering work by Kolmogoroff, Petrovsky and Piscounoff (= KPP) [48] and by Fisher [49] on the nonlinear diffusion equation

$$\partial_t \phi = \partial_x^2 \phi + f(\phi) \ , \tag{1.1}$$

where $f(\phi)$ is such that it has a homogeneous stable state $\phi = 1$ and a homogeneous unstable state $\phi = 0$. Both of these papers [48,49] were motivated by the biological problem of gene spreading in a population. Since this work, the nonlinear diffusion equation (1.1), in particular the one with a simple nonlinearity of the type

$$f = f_{\rm KPP}(\phi) = \phi - \phi^k \ , \ k > 1, \ \ \text{e.g., } k = 2 \text{ or } 3 \ , \tag{1.2}$$

has become a standard problem in the mathematical literature [30,32,36,50–54]. For the F-KPP equation defined by (1.1) and (1.2), there exist dynamically stable uniformly translating front solutions $\phi(x,t) \equiv \Phi_v(x - vt)$ for every velocity $v \geq v^* = 2\sqrt{f'(0)}$, and hence every one of these solutions is a possible attractor of the dynamics for long times t. The resulting dynamical behavior or "velocity selection" depends on the initial conditions and has been investigated by a variety of methods [48–50,52] and essentially all its relevant properties have been derived rigorously [50]. E.g., following the lines of KPP [48], Aronson and Weinberger proved rigorously [50], that every initial condition, that decays spatially at least as fast as $e^{-\lambda^* x}$ ($\lambda^* = v^*/2$) into the unstable state for $x \to \infty$, approaches for large times the front $\Phi_{v^*}(x - v^* t)$ with the smallest possible velocity v^*. Most of the rigorous mathematical methods can, however, not be extended to higher order equations [55].

In physics, the interest in front propagation into unstable states initially arose from a different angle. Since the late fifties, the growth and advection of linear perturbations about a homogeneous unstable state has been analyzed through an asymptotic long time analysis of the Green's function of the linear equations [56–58]. Only ten to fifteen years ago did it become fully clear in the physics community [59–69], that there was actually an empirical but deep connection between the rigorous results for the second order equations and some aspects of the more general and exact but nonrigorous results for the growth of linear perturbations. This has given rise to a number of reformulations and intuitive scenarios aimed at understanding the general front propagation problem into unstable states [60,61,63,65–69].

Although our results bear on many of these approaches, our aim is *not* to introduce another intuitive or speculative scenario. Rather, we will introduce what we believe to be the first systematic analysis of the rate of convergence or "relaxation" of the front velocity and profile in the so-called "linear marginal stability" [63,65] or "pulled" [59,68,69] regime. In this regime the asymptotic front velocity is simply the linear spreading speed determined by the Green's function of the linearized equations. Quite surprisingly, our analysis even yields a number of *new* and *exact* results for the celebrated nonlinear diffusion equation (1.1), but it applies equally well to (sets of) higher order partial differential equations that admit uniformly translating fronts, to difference equations, or to integro-differential equations. After a general discussion, we will illustrate this explicitly on
1) the extended Fisher-Kolmogoroff (EFK) equation [64,65,70]

$$\partial_t \phi = -\gamma \partial_x^4 \phi + \partial_x^2 \phi + f(\phi) \quad \text{for } 0 < \gamma < 1/12 \ , \tag{1.3}$$

where it generates uniformly translating fronts,
2) an example of coupled differential equations, namely those for planar negative streamer fronts,

$$\begin{aligned} \partial_t \sigma &= D \partial_x^2 \sigma + \partial_x(\sigma E) + |E| e^{-1/|E|} \ , \ \sigma(x \gg 1, t) = 0 \ , \\ \partial_t E &= -D \partial_x \sigma - \sigma E \ , \ E(x \gg 1, t) = E^+ < 0 \ , \end{aligned} \tag{1.4}$$

describing the coupled electron density σ and electric field E in a dielectric discharge [15],
3) a difference-differential equation (see, also [71])

$$\partial_t C_i(t) = -C_i + C_{i-1}^2 \ , \ C_0(t) = 0 \ , \ C_{i \gg 1}(t) = 1 \ , \tag{1.5}$$

which occurs in the calculation of the Lyapunov exponent in kinetic theory [17],

4) the extension of the nonlinear diffusion equation with a second temporal derivative,

$$\tau_2 \frac{\partial^2 \phi}{\partial t^2} + \frac{\partial \phi}{\partial t} = \frac{\partial^2 \phi}{\partial x^2} + \phi - \phi^3 \ , \tag{1.6}$$

5) an extension of the nonlinear diffusion equation with a memory kernel,

$$\partial_t \phi(x,t) = \partial_x^2 \phi(x,t) + \int_0^t dt' K(t-t') \phi(x,t') - \phi^k(x,t) \ , \tag{1.7}$$

6) and discretized versions of the nonlinear diffusion equation as they arise in numerical finite difference codes

$$\frac{\partial \phi(x,t)}{\partial t} \ \longrightarrow \ \frac{\phi_i(t+\Delta t) - \phi_i(t)}{\Delta t} \quad \text{etc.} \tag{1.8}$$

For all these equations, the results have a remarkable degree of simplicity and universality: as summarized in Sect. I C and Table I below, pulled fronts always converge in time with *universal power laws and prefactors* that are independent of the precise form of the equations *and* independent of the precise initial conditions as long as they obey a certain steepness criterion. All these predictions are fully confirmed by extremely precise numerical simulations. Taken together, these results therefore yield the understanding of the pulled front mechanism that so many authors [8,61,63–65,67–69,72] have sought for.

The asymptotic long time behavior can be worked out in detail and to high orders for the F-KPP equation (1.1), (1.2) in an asymptotic expansion in $1/\sqrt{t}$. These results are presented in detail in this paper. Once we will have laid out the structure of this expansion by our detailed analysis, it is clear that essentially the same expansion can be applied to other more complicated types of equations, provided that they admit a family of uniformly translating front solutions in the neighborhood of the asymptotic "pulled" velocity v^*. Moreover, from the structure it becomes transparent that the two lowest order equations in the $1/\sqrt{t}$ expansion suffice to calculate the universal convergence, and that the structure of these equations is virtually independent of the precise form of the dynamical equation. For the other type of equations, like higher order partial differential equations, we limit the discussion of our method to the motivation and analysis of these two equations. Although we will give some discussion of the assumptions that underly the expansion (like the one that there is a nearby family of moving front solutions), a full analysis of these as well as of the extension to nonuniformly translating fronts, such as those arising in the EFK equation (1.3) for $\gamma > 1/12$, in the Swift-Hohenberg equation [73], or in the complex Ginzburg-Landau equation [66], will be left to future publications [74–76].

Previous work on the rate of convergence of moving pulled fronts appears to be quite limited. For Eq. (1.1) with nonlinearity (1.2), Bramson [77] proved rigorously that the convergence to the asymptotic velocity v^* is $v(t) = v^* - 3/(2\lambda^* t)$ uniformly, i.e., independent of the amplitude ϕ whose position one tracks. Here, as before, $\lambda^* = v^*/2 = \sqrt{f'(0)}$. The factor $3/2$ in this expression has often been considered puzzling, since the *linear* diffusion equation with localized initial conditions yields $v(t) = v^* - 1/(2\lambda^* t)$. In [65], it was argued that the factor $3/2$ in this result applies more generally to higher order equations as well, but a systematic analysis or an argument for why the convergence is uniform, was missing. Apart from this and a recent rederivation [72] of Bramson's result along lines similar in spirit to ours[1] and a few papers similar in spirit to that of Bramson [52,79,80], we are not aware of systematic investigations of this issue. Even for the convergence of the velocity in the nonlinear difusion equation, our results go beyond those of Bramson.

Our results are not only of interest in their own right, but they have important implications as well. Since the asymptotic convergence towards the attractor Φ^* is algebraic in time, the attractor alone might not give sufficient information about the front after long but finite times, since algebraic convergence has no characteristic time scale. In particular, there is no time beyond which convergence can be neglected. Such slow convergence means that in many cases, experimentally as well as theoretically, one observes transients and not the asymptotic behavior. In fact, in the very first explicit experimental test of front propagation into unstable states in a pattern forming system [2], viz. Taylor-Couette flow, the initial discrepancy between theory and experiment was later shown to be related to the existence of slow transients [16]. The slow convergence is important for theoretical studies as well: it is a common experience (see, e.g., [12,64,81]) that when studying front propagation in the "pulled" regime numerically, the measured front velocity is often below v^*, even though the asymptotic front speed can never be below v^*, because no slower attractor of the dynamics exists. This observation finds a natural explanation in our finding that the rate of convergence is always power law slow, and that the front speed is always approached *from below*.

---

[1] The main focus of the work by Brunet and Derrida [72] is actually the correction to the asymptotic velocity if the function $f(\phi)$ has a cutoff h such that $f_h(\phi) = 0$ for $\phi < h$. The method the authors use to derive this, is actually closely related to the one they use to rederive Bramson's result, and to our approach. See in this connection also the recent paper by Kessler *et al.* [78].

A second important implication of the absence of an intrinsic time scale of the front convergence is the following. When we consider the propagation of such fronts in more than one dimension in which there is a coupling to another slow field (as, e.g., in the phase field models [39,82,83]), the front dynamics does not adiabatically decouple from the dynamics of the other field and from the evolution of the curvature and shape of the front itself. This implies that the standard moving boundary approximation [38,39,84] (which actually rests on the assumption that the convergence on the "inner scale" is exponential) can not be made. Though this is intuitively quite obvious from the power law behavior of the front convergence process, the connection between the convergence and the breakdown of a moving boundary approximation also emerges at a technical level: the divergence of the solvability integrals that emerge when deriving a moving boundary approximation turns out to be related to the continuity of the stability spectrum of pulled fronts [37]. The break-down of the solvability analysis for perturbations of the asymptotic front in the pulled regime also has consequences for the evaluation of multiplicative noise in such equations [37].

B. Pushed versus pulled fronts, selection and convergence

Let us return to the well understood nonlinear diffusion equation (1.1) and discuss to which nonlinearities $f(\phi)$ our prediction of algebraic convergence applies and why. If $f'(0) < 0$, the invaded state $\phi = 0$ is linearly stable, and the construction of a uniformly translating front $\phi(x,t) = \Phi_v(x-vt)$ poses a nonlinear eigenvalue problem. The solution with the largest eigenvalue v is the unique stable and dynamically relevant solution (unique up to translation invariance, of course). It is also well known and rederived in Section II, that any initial front, that separates the (meta)stable state $\phi = 0$ at $x \to \infty$ from another stable state at $x \to -\infty$, will converge exponentially in time to this front solution Φ_v, which is unique up to translation. However, whenever $f'(0) > 0$, $\phi = 0$ is unstable, and there is not a unique asymptotic attractor Φ_v, but a continuous spectrum of nonlinear eigenvalues v, which constitute the velocities of possible attractors Φ_v. The existence of a continuum of attractors of the dynamics poses a so-called *selection problem*: From which initial conditions will the front dynamically approach which attractor? The attractor with the smallest velocity plays a special role, as its basin of attraction are all "sufficiently steep" initial conditions, as defined in Section II. It therefore will be refered to as *the selected* front solution.

When we concentrate on these "sufficiently steep" initial conditions and analyze the dependence from the nonlinearity f in (1.1), the transition from exponential to algebraic convergence does *not* coincide with the transition from stability to instability of the invaded state $\phi = 0$, but with the transition between two different mechanisms of front propagation into unstable states. Indeed, it is known (see also Sect. II), that for $f'(0) > 0$, there are also two different possibilities depending on f of how the selected front Φ_{sel} and its speed v_{sel} are determined. Either Φ_{sel} is found by constructing a so-called strongly heteroclinic orbit for Φ_v from the full nonlinear equation. This case is known as case II [61] or nonlinear marginal stability [63,65], or as pushing [59,68,69]. Or, the selected velocity v_{sel} is determined by linearizing about the unstable state $\phi = 0$, which case is known as case I or linear marginal stability, or as pulling. We henceforth will use the terms "pushing" and "pulling" for the two different propagation mechanisms of a selected front, since they very literally express the different dynamical mechanisms.

In a pushed front just like in a front propagating into a (meta)stable state, the dynamics is essentially determined in the nonlinear "*interior part*" of the front, where ϕ varies from close to $\phi = 0$ to close to the stable state. The construction of the selected front as a strongly heteroclinic orbit in the pushed case continuously extends into the construction of the heteroclinic orbit of the unique attractor, if the invaded state is (meta)stable ($f'(0) < 0$). For both pushed fronts and fronts propagating into linearly stable states, the spectrum of linear perturbations is bounded away from zero, so that convergence towards the asymptotic front is exponential in time.

In a pulled front, the dynamics is quite different: As we shall see, it is determined essentially in the region linearized about the unstable state. We call this region the leading edge of the front. Eq. (1.1) is appropriate for analyzing the front interior. We will see in Section II D, that a stability analysis performed in this representation is not able to capture the convergence of a steep initial condition towards a pulled front. Rather the substitution

$$\psi = \phi\, e^{\lambda^* \xi} \ , \quad \xi = x - v^* t \ , \tag{1.9}$$

which we shall term the *leading edge representation*, transforms (1.1) into

$$\begin{aligned} \partial_t \psi &= \partial_\xi^2 \psi + \bar{f}(\psi, \xi) \ , \\ \bar{f} &\equiv e^{\lambda^* \xi} \left[f\left(\psi e^{-\lambda^* \xi}\right) - f'(0)\, \psi e^{-\lambda^* \xi} \right] \\ &= O\left(\psi^2\, e^{-\lambda^* \xi}\right) \ . \end{aligned} \tag{1.10}$$

This equation will turn out to be appropriate for analyzing a leading edge dominated dynamics. Note that $\bar{f}$ is at least of order ψ^2 with an exponentially small coefficient as $\xi \to \infty$. For large ξ, the dynamics is purely diffusive. If the nonlinearity obeys $f(\phi) - f'(0)\phi < 0$ for all $\phi > 0$ — which is known as a sufficient criterion for pulling — the nonlinearity $\bar{f}$ is always negative. Then $\bar{f}$ purely damps the dynamics in the region of smaller ξ. The dynamics evolving under (1.10) is equivalent to simply linearizing (1.1) about the unstable state in the large ξ region — there is only one subtle but important ingredient from

the requirement that the dynamics in the linear region crosses over smoothly to the nonlinear front behavior at smaller ξ, that actually enters our leading edge analysis in the form of a boundary condition. In the leading edge representation (1.10), this is brought out by the presence of the sink-type term $\bar{f}$ which is nonzero in a localized region behind the leading edge. With this small caveat[2], we can conclude that the leading edge of the front "pulls the rest of the front along", and that this is precisely the mechanism that gives rise to the universal algebraic convergence behavior. In a pushed front, in contrast, the nonlinearity "pushes the leading edge forward" and convergence is exponential.

To illustrate this discussion by a concrete example, we note that when the function $f(\phi)$ in the nonlinear diffusion equation is of the form

$$f = f_\epsilon(\phi) = \epsilon\phi + \phi^{n+1} - \phi^{2n+1} \quad , \quad n > 0 \; . \qquad (1.11)$$

we can rely on known analytic solutions for Φ_v. In this case, the state $\phi = 0$ is (meta)stable for $\epsilon < 0$. For $0 < \epsilon < (n+1)/n^2$, the selected front is pushed, and for $\epsilon > (n+1)/n^2$, it is pulled (see Appendix A).

At this point, a brief explanation of our use of the word "metastable" may be appropriate. For systems with a Lyapunov function, the word metastable is often used in physics to denote a linearly stable state, which does not correspond to the absolute minimum of the Lyapunov function (in analogy with the free energy). A domain wall or front between the absolutely stable and a metastable state then moves into the metastable domain; one may therefore loosely call a linearly stable state "metastable", if it is invaded by another "more stable" state through the motion of a domain wall or front.

The understanding of the two different dynamical mechanisms of pushing and pulling in the nonlinear diffusion equation (1.1) lays the basis for the analysis of equations (1.3) – (1.8). The essential step towards a generalization of the leading edge representation (1.10) is done by a saddle point analysis, that identifies which Fourier modes of linear perturbations of the unstable state will dominate the long time dynamics. This analysis yields the parameters v^*, λ^*, the diffusion constant D and possible higher order terms required for the leading edge representation.

C. Sketch of method and results on front relaxation in the pulled regime

Bramson's method [77] to calculate algebraic convergence is specifically adapted to equations of type (1.1). It is based on a representation of the diffusion equation by Brownian processes, which are evaluated probabilistically. Instead, we construct the asymptotic convergence trajectory towards a known asymptotic state by solving the differential equations in a systematic asymptotic expansion which, though nonrigorous, extends immediately to higher order equations. Our approach leads to *exact* results, since the expansion parameter are inverse powers of the time t, so these terms become arbitrarily small in the asymptotic regime.

The idea of the method is that in a pulled front, the speed is essentially set in the leading edge, where linearization of the equation of motion about the unstable state is justified. This leading edge has to be connected to what we will refer to as the interior part of the front, defined to be the region where we have to work with the full nonlinear equation. For the interior, we use the fact that for large times the shape of the converging front will resemble the asymptotic front, and thus can be expanded about it. We also explicitly make use of the fact that the initial state $\phi(x,0)$ for large x is steeper than $\Phi^* = \Phi_{v^*}$ in the leading edge, i.e., $\phi(x,0)\, e^{\lambda^* x} \to 0$ as $x \to \infty$, and that the final state is Φ^*. The structure of the problem then dictates that we have to expand in $1/\sqrt{t}$.

The structure of the expansion in $1/\sqrt{t}$ is the only real input of the analysis; its selfconsistency becomes clear a posteriori and it can be motivated from the earlier work on the long time expansion of the Green's function of the linearized equations, or, equivalently, from the observation that the equation governing the convergence towards the asymptotic front profile (1.10) reduces essentially to a diffusion equation in the leading edge of the front. Based on this ansatz, we derive the following exact results:

For equations such, that the selected front is a uniformly translating pulled front, and for sufficiently steep initial conditions such that $\lim_{x\to\infty} \phi(x,0)\, e^{\lambda^* x} = 0$, we derive that the asymptotic velocity convergence is given by the universal law

$$v(t) = v^* + \dot{X} \; ,$$
$$\dot{X} = -\frac{3}{2\lambda^* t}\left(1 - \sqrt{\frac{\pi}{(\lambda^*)^2 D t}}\right) + O\left(\frac{1}{t^2}\right) \; . \qquad (1.12)$$

The three constants, the velocity v^*, the inverse length λ^* and the diffusion constant D, are in general obtained from a saddle point expansion [58] for the equation of motion linearized about the unstable state. To write these results, define $\omega(k)$ as the dispersion of a Fourier mode $e^{-i\omega t + ikx}$ of the equations linearized about the unstable state into which the front propagates. In a frame moving with velocity v^*, the quickest growing mode k^* is identified by the complex saddle point equation $\partial_k \left[\omega(k) - v^* k\right]|_{k=k^*} = 0$. In the more usual decomposition into real functions this implies, that [56,61,63,65]

[2]Note though, that this subtle point is quite important — as we shall see, the saddle point or pinch point analysis gives precisely the wrong prefactor for the leading $1/t$ convergence term because this boundary condition is not satisfied.

$$\left.\frac{\partial \mathrm{Im}\ \omega}{\partial \mathrm{Im}\ k}\right|_{k^*} = v^* \ , \quad \left.\frac{\partial \mathrm{Im}\ \omega}{\partial \mathrm{Re}\ k}\right|_{k^*} = 0 \ . \tag{1.13}$$

The speed of the frame is asymptotically the same as the speed of the front, if

$$\frac{\mathrm{Im}\ \omega(k^*)}{\mathrm{Im}\ k^*} = v^* \ . \tag{1.14}$$

For the uniformly translating fronts that we will analyze here, we have

$$\mathrm{Im}\ k^* \equiv \lambda^* > 0 \ , \quad \mathrm{Re}\ k^* = 0 \ , \quad \mathrm{Re}\ \omega(k^*) = 0 \ , \tag{1.15}$$

and a real positive diffusion coefficient D

$$D = \left.\frac{i\partial^2\omega}{2\partial k^2}\right|_{k^*} = \left.\frac{\partial^2 \mathrm{Im}\ \omega}{2\partial\lambda^2}\right|_{k^*} \ . \tag{1.16}$$

For equations (1.1), (1.2) we simply have $v^* = 2$, $\lambda^* = D = 1$, and the first term in (1.12) then reduces to the result of Bramson. The general form of this term was conjectured earlier by one of us [65]. We confirm this conjecture, identify the $1/t$ term as the first non-vanishing term in our asymptotic expansion in $1/\sqrt{t}$, and explicitly calculate the $1/t^{3/2}$ term which is new even for equation (1.1). The $1/t^2$ term will depend on initial conditions, and is thus non-universal.

Of course, while the velocity of a front is converging, so is the profile shape. Note that $v(t)$ (1.12) does not depend on the "height" $\phi = h$, which is being tracked. In fact, if we define the velocity v_ϕ of the fixed amplitude $\phi = h$ through $\phi\left(x + \int^t d\tau\ v_\phi(\tau)\ ,\ t\right) = h$, then up to order $1/t^2$ the velocity $v_\phi(t) = v^* + \dot{X}$ is *independent of the "height"* $\phi = h$. Moreover, it is determined solely by properties of the equation linearized about the unstable state, as Eqs. (1.13)–(1.16) show. In this sense, we can indeed speak of pulling of the front by the leading edge of the front.

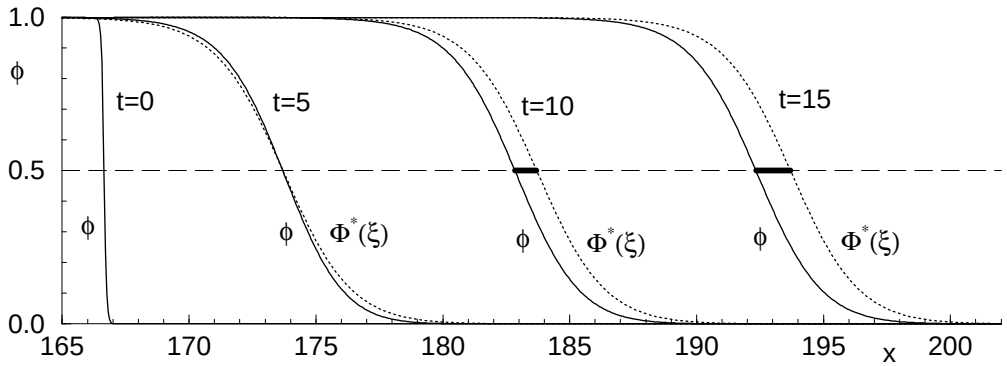

FIG. 1. Illustration of the fact, that even though the shape of a front profile is quite close to Φ^*, the position of a front is shifted logarithmically in time relative to the uniformly translating profile $\Phi^*(\xi)$.
Solid lines: evolution of some initial condition $\phi(x,0)$ of the form (4.4) under $\partial_t\phi = \partial_x^2\phi + \phi - \phi^3$ at times $t = 5, 10, 15$. Dotted lines: evolution of $\phi(x,t) = \Phi^*(\xi)$, $\xi = x - 2t$, at times $t = 5, 10, 15$. Φ^* is placed such, that the amplitude $\phi = 1/2$ coincides with that of $\phi(x,t)$ at time $t = 5$. The logarithmic temporal shift is indicated by the fat line.

The shape convergence is also obtained explicitly from our analysis. The crucial input for the analysis is the right frame and structure to linearize about. At first sight, a natural guess would be that for large times, the actual shape of the front $\phi(x,t)$ should be linearizable about the shape of the asymptotic front $\Phi^*(x - v^*t)$. However, the algebraic velocity convergence (1.12) implies, that if a converging front profile ϕ is close to the asymptotic uniformly translating front profile $\Phi^*(x - v^*t)$ at some time t_0, the distance between the actual profile and Φ^* will diverge at large times t as $X(t) = -(3/2\lambda^*)\ln(t/t_0) + \ldots$. This result, which is illustrated in Fig. 1, implies that if we want to linearize ϕ about Φ^* at all times, *we have to move* Φ^* *along with the non-asymptotic velocity* $v(t)$ *(1.12) of the converging front.* A crucial step for the analysis is thus to linearize about $\Phi^*(\xi)$ in a coordinate system

$$(\xi_X, t) \quad , \quad \xi_X \equiv \xi - X(t) = x - v^*t - X(t) \ , \tag{1.17}$$

moving with the converging front. If we expand ϕ about $\Phi^*(\xi)$ with ξ from (1.17) and then resum, we find that the interior shape of the front is given by

$$\phi(x,t) = \Phi_{v(t)}(\xi_X + x_0) + O\left(\frac{1}{t^2}\right) \tag{1.18}$$

for $\xi_X \ll \sqrt{4Dt}$. x_0 expresses the translational degree of freedom of the front. The uniformly translating front $\Phi_v(\xi)$ is a solution of the ordinary differential equation for the uniformly translating profile $\phi(x,t) = \Phi_v(x - vt)$ but with v replaced by the *instantaneous* value $v(t)$ of the velocity. E.g., for the nonlinear diffusion equation (1.1), $\Phi_v(\xi)$ is the solution of

$$-v\partial_\xi\Phi_v(\xi) = \partial_\xi^2\Phi_v(\xi) + f(\Phi_v(\xi)) \ . \tag{1.19}$$

Eq. (1.18) also confirms that to leading order the interior is slaved to the slow dynamics of the leading edge. The

transient profiles $\Phi_{v(t)}$ in (1.18) propagate with velocity $v(t)$ smaller than v^*, according to (1.12).

For the special case of Eq. (1.1) it is well known (see also Section II), that when constructing a front Φ_v starting from $\Phi_v = 1$ at $\xi \to -\infty$, it eventually will become negative for finite ξ whenever $v < v^*$, and that globally such fronts either do not exist or are dynamically unstable, depending on the properties of f for negative ϕ. However, only the positive part of $\Phi_{v(t)}$ from $\xi \to -\infty$ up to $\xi \ll \sqrt{t}$ plays a role as a transient. That the convergence trajectory is approximately given by $\Phi_{v(t)}$, was already observed numerically in equations of type (1.1) by Powell *et al.* [67]. Our analytical derivation of this result actually holds for a larger class of equations, but at the same time we find that it only holds up to a correction term of order $1/t^2$. This non-universal correction is always non-vanishing.

For $\xi_X \gg \sqrt{4Dt}$, the transient crosses over to

$$\phi(x,t) = \alpha \xi_X \; e^{-\lambda^* \xi_X \; - \xi_X^2/(4Dt)} \times \left(1 + O\left(\frac{1}{\sqrt{t}}\right) + O\left(\frac{1}{\xi_X}\right)\right). \tag{1.20}$$

The analytical expression for the universal correction of order $1/\sqrt{t}$ is given in Eqs. (5.39) or (5.69) below, while the correction of order $1/t$ will depend on initial conditions, and is thus non-universal.

A crucial insight implemented above is, that the front consists of different dynamical regions, which have to be matched to each other. The situation is sketched in Fig. 2. For a pulled front, the Gaussian region (1.20) of the leading edge essentially determines the velocity, while the front interior (1.18) is slaved to leading order. The Gaussian region might be preceeded by a region of "steepness" λ being conserved in time, which for sufficiently steep initial conditions $\lambda > \lambda^*$ has no dynamical importance (where the steepness λ is defined in Eq. (2.6) below). Likewise, for flat initial conditions, the dynamics is dominated by the conserved λ region, while pushed dynamics is dominated by the front interior. In both of these cases, the intermediate Gaussian region is absent. For the nonlinear diffusion equation (1.1), the different cases are discussed in Section II and summarized in Table III.

Our results (1.12) – (1.20) are universal in three ways:
• The predicted convergence behavior is independent of the precise initial conditions, provided they decay quicker than $e^{-\lambda^*|x|}$ far in the unstable regime.
• The leading edge behavior (1.12) and (1.20) is independent of the precise nonlinearities. For Eq. (1.1), the constants v^*, λ^* and D depend on $f'(0)$ only. For the more general equations, these constants are completely determined by the saddle point expansion in the equation linearized about the unstable state.
• If we analyze general equations like (1.3) – (1.8), also our prediction for the interior part of the front (1.18) stays unchanged, as long as the front speed stays determined by the linearization about the unstable state, i.e., the front stays pulled, and as long as the state behind the front stays homogeneous. The effect of the nonlinearities just gets absorbed in appropriate functions Φ_v.

The results summarized in this Subsection are the most central new results of this paper. They are summarized, for easy reference in Table I.

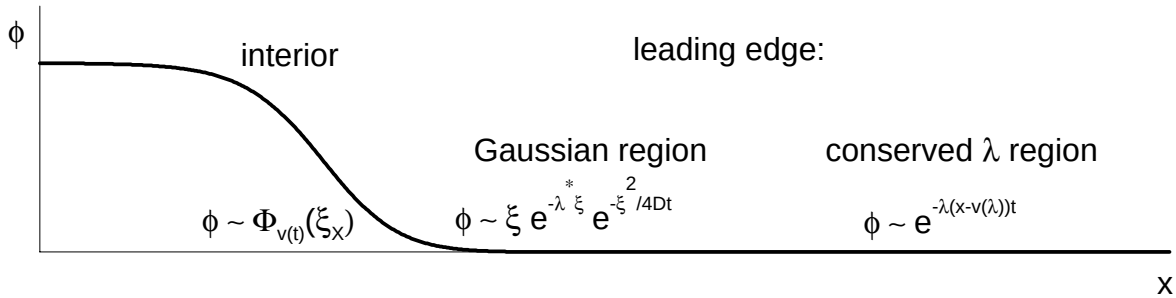

FIG. 2. Sketch of a front with the different dynamical regions: interior = nonlinear region, leading edge = region linearized about the unstable state. Depending on the initial conditions, the leading edge might still consist of two different regions: a Gaussian region and a region of conserved steepness λ.
The most familiar case is the interior dominated or "pushed" front (Cases I and II in Table III). To such fronts, standard tools of perturbation theory like linear stability analysis apply, as we discuss in Section II. Leading egde dominated fronts can either be governed by the conserved λ region (Case III), if they start with "flat" initial conditions, or by the Gaussian region (Case IV), if the initial conditions are "sufficiently steep". The Case IV fronts are also called "pulled". Their universal algebraic relaxation is analyzed for the nonlinear diffusion equation in Sections III and IV, and for general equations in Section V.

Height independent velocity:

$$v(t) = v^* + \dot{X}$$
$$= v^* - \frac{3}{2\lambda^* t}\left(1 - \sqrt{\frac{\pi}{(\lambda^*)^2 Dt}}\right) + O\left(\frac{1}{t^2}\right) ,$$

where the saddle point analysis of the linearized equation yields v^*, λ^*, D, cf. Table IV.

$\Rightarrow$ Use the coordinate: $\xi_X = x - v^* t - X(t)$.

Front for $\xi_X \ll \sqrt{4Dt}$ (front interior) :

$$\phi(x,t) = \Phi_{v(t)}(\xi_X) + O\left(\frac{1}{t^2}\right) ,$$
$$= \Phi^*(\xi_X) + \dot{X}\, \eta_{\rm sh}(\xi_X) + O\left(\frac{1}{t^2}\right) ,$$

where $\Phi_v(\xi)$ solves $\phi(x,t) = \Phi_v(x - vt)$, and $\eta_{\rm sh}(\xi) = \delta\Phi_v(\xi)/\delta v|_{v^*}$.

Front for $\xi_X \gg \sqrt{4Dt}$ (leading edge) :

$$\phi(x,t) = \alpha \xi_X\, e^{-\lambda^* \xi_X}\, e^{-\xi_X^2/(4Dt)} + \dots .$$

Table I: The central results on the universal algebraic relaxation towards uniformly translating pulled fronts, see also Fig. 2. These results apply to steep initial conditions in the nonlinear diffusion equation in the pulled regime (Case IV of Table III, see Sections III and IV) and to more general equations (see Section V).

D. Organization of the paper

Before embarking on our explicit calculation of the velocity and shape convergence in the pulled regime, we review in Section II a number of properties of propagating fronts in the nonlinear diffusion equation. Most of these are well known, but they either play a role in the later analysis or in the motivation thereof: *(i)* The existence of a family of fronts is essential for the convergence in the inner front region, as Eq. (1.18) illustrates already. *(ii)* The stability analysis illustrates that pushed fronts converge exponentially, but that the convergence of pulled fronts does not follow simply from the stability analysis. *(iii)* For completeness, we point out that the convergence of fronts emerging from initial conditions that are not sufficiently steep (both in the pushed and pulled regime) can be understood to a large extent from the stability calculation. *(iv)* Many of the arguments that were previously made partially intuively [63,65] for the connection between front stability and selection, are reformulated in a more precise way in this Section. *(v)* The connection between the front convergence and the breakdown of the standard moving boundary approximation arises through the properties of the stability operator. Some of the results collected Section II therefore lay the basis for the discussion of these connections in a later paper.

Readers who are familiar with most of the results of Section II or who want to focus right away on the convergence calculation can, after skimming Section II A proceed to Section III, where the detailed analysis of pulled front relaxation in the the nonlinear diffusion equation (1.1) is given. The detailed numerical simulations that confirm our analytical predictions are presented in Section IV. In Section V we then extend our analysis to more general equations, discuss the example equations (1.3) – (1.8), and present numerical results, again in excellent agreement with our analytical predictions. We then close the main body of the paper with a summary and outlook in Section VI.

Since this is a long paper with a large number of detailed results of various types, and since we have made an attempt to make our results accessible for readers from different fields, we introduce Table II as a "helpdesk" for the reader who wants to focus on a particular aspect of the front propagation problem only, or who wants to get only an idea of the essential ingredients of our approach

and the main results.

We finally note that a brief sketch of our results can be found in [85], while the lecture notes in [86] provide further background information and insight into how the convergence analysis presented here arose from the study of moving boundary approximations.

THE READER'S HELPDESK	
If.....	*Then our advice is.....*
you do not want to study the stability calculation or are not interested in the connection between stability and front selection	if you know what is meant with the "pulled" velocity v^* you can start with Section III immediately; if not, read Section II E, II F and possibly Section V C 1 first
you are already familiar with previous ideas concerning front selection in the physics literature, but want to get an idea of our change of emphasis and of the new detailed results of this paper	to skim Section II A for notation and terms, to then read Section II E 2 and II F, to check Table III and then to proceed to Section III
you (mainly) want to read about the connection between stability, selection and relaxation	to read Section II with Table III and for the generalization Sections V B and V C with their appendices
you only want to get an idea of the conceptual basis of the algebraic convergence	to read Section III A and possibly Sections V C–V E for the arguments concerning higher order partial differentiel equations or other types of equations
you are unfamiliar with the concept of pulled velocity v^* for higher order equations and want to know how it is determined	to read Sections III A and V C 1 (and possibly parts of Sections V D and V E)
you just want to see the numerical support for the algebraic relaxation prediction from Tables I and IV	read Section IV on the nonlinear diffusion equation and Section V F for higher order and coupled equations
you just want a toolkit for when to apply the predictions from Tables I and IV	to read Section VI E

Table II: A guide through the paper for the reader who is not interested in every detail of the work presented in this paper.

II. STABILITY, SELECTION AND CONVERGENCE IN THE NONLINEAR DIFFUSION EQUATION

In this Section, we first review a number of results on the multiplicity and stability of uniformly translating front solutions of the nonlinear diffusion equation in Sections II A – II C. In Sec. II D, we discuss to which extent the linear stability analysis of these uniformly translating fronts allows us to solve the selection problem, i.e., to determine the basins of attraction of these solutions in the space of initial conditions. We also address the question to what extent it enables us to determine the convergence mechanism and convergence rate.

Though several elements of the analysis have appeared in one form or another at scattered places in the literature [36,38,53,61,65–69,87–94], the aim of this Section is is *(i)* to define the concept of the *steepness* of a front in the leading edge and show that this concept plays a central and ordering role in the discussion of stability, selection and convergence: We define "*sufficiently steep*" initial conditions as all initial conditions, that for large times approach the so-called selected front. *(ii)* to discuss the two distinct propagation mechanisms, namely the interior dominated dynamical regime, and a leading edge dominated dynamics. The dynamics of initial conditions, that are very flat in the leading edge, will always be dominated by this leading edge. The dynamics of steep initial conditions can be dominated by either the interior (*pushed*) or the leading edge (*pulled*). We reserve the names "pushed" and "pulled" to the interior or leading edge dominated convergence of steep initial conditions towards the selected front. *(iii)* to show why convergence towards *pulled* fronts can not be obtained by means of a linear stability analysis. *(iv)* to introduce the "leading edge representation" and demonstrate its predictive power. *(v)* to lay the ground for the calculation of Section III as well as for our future discussion of the breakdown of moving boundary approximations for pulled fronts.

A. Notation and statement of problem

In Sections II – IV, we analyze the nonlinear diffusion equation

$$\partial_t \phi(x,t) = \partial_x^2 \phi + f(\phi) \ , \tag{2.1}$$

where $f(\phi)$ is assumed to be continuous and differentiable. For studying front propagation into unstable states, it is convenient to take

$$\begin{aligned} &f(0) = 0 = f(1) \ , \ f'(0) = 1 \ , \\ &f(\phi) > 0 \ \text{ for all } \ 0 < \phi < 1 \ . \end{aligned} \tag{2.2}$$

so that in the interval $[0,1]$ $f(\phi)$ has one unstable state at $\phi = 0$ and only one stable state at $\phi = 1$. Eq. (2.2) implies, that $f'(1) < 0$. Note, that we here have defined $f(\phi)$ only on the interval $0 \le \phi \le 1$. It can be shown by comparison arguments [50,95] that an initial state with $0 \le \phi(x,0) \le 1$ for all x, conserves this property in time under the dynamics of (2.1), (2.2).

For a nonlinearity like (1.11), a general equation of the form

$$\begin{aligned} \partial_\tau \varphi = D\partial_y^2 \varphi + F_\epsilon(\varphi) \ \ , \ \ F_\epsilon(0) = 0 = F_\epsilon(\varphi_s) \ , \\ F'_\epsilon(0) = \epsilon \ \ , \ \ \varphi_s > 0 \ , \end{aligned} \tag{2.3}$$

results. It allows ϵ to take either sign. For $\epsilon < 0$, the state $\phi = 0$ is linearly stable, for $\epsilon > 0$, it is unstable. Fronts propagating into metastable states ($\epsilon < 0$) will be discussed briefly in Section II D for comparison. If $\epsilon > 0$, (2.3) transforms to the normal form (2.1) as

$$t = \epsilon\tau \ , \ x = \sqrt{\epsilon/D}\, y \ , \ \phi = \varphi/\varphi_s \ , \ f(\phi) = \frac{F(\varphi)}{\epsilon\, \varphi_s} \ . \tag{2.4}$$

Accordingly, velocities transform as $dx/dt = [dy/d\tau]/\sqrt{D\epsilon}$.

The front propagation problem can now be stated as follows. Suppose, that some initial condition $0 \le \phi(x,0) \le 1$ with

$$\lim_{x\to\infty} \phi(x,0) = 0 \ \ , \ \ \phi(x,0) > 0 \text{ for some } x \ , \tag{2.5}$$

is inserted into the equation of motion (2.1) with (2.2). Which shape will the resulting front approach asymptotically as time $t \to \infty$, if any? How quick will the convergence to this asymptotic front be? Can we identify the mechanisms that generate such dynamical behavior? Can we rephrase it such, that we can generalize results to equations other than (2.1)? These questions essentially concern the nature of the front selection mechanism.

As is well known [32,38,48–50,61,63,65,66,68,69,72], the answers to these questions depend on more specific properties of the initial condition as well as of the nonlinearity $f(\phi)$. Our discussion of these results will focus more than earlier work on the central and unifying role of the *steepness* λ of the leading edge of a front, defined as the asymptotic exponential decay rate:

$$\phi(x,t) \overset{x\to\infty}{\sim} e^{-\lambda x} \quad \Leftrightarrow \quad \lambda = -\lim_{x\to\infty} \left(\frac{\partial \ln \phi}{\partial x} \right) \ . \tag{2.6}$$

When $\phi(x,t)$ decays faster than exponential as $x \to \infty$, this implies $\lambda = \infty$.

We will call an initial condition *sufficiently steep*, if

$$\lim_{x\to\infty} e^{\lambda_{steep} x}\, \phi(x,0) = 0 \ , \tag{2.7}$$

otherwise we call it *flat*. How λ_{steep} is determined by $f(\phi)$, will be discussed in Section II D. We will see, that always $0 < \lambda_{steep} \le 1$ for Eq. (2.1), and, in particular, that for pulled fronts $\lambda_{steep} = 1$ and for pushed fronts

$\lambda_{steep} < 1$. The criterion (2.7) for steepness includes all initial conditions with bounded support or, e.g., the initial condition $\phi(x,0) = \theta(-x)$ with θ the step function. Why all such sufficiently steep initial conditions lead to a sharp selection of a front with velocity v_{sel} for $t \to \infty$ (in the sense as explained in the introduction), will be reviewed later in this Section. In contrast, a flat exponentially decaying initial condition whose steepness is smaller than λ_{steep},

$$\phi(x,0) \overset{x\to\infty}{\sim} e^{-\lambda x} \quad , \quad \lambda < \lambda_{steep} \ , \tag{2.8}$$

evolves under the dynamics into a uniformly translating front with a constant velocity $v(\lambda) > v_{sel}$, as we shall discuss.

Another important distinction that we wish to bring to the forefront in our discussion below is that between *leading edge dominated* or *interior dominated* dynamics. The purest form of leading edge dominated dynamics results from flat exponential initial conditions (2.8) with finite steepness λ. In this case, the asymptotic front speed is just the speed $v(\lambda) = \lambda + 1/\lambda$ with which the exponential tail $e^{-\lambda x}$ propagates according to the dynamical equation

$$\partial_t \phi = \partial_x^2 \phi + \phi + o(\phi^2) \ . \tag{2.9}$$

This equation is obtained by linearizing about the unstable state $\phi = 0$, and is appropriate in the leading edge region. Also the convergence towards $v(\lambda)$ is in this case determined by the dynamics in the leading edge — see Sections II D and II E. The more important leading edge dominated dynamics occurs, however, for sufficiently steep initial conditions (2.7) converging to a *pulled* front. As already mentioned, for pulled fronts the asymptotic front speed is just the linear spreading velocity v^* of the leading edge. It occurs when the nonlinearities in $f(\phi)$ are mostly saturating so that they slow down the growth. A well-known sufficient criterion for pulling is

$$f'(0) = \sup_{0<\phi<1} \frac{f(\phi)}{\phi} \ . \tag{2.10}$$

(We briefly rederive this criterion with the help of our leading edge transformation in Appendix A, since this form of a proof is generalizable to other equations.) Pulled fronts are actually at the margin of leading edge domination: although the linearized equation (2.9) is sufficient to determine $v_{sel} = v^* = 2$, the convergence towards this velocity is governed by a nontrivial interplay of dominating leading edge and "slaved" interior. This algebraic and universal convergence we discuss in Sections III and IV and then for more general equations in Section V, building on concepts developed in the present Section.

Leading edge dominated dynamics contrasts with *interior dominated* dynamics, which occurs when the nonlinear function $f(\phi)$ is such that steep initial conditions give rise to *pushed* fronts. For interior dominated or *pushed* dynamics, v_{sel} is associated with the existence of a strongly heteroclinic orbit in the phase space associated with $\Phi_v(\xi)$ (see Section II B below). This means that the whole nonlinearity $f(\phi)$ is needed for constructing v_{sel}. The linear stability analysis leads to the amoung physicists well-known Schrödinger problem reviewed in Section II C. As a consequence, convergence towards the asymptotic solution is exponential in time, as discussed in Section II D. This type of dynamics extends smoothly towards fronts propagating into metastable states, i.e., towards $\epsilon < 0$ in (2.3).

While in this Section we consider the nonlinear diffusion equation (2.1), (2.2) only, many of our results can be generalized rather straightforwardly to a more general class of spatially second order nonlinear diffusion equations. We refer to Appendix B for an explicit analysis of the transformation that maps the resulting stability problem onto the one discussed here.

B. Uniformly translating fronts: candidates for attractors and transients

In this Section, we recall some well known properties [48–50,61,63,65,69] of uniformly translating front solutions of the nonlinear diffusion equation (2.1), (2.2), which play a role in the subsequent analysis. The properties of uniformly translating fronts can be derived by standard methods [96–98]. We transform to a coordinate system moving with uniform velocity v: $(x,t) \to (\xi,t)$, $\xi = x - vt$. The temporal derivative then transforms as $\partial_t\big|_x = \partial_t\big|_\xi - v\partial_\xi\big|_t$. For a front $\phi(x-vt) = \Phi_v(\xi)$ translating uniformly with velocity v, the time derivative vanishes in the comoving frame $\partial_t\big|_\xi \Phi_v = 0$, and so $\Phi_v(\xi)$ obeys the ordinary differential equation

$$\partial_\xi^2 \Phi_v + v\partial_\xi \Phi_v + f(\Phi_v) = 0 \ . \tag{2.11}$$

In view of the initial condition (2.5), we focus on the right-moving front and so we impose the boundary conditions

$$\begin{aligned} &\Phi_v(\xi) \to 1 \ \text{ for } \xi \to -\infty \ , \\ &\Phi_v(\xi) \to 0 \ \text{ for } \xi = \bar{\xi} \ , \end{aligned} \tag{2.12}$$

where $\bar{\xi}$ is either finite or ∞. Note that a more detailed discussion of $\bar{\xi}$ requires to eliminate the translation invariance $\Phi_v(\xi) \to \Phi_v(\xi + \xi_0)$ from the problem.

Close to the stable state $\phi = 1$, the differential equation can be linearized about $\phi = 1$ and solved explicitely. The general local solution is a linear combination of $e^{-\tilde{\lambda}_\pm \xi}$ with

$$\tilde{\lambda}_\pm = \frac{v \pm \sqrt{v^2 - 4f'(1)}}{2} \ . \tag{2.13}$$

According to (2.2), $f'(1)$ is negative. Thus for any real v, $\tilde{\lambda}_+$ is positive and $\tilde{\lambda}_-$ is negative. With the convention (2.12), only the negative root is acceptable. So

$$\Phi_v(\xi) = 1 \pm e^{-\tilde{\lambda}_-(\xi-\xi_0)} + o(e^{-2\tilde{\lambda}_-\xi}) \text{ for } \xi \to -\infty \ . \tag{2.14}$$

The free integration constant multiplying $e^{-\tilde{\lambda}_-\xi}$ here has been decomposed into a sign $\pm$ and a free parameter ξ_0 accounting for translation invariance. Apart from translation invariance, there are two solution for Φ_v close to $\phi = 1$ distinguished by $\pm$.

A global view of the nature and multiplicity of solutions can be obtained with a well known simple particle-in-a-potential analogy. This analogy has of course been exploited quite often in various types of approaches [61,99–101], and only works for the nonlinear diffusion equation, not for equations with higher spatial derivatives; for these, we have to rely on a construction of solutions as trajectories in phase space as sketched around Eq. (2.22). The particle-in-a-potential analogy is based on the identification of equation (2.11) with the equation of motion of a classical particle with friction in a potential. One identifies Φ_v with a spatial coordinate, ξ with time, v with a friction coefficient, and f with the negative force, $f = -\text{force} = \partial_\phi V(\phi)$ derived from the potential $V(\phi) = \int^\phi d\phi' \ f(\phi')$. The potential has a maximum at $\phi = 1$ and a minimum at $\phi = 0$. The construction of Φ_v is equivalent to the motion of a classical particle with "friction" v in this potential, where at "time" $-\infty$ the particle is at rest at the maximum of V. Obviously for any positive "friction" $v > 0$, the particle will never reach the minimum at $\phi = 0$, if it takes off from the maximum at $\phi = 1$ towards $\phi > 1$. It will always reach $\phi = 0$, if it takes off towards $\phi < 1$. We conclude that for every $v > 0$, there is a unique uniformly translating front (unique up to translation invariance), that starts as (2.12) and reaches $\phi = 0$ monotonically. Close to $\phi = 1$, it is given by the $-$ branch in Eq. (2.14).

Let us be more specific on how $\phi = 0$ is approached. If the "friction" v is sufficiently large, the motion of the particle will be overdamped, when it first approaches $\phi = 0$, and it will reach $\phi = 0$ only for "time" $\xi \to \infty$. The critical value of the "friction" where this behavior starts, defines the critical velocity v_c. If $v < v_c$, the particle will reach $\phi = 0$ at a finite "time" ξ and cross it. What then happens, depends on $f(\phi)$ for negative arguments. If $f'(0) = 1$ also on approach from negative arguments ϕ as in the case of the nonlinearities (1.2) or (1.11), the particle might oscillate a finite or an infinite number of times through $\phi = 0$ and reach $\phi = 0$ asymptotically for $\xi \to \infty$[3]. We will see in Sect. II C, that a uniformly translating front Φ_v is dynamically stable, if and only if $v \geq v_c$.

The critical velocity v_c is the smallest velocity at which $\Phi_v(\xi)$ monotonically reaches $\Phi_v(\xi) \to 0$ at $\xi \to \infty$. It can be determined by two different mechanisms which will turn out to distinguish pushed or pulled fronts. These different mechanisms are determined by the nonlinearity $f(\phi)$ or the "potential" $V(\phi)$, resp. To see this, let us linearize about the unstable state, and let us assume for simplicity, that $f'(0) = 1$ from either side. The general solution close to $\phi = 0$ is

$$\Phi_v(\xi) = \begin{cases} A_v \ e^{-\lambda_-\xi} + B_v \ e^{-\lambda_+\xi} & \text{for } v > 2 \ , \\ (\alpha\xi + \beta) \ e^{-\lambda^*\xi} & \text{for } v = v^* = 2 \ , \\ C_v \ e^{-\lambda_0\xi} \ \cos k(\xi - \xi_2) & \text{for } |v| < 2 \ , \end{cases} \tag{2.15}$$

where

$$\lambda_\pm(v) = \lambda_0(v) \pm \mu(v) \ \ (v > 2) \ , \ \ \lambda_0(v) = \frac{v}{2} \ \ (\text{all } v) \ , \tag{2.16}$$

$$\mu(v) = \frac{\sqrt{v^2 - 4}}{2} \ \ (v > 2) \ , \ \ k(v) = \frac{\sqrt{4 - v^2}}{2} \ \ (v < 2) \ , \tag{2.17}$$

$$\lambda^* = \lambda_0(v^*) \ = \ \lambda_\pm(v^*) \ = \ 1 \ \ (v = v^* = 2) \ . \tag{2.18}$$

The special value $v^* = 2$ thus is determined by linearization about the unstable state. At this value of the velocity, the two roots λ_+ and λ_- coincide; as a result, at this point the asymptotic profile is not the sum of two exponentials, but an exponential times a first order polynomial in ξ. The solution (2.15) of the linearized equation for every v contains two free parameters. These parameters are determined by the unique approach of the front Φ_v from $\phi = 1$ and will in general be non-vanishing. The fact that $\alpha \neq 0$ in (2.15) generically, will turn out to have important consequences for the convergence of pulled fronts, as we shall see in Section III.

From (2.15) we can conclude immediately, that fronts with velocity $v < v^* = 2$ will cross $\phi = 0$ at a finite value of ξ. So the critical value of v is certainly $v_c \geq v^* = 2$. Whether $v_c = v^*$ or $v_c > v^*$, depends on the nonlinearities. Suppose first that upon lowering v the front solutions Φ_v remain monotonic till $v = v^*$. In this case,

[3]Note that for, e.g., the modification $f(\phi)=|\phi|\left(1-\phi^{k-1}\right)$, $k > 1$, of the nonlinearity $\phi-\phi^k$ (1.2), and for $v < v_c$, the trajectory will be the same for positive ϕ, but will not reach $\phi = 0$ for $\xi \to \infty$, as the potential V then only has an inflection point at $\phi = 0$, not a minimum. For our analysis of the velocity convergence in the nonlinear diffusion equation, we do not need the behavior of the fronts for negative ϕ, so in that case it does not matter for our fronts between $\phi = 0$ and $\phi = 1$, whether the nonlinearity is, e.g., $\phi - \phi^k$ or $|\phi|\left(1-\phi^{k-1}\right)$. For the linear stability analysis (Sec. II C), Φ_v does need to be defined, of course, on the whole interval from $-\infty$ to $+\infty$, so then the behavior of $f(\phi)$ for negative ϕ needs to be specified when analyzing fronts Φ_v with $v < v_c$. Also, for higher order equations, it is not guaranteed that negative values of the field do not play a role in the convergence behavior.

$v_c = v^*$. A second possibility is the following. At very large v, the front solution is certainly monotonic, as in the particle-on-the-hill analogy, the particle slowly creeps to the minimum of the potential for large "friction" v. Hence A_v in (2.15) is positive for large v. Now, upon lowering v, it may, depending on the nonlinearities, happen that at some velocity $v = v^\dagger$, $A_{v^\dagger} = 0$. In this case, the front is nonmonotonic for $v < v^\dagger$ as A_v will be negative for $v < v^\dagger$. Hence in this case, $v_c = v^\dagger$.

For uniformly translating pulled fronts we will use the short hand notation $\Phi^* \equiv \Phi_{v^*}$. For large ξ they are asymptotically

$$\Phi^*(\xi) \equiv \Phi_{v^*}(\xi) \stackrel{\xi\to\infty}{\sim} \xi\, e^{-\xi} \ , \tag{2.19}$$

since in general the coefficient α in (2.15) is nonzero. For fronts with velocity $v > v^*$, the smaller λ will dominate the large ξ asymptotics, so generically

$$\Phi_v(\xi) \stackrel{\xi\to\infty}{\sim} e^{-\lambda_- \xi} \ . \tag{2.20}$$

However, for a front solution with velocity $v^\dagger$, we have $A_{v^\dagger} = 0$, and so

$$\Phi^\dagger(\xi) \equiv \Phi_{v^\dagger}(\xi) \stackrel{\xi\to\infty}{\sim} e^{-\lambda_+ \xi} \ . \tag{2.21}$$

More mathematically, a construction of front solutions of Eq. (2.11) is equivalent to a construction of trajectories in a phase space $(\Phi_v, \Psi_v \equiv \partial_\xi \Phi_v)$ in which the flow is given by

$$\partial_\xi \begin{pmatrix} \Phi_v \\ \Psi_v \end{pmatrix} = \begin{pmatrix} \Psi_v \\ -v\Psi_v - f(\Phi_v) \end{pmatrix} \ . \tag{2.22}$$

Front solutions correspond to trajectories between the fixed points $(\Phi_v, \Psi_v) = (1, 0)$ and $(0, 0)$. These are thus heteroclinic orbits in phase space. Coming out of the $(1, 0)$ fixed point there are according to (2.14) two trajectories. When we follow the one for which Φ_v decreases for increasing ξ, its behavior near the $(0, 0)$ fixed point is given by (2.15). Now, since the flow depends continuously on v, so will A_v and B_v in (2.15). For large v, A_v is positive, and from the construction of the flow in phase space, one sees that A_v may change sign on lowering v. The largest v with $A_v = 0$ determines the change from monotonic to non-monotonic fronts. At this $v = v^\dagger$, the trajectory flows into the stable $(0, 0)$ fixed point along the most strongly contracting eigendirection — this is precisely what is expressed in (2.21). For this reason, the solution $\Phi^\dagger$ is referred to as a strongly heteroclinic orbit [104]. In [66], this solution was referred to as "the nonlinear front solution".

In summary, the main results of the preceding analysis are:

• For every $v \geq v_c$, there is a uniformly translating front Φ_v with velocity v, which monotonically connects $\phi = 1$ at $\xi \to -\infty$ to $\phi = 0$ at $\xi \to \infty$. All Φ_v with these properties are uniquely determined by v up to translation invariance.

• For every $0 < v < v_c$, there is a unique front solution Φ_v, that translates uniformly with velocity v, and that monotonically connects $\phi = 1$ at $\xi \to -\infty$ to $\phi = 0$ at some finite $\xi = \bar{\xi}$.

• Depending on the nonlinearities, the change from monotonic to nonmonotonic behavior can either occur at the velocity v^*, with $v^* = 2$ for (2.1) and (2.2), or at a larger velocity $v^\dagger$: $v_c = \max[v^*, v^\dagger]$. If $v^\dagger$ exists, it is the largest velocity at which there is a strongly heteroclinic orbit.

The results for invasion into either metastable ($f'(0) < 0$) or unstable states ($f'(0) > 0$) and for $v_c = v^\dagger > v^*$ and $v_c = v^*$ are summarized in $v(\lambda)$ plots in Fig. 3, which show the multiplicity of stable uniformly translating fronts Φ_v parametrized by either v or λ.

The results of this subsection play a role in the subsequent analysis:

(i) There are important connections [61] between the properties of the uniformly translating front solutions and the stability of these fronts (see Section II C). In particular front solutions with velocity $v \geq v_c$ are dynamically stable and possible attractors of the long time dynamics. Fronts with velocity $v < v_c$ either do not exist or are unstable.

(ii) The results for front selection can be easily formulated in terms of the properties of these uniformly translating solutions [61,63,65]: for sufficiently steep initial conditions the dynamically selected velocity coincides with v_c: $v_{sel} = v_c$. If $v_{sel} = v^\dagger$, we speak of the *pushed* regime, while if $v_{sel} = v^*$ we speak of *pulled* fronts.

(iii) We will see in Section III, that the front solutions with $v < v^*$ play a role in the convergence behavior in the interior region of the pulled fronts.

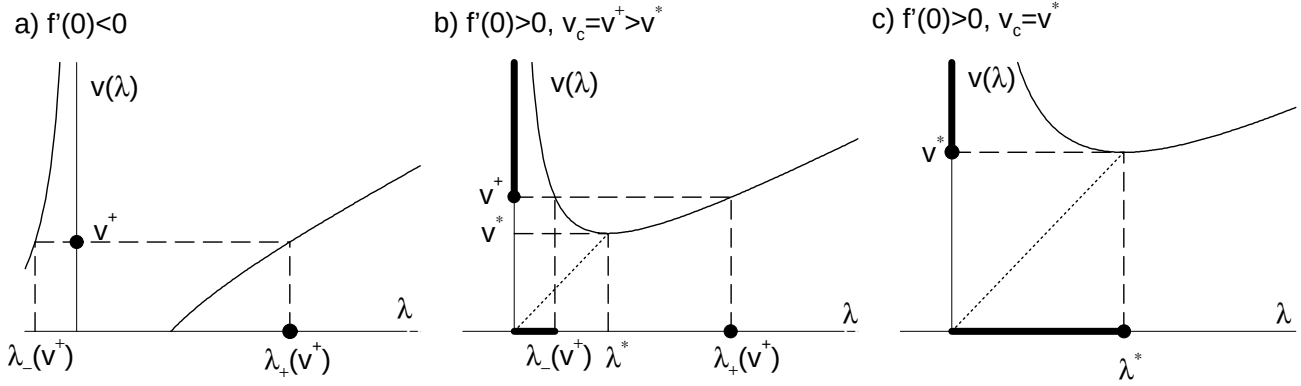

FIG. 3. Steepness λ (2.6) versus velocity $v(\lambda) = \lambda + f'(0)/\lambda$ with solid line for real λ and dotted line for real part of complex λ. $v^\dagger$ is the pushed velocity derived from global analysis, v^* the linear spreading velocity. A fat line or point on the axes denotes the possible attractors $\Phi_v(x - vt)$ of the dynamics, parametrized either by velocity v or by steepness λ. *a*) The case $f'(0) < 0$ corresponding to front propagation into a (meta)stable state. In this case, there is a unique attractor with velocity $v^\dagger$ and steepness $\lambda_+(v^\dagger)$. *b*) and *c*) The case $f'(0) > 0$ corresponding to front propagation into an unstable state. In this case there is a continuum of attractors parametrized by $v \geq v_c$. *b*) The pushed regime: $v_c = v^\dagger > v^*$. The steepness $\lambda_+(v^\dagger)$ of the steepest attractor is isolated just as in case *a*). *c*) The pulled regime: $v_c = v^*$. The steepness λ^* of the steepest attractor is at the margin of the λ-continuum.

C. Linear stability analysis of moving front solutions

Having constructed uniformly translating fronts as possible attractors of the long time dynamics, we now turn to the stability of these moving front solutions. In Section II C 1 we recall the transformation of the linear stability problem to the eigenfunction and eigenvalue problem of a Schrödinger equation [88,36,61,98], a problem well known to physicists (for earlier as well as more mathematical approaches, see [88–93,54]). We then argue, that this space of eigenfunctions in general will be insufficient to discuss the general linear stability problem or the whole basin of attraction of a given uniformly translating front Φ_v. We then in Section II C 2 extend the linear stability analysis to functions outside the Hilbert space associated with the Schrödinger problem. The discussion of these perturbations follows concepts outlined in the Appendix of [63]. As will be discussed in Section II D, this extended space of linear perturbations gives an essentially complete picture of the basins of attraction of uniformly translating fronts and of the rates of convergence. However, we will see, that *even after extending linear stability analysis beyond the Hilbert space, it is not possible to derive the convergence of pulled fronts with this tool of analysis.*

To study the linear stability of a uniformly translating front Φ_v, we linearize about it in the frame $\xi = x - vt$ moving with the constant velocity v, by writing

$$\phi(\xi, t) = \Phi_v(\xi) + \eta(\xi, t) \ . \tag{2.23}$$

Inserting (2.23) into (2.1), we find to linear order the equation of motion for $\eta(\xi, t)$

$$\partial_t \eta = \mathcal{L}_v \eta + O(\eta^2) \tag{2.24}$$

with the linear operator

$$\mathcal{L}_v = \partial_\xi^2 + v\partial_\xi + f'\Big(\Phi_v(\xi)\Big) \ . \tag{2.25}$$

$\mathcal{L}_v$ is not self-adjoint, so left and right eigenfunctions will differ. The trouble is caused by the linear derivative $v\partial_\xi$. It can be removed by the following transformation [88,61]:

$$\psi = e^{v\xi/2}\, \eta \ , \tag{2.26}$$

$$\mathcal{H}_v = -\, e^{v\xi/2}\, \mathcal{L}_v\, e^{-v\xi/2} \ . \tag{2.27}$$

so that $\mathcal{H}_v$ becomes the linear operator

$$\mathcal{H}_v = -\partial_\xi^2 + V(\xi) \quad , \quad V(\xi) = \tfrac{v^2}{4} - f'\Big(\Phi_v(\xi)\Big) \ . \tag{2.28}$$

The equation of motion (2.24) then becomes

$$-\partial_t \psi = \mathcal{H}_v \psi + O\left(\psi^2\, e^{-v\xi/2}\right) \ . \tag{2.29}$$

Transformation (2.26) from η to ψ increases the weight of the leading edge ($\xi \to \infty$) by a factor $e^{v\xi/2}$, while it enhances convergence at $\xi \to -\infty$. Note that the so-called leading edge representation of the equation of motion already mentioned in (1.10) and further discussed in Sections II E, III and V is based on a similar transformation. However, we there will transform the complete function ϕ, and not only the linear perturbation $\eta = \phi - \Phi_v$.

Let us return to (2.29). Since $\mathcal{H}_v$ is self-adjoint, we can decompose functions, that lie in the Hilbert space of $\mathcal{H}_v$, into the orthonormal set of eigenfunctions of $\mathcal{H}_v$. Eigenfunctions in this Hilbert space form a complete set. However, it is obvious that not all linear perturbations with $|\eta| \ll 1$ are in this space: Only perturbations with

$$\lim_{\xi\to\infty} |\eta|\, e^{\,\lambda_0(v)\,\xi} < \infty \quad \text{with } \lambda_0(v) = \frac{v}{2} \tag{2.30}$$

can lie in the Hilbert space (which consists of square integrable functions and of solutions proportional to plane waves $e^{ik\xi}$ as $\xi \to \pm\infty$).

1. Schrödinger stability analysis

The general properties of the spectrum and eigenfunctions of $\mathcal{H}_v$ within the Hilbert space can be immediately obtained from a few well known results which to physicists are known from quantum mechanics (see, e.g., [102]), since $\mathcal{H}_v$ is the Hamiltonian operator for a (quantum) wave in a potential in one dimension. The potential is asymptotically lower on the right than on the left, since

$$V(\infty) = \tfrac{v^2}{4} - f'(0) \;\; < \;\; \tfrac{v^2}{4} - f'(1) = V(-\infty)\ , \tag{2.31}$$

according to (2.2). If we write the temporal behavior of an eigenfunction as $\tilde{\psi}_\sigma(\xi)\, e^{-\sigma t}$, one finds that the spectrum of

$$\mathcal{H}_v \tilde{\psi}_\sigma = \sigma \tilde{\psi}_\sigma \tag{2.32}$$

is continuous for $\sigma \geq V(\infty)$, and that the eigenfunctions are distributions, i.e., essentially plane waves $e^{ik\xi}$ with $k = \pm\sqrt{\sigma - V(\infty)}$ as $\xi \to \infty$. One immediately concludes, that a front Φ_v with velocity $v < v^* = 2\sqrt{f'(0)}$ will be unstable against the continuous spectrum of linear perturbations with "energies" $V(\infty) < \sigma < 0$.

For a front Φ_v with velocity $v \geq v^* = 2\sqrt{f'(0)}$, there still might be a point spectrum of bound and square integrable states with $\sigma < 0$. Bound states have a finite number of nodes, and there is a one-to-one correspondence between the number of nodes and the eigenvalue of the bound state "wavefunction" ψ_σ: the eigenfunction with the lowest eigenvalue σ is nodeless (if it exists), the eigenfunction corresponding to the next largest bound state eigenvalue has one node, etc. Therefore, the point spectrum is bounded from below by the "energy" σ of the nodeless eigenfunction, if it exists. Now, one eigenfunction is known: the translation mode $\tilde{\psi}_0$ clearly has $\sigma = 0$. The translation mode can be generated by an infinitesimal translation of Φ_v:

$$\tilde{\psi}_0 = e^{\lambda_0(v)\xi}\, \partial_\xi \Phi_v \quad , \quad \mathcal{H}_v \tilde{\psi}_0 = 0\ . \tag{2.33}$$

If Φ_v is monotonic, $\tilde{\psi}_0$ will be nodeless. If Φ_v is non-monotonic, $\tilde{\psi}_0$ will have nodes.

From this, one might be tempted to immediately draw conclusions on the stability of monotonic or non-monotonic front solutions. However, this is only possible, if $\tilde{\psi}_0$ is in the Hilbert space! Comparison with (2.15) shows, that this is the case, if either $v = v^*$ and $\alpha = 0$, or if $v > v^*$ and $A_v = 0$, i.e., for one of the strongly heteroclinic orbits.

If a front Φ_v obeys one of these conditions and if it is monotonic, then $\tilde{\psi}_0$ is the eigenfunction in the Hilbert space with the lowest "energy" $\sigma = 0$. Therefore all other eigenfunctions will have $\sigma > 0$ and will decay in time as $e^{-\sigma t}$. An arbitrary linear perturbation in the Hilbert space can be decomposed into the complete set of eigenfunctions, and therefore it will decay, too — where special attention will have to be payed to the nondecaying translation mode $\tilde{\psi}_0$.

If such a front Φ_v is non-monotonic, it will have n extrema, with $n > 0$ some integer. The translation mode then has n nodes, and hence there are then n bound eigenfunctions $\tilde{\psi}_\sigma$ with negative σ. The front profile is then linearly unstable with respect to these modes. Since any generic initial condition will have a nonvanishing contribution from these destabilizing modes, a non-monotonic Φ_v will generically not be approached for long times. Such a Φ_v is called dynamically unstable.

The analysis of the spectrum and eigenfunctions of the Schrödinger operator in the Hilbert space therefore yields the following results:

1) A front Φ_v with velocity $v < v^*$ is intrinsically unstable against a continuous band of linear perturbations from the Hilbert space. Such a front generically will not be approached under the dynamics.

2) A front Φ^* with velocity $v = v^*$ and $\alpha = 0$ is unstable against perturbations from the Hilbert space, if it is non-monotonic, and it is stable, if it is monotonic. There is a continuous band of linear perturbations with $\sigma \geq 0$, that continuously extends down to $\sigma = 0$. Accordingly, there is no gap in the excitation spectrum, which already hints at the non-exponential convergence towards a monotonic Φ^*.

3) A strongly heteroclinic orbit Φ_v with $v > v^*$ and $A_v = 0$, if it exists, is unstable against perturbations from the Hilbert space, if it is non-monotonic, and it is stable, if it is monotonic. If strongly heteroclinic orbits exist, by construction (see Section II B), only the one with the largest velocity $v = v^\dagger$ is monotonic, and the front Φ^* with velocity $v = v^* < v^\dagger$ is non-monotonic and thus unstable. So only for $\Phi^\dagger$, the spectrum of linear perturbations is purely positive: $\sigma \geq 0$. For $\Phi^\dagger$, there is at best a discrete spectrum of linear perturbations in the Hilbert space in the range $0 < \sigma < V(\infty) = ({v^\dagger}^2 - {v^*}^2)/4$, and the continuous spectrum begins at $\sigma \geq V(\infty)$. Convergence of all perturbations in the Hilbert space will thus be exponential in time like $e^{-\sigma t}$, with σ the smallest positive eigenvalue.

Note the restrictions of this analysis:

(a) Up to now, we have no predictions for fronts with velocity $v \geq v^*$, whose translation mode $\tilde{\psi}_0$ (2.33) is outside the Hilbert space. We will see, that the equivalence of stability and monotonicity extends beyond the Hilbert space analysis.

(b) The analysis of general initial conditions might require linear perturbations, that lie outside the Hilbert space, even if $\tilde{\psi}_0$ is in the Hilbert space.

2. Linear perturbations outside the Hilbert space

The mapping to the Schrödinger problem is a powerful method for perturbations η about a front Φ_v, that lie within the Hilbert space, because we then can work with a complete set of orthogonal functions. However, this space of perturbations needs to be completed by functions from outside the Hilbert space.

To see this, consider for simplicity an initial condition, that is close to some Φ_v with $v \geq v^*$, but steeper than this asymptotic front: $\lim_{x\to\infty} \phi(x,0)/\Phi_v(x) = 0$. Then the steepness in the leading edge of $\eta = \phi - \Phi_v$ will be dominated by Φ_v, and

$$\psi = \eta\, e^{\lambda_0(v)\xi} \overset{\xi\to\infty}{\sim} \begin{cases} \alpha\xi + \beta & \text{for } v = v^* \\ e^{-\mu(v)\xi} & \text{for } v = v^\dagger \text{ or generally} \\ & \text{for } v > v^* \text{ and } A_v = 0 \\ e^{\,\mu(v)\xi} & \text{for } v > v^* \text{ and } A_v \neq 0 \end{cases} \tag{2.34}$$

with $\mu(v) = \sqrt{v^2/4 - 1} > 0$ from (2.15). Accordingly, only for a pushed front propagating with velocity $v = v^\dagger$ (or more generally for a strongly heteroclinic orbit with $v > v^*$ and $A_v = 0$) or for a pulled front with velocity v^* and $\alpha = 0$, the linear perturbation $\eta\, e^{\lambda_0(v)\xi}$ is in the Hilbert space of $\mathcal{H}_v$. The decay of the zero mode $\tilde{\psi}_0$ (2.33) is asymptotically the same as that of ψ in (2.34). So a treatment of linear perturbations outside the Hilbert space is clearly called for.

A perturbation η, that we want to decompose, in general obeys

$$\lim_{\xi\to\pm\infty} |\eta(\xi,t)| \ll 1 \ . \tag{2.35}$$

This is required for the linearization of ϕ about Φ_v in (2.24). We aim at a decomposition of $\eta(\xi,t)$ into eigenfunctions $\eta_\sigma(\xi)\, e^{-\sigma t}$. We therefore return to the eigenvalue equation for such an eigenmode, which according to (2.24) and (2.25) is given by

$$\left[\partial_\xi^2 + v\partial_\xi + f'\Big(\Phi_v(\xi)\Big) + \sigma\right] \eta_\sigma = 0 \ . \tag{2.36}$$

Our previous analysis in the Hilbert space already has identified many of these eigenmodes, in fact all those, which obey (2.30). This criterium on η_σ is too strict at $\xi \to \infty$, so we now need to additionally analyze perturbations with $e^{-\lambda_0(v)\xi} < |\eta_\sigma(\xi)| < 1$ as $\xi \to \infty$, which lie outside the Hilbert space. On the other hand, for $\xi \to -\infty$, Eq. (2.30) is less restrictive than (2.35). This gives us the freedom to impose only $|\eta_\sigma(\xi)| \lesssim e^{\lambda_0(v)|\xi|}$ as $\xi \to -\infty$, since such a divergence can be compensated for by perturbations from inside the Hilbert space, where we make use of its completeness. We therefore now impose the boundary conditions

$$\lim_{\xi\to\infty} |\eta_\sigma(\xi)| < \infty \quad , \quad \lim_{\xi\to-\infty} e^{\lambda_0(v)\xi}|\eta_\sigma(\xi)| < \infty \ , \tag{2.37}$$

where perturbations that additionally obey $e^{-\lambda_0(v)\xi}|\eta_\sigma(\xi)| < \infty$ as $\xi \to \infty$, are in the Hilbert space of $\mathcal{H}_v$.

First of all, we note, that the translation mode $\eta_0(\xi) = \partial_\xi \Phi_v(\xi)$ (2.33) now is always included in the larger space (2.37) of perturbations.

Second, solve (2.36) for $\xi \to \infty$ and find in analogy to (2.15), that

$$\eta_\sigma(\xi) = A_\sigma e^{-\Lambda_-\xi} + B_\sigma e^{-\Lambda_+\xi} \ , \tag{2.38}$$

with

$$\Lambda_\pm(\sigma, v) = \frac{v}{2} \pm \sqrt{\frac{v^2}{4} - f'(0) - \sigma} \ . \tag{2.39}$$

For brevity of notation, we here allowed $\Lambda_\pm(\sigma, v)$ to be complex. In Fig. 4 we plot $\Lambda_\pm$ versus σ, both for the case of a front propagating into an unstable state ($f'(0) > 0$), and for the case of a front between a stable and a metastable state ($f'(0) < 0$), and for $f'(0) > 0$, we furthermore distinguish between $v > v^*$ and $v = v^*$. The leading edge solution (2.38), of course, precisely coincides with the leading edge behavior of the Hilbert space functions, except that one case was excluded from the Hilbert space: A leading edge with $A_\sigma \neq 0$ and $\sigma \leq V(\infty) = v^2/4 - f'(0)$ does not obey the boundary condition (2.30). It does obey the boundary condition (2.35), if $\sigma \geq -f'(0)$. Let us therefore now focus on the additional perturbations with

$$-f'(0) < \sigma \leq V(\infty) = \frac{v^2}{4} - f'(0) \ . \tag{2.40}$$

If $A_\sigma \neq 0$, such perturbations are outside the Hilbert space, but they do obey (2.37).

Are there such perturbations for a given σ, and how many? For answering this question, we need to analyze η_σ globally, in close analogy to the global analysis of the Φ_v as a function of v in Section II B. Solving (2.36) at $\xi \to -\infty$ yields two exponents

$$\begin{aligned} \tilde{\Lambda}_\pm(\sigma, v) &= \frac{v}{2} \pm \sqrt{\frac{v^2}{4} - f'(1) - \sigma} \\ &= \lambda_0(v) \pm \sqrt{V(-\infty) - \sigma} \ , \end{aligned} \tag{2.41}$$

in analogy with (2.13) and (2.14). Since $V(-\infty) > V(\infty)$ (2.32), for $\sigma \leq V(\infty)$ we certainly have $V(-\infty) - \sigma > 0$. The coefficient of $e^{-\tilde{\Lambda}_+(\sigma,v)\xi}$ therefore needs to vanish for η_σ to obey (2.37). Behind the front for $\xi \to -\infty$, we therefore find that

$$\eta_\sigma(\xi) = \pm e^{-\tilde{\Lambda}_-(\xi-\xi_0)} + o\left(e^{-2\tilde{\Lambda}_-\xi}\right) \ , \tag{2.42}$$

for an η_σ obeying (2.37) and (2.40). Eq. (2.42) determines η_σ uniquely, because the arbitrary constant coefficient $\pm e^{\tilde{\Lambda}_-\xi_0}$ can be scaled out of a linear equation like (2.36). Such a linear equation can always be integrated

towards $\xi \to \infty$, where it uniquely determines the coefficients A_σ and B_σ in (2.38). Accordingly, A_σ and B_σ generically are non-vanishing, in complete analogy to the argument for A_v and B_v in (2.15) to be generically non-vanishing in Φ_v.

What do we gain with these extra solutions? The eigenfunctions in the Hilbert space had a continuous spectrum for $\sigma \geq V(\infty) = (v^2 - v^{*2})/4 \geq 0$ and at best a discrete spectrum defined by $A_\sigma = 0$ for $\sigma < V(\infty)$. Adding the solutions, that obey (2.37), we extend the continuous spectrum down to $\sigma \geq -f'(0) = V(\infty) - v^2/4 < 0$ and find at best a discrete spectrum defined by $A_\sigma = 0$ for $\sigma < -f'(0)$. These discrete solutions for $\sigma < -f'(0)$ all lie in the Hilbert space.

Let us now look at the steepness in the leading edge of the solutions outside the Hilbert space. They have a σ from the interval (2.40), and $A_\sigma \neq 0$. For these we observe (cf. Fig. 4) that

$$\begin{aligned} &\Lambda_-(\sigma, v) > \lambda_-(v) \quad \text{for} \quad \sigma > 0 \quad \text{(decaying)} , \\ &\Lambda_-(\sigma, v) < \lambda_-(v) \quad \text{for} \quad \sigma < 0 \quad \text{(destabilizing)} , \\ &\Lambda_-(0, v) = \lambda_-(v) \quad \text{for} \quad \sigma = 0 \quad \text{(marginal)} , \end{aligned} \tag{2.43}$$

with $\lambda_-(v)$ from (2.14). This means, that these linear eigenmodes η_σ of Φ_v will decay ($\sigma > 0$), if they are steeper than $e^{-\lambda_-(v)\,\xi}$, and that they will destabilize a front Φ_v, if they are flatter. Note that the spectrum of decaying modes is continuous down to zero, as $\sigma \downarrow 0$ as $\Lambda_- \downarrow \lambda_-$.

It is tempting to conclude here immediately, that a front $\Phi_v(\xi)$ with velocity $v \geq v^*$ will be stable against all perturbations, which are steeper in the leading edge than $e^{-\lambda_-(v)\xi}$. However, the possible existence of the discrete set of solutions with $A_\sigma = 0$ and $\sigma < 0$ requires special attention, since these perturbations are steeper than $e^{-\lambda_0(v)\xi}$, but destabilizing ($\sigma < 0$). Now, if Φ_v is strongly heteroclinic ($A_v = 0$), we already found in Section II C 1, that such destabilizing perturbations exist, if and only if Φ_v is non-monotonic. We now need to show that this argument also holds for fronts Φ_v with $v > v^*$ and $A_v \neq 0$ or for fronts Φ^* with velocity v^* and $\alpha \neq 0$. The following five steps *(i)–(v)* prove this: (*i*) Impose (2.42) at $\xi \to -\infty$. This defines a unique solution of equation (2.36) for η_σ for every $\sigma < V(-\infty)$. In fact, we only need to analyze $\sigma < V(\infty)$, since we know the spectrum for larger σ. (*ii*) Integrate (2.36) forward towards $\xi \to \infty$ for a very large negative σ. The variation of $f'(\Phi_v(\xi))$ in space then can be almost neglected. Therefore at $\xi \to \infty$, we will find (2.38) with $|A_\sigma/B_\sigma| \gg 1$. For our further construction it is crucial to observe, that such a perturbation for sufficiently large negative σ will be nodeless. It does not matter, on the other hand, that this solution typically will not obey our bound (2.37), since we only use it as a means for constructing the solutions with $A_\sigma = 0$, which will not only obey (2.37), but even lie inside the Hilbert space. (*iii*) Upon increasing σ continuously, at discrete values of $\sigma < V(\infty)$, η_σ will gain an extra node. Since the generation of every new node is associated with a change of sign of the perturbation at $\xi \to \infty$, if the sign at $\xi \to -\infty$ is kept fixed, the appearance of an additional mode can only occur at a σ, where the sign of A_σ changes. (*iv*) We know the number of nodes of the zero mode η_0. It is identical to the number of extrema of Φ_v. We therefore know the number of particular perturbations with $A_\sigma = 0$ and $\sigma < 0$. (*v*) From this it follows that if Φ_v is monotonic, there are no particular perturbations with $A_\sigma = 0$ and $\sigma < 0$. If Φ_v is non-monotonic, there are such perturbations.

Summarizing the Schrödinger analysis and the present results, we can conclude immediately:

1) Non-monotonic fronts are intrinsically unstable, and generically will not be approached by any initial conditions.

2) Monotonic fronts propagating with velocity v are stable against perturbations steeper than $e^{-\lambda_-(v)\xi}$. The role of the zero mode η_0 will require special attention.

As to the formal derivation of these results let us remark:

(*i*) In Section II B, we have counted the multiplicity of front solutions Φ_v as a function of v. Here we have counted the multiplicity of perturbations η_σ of a front Φ_v as a function of σ. This counting was based on the proper asymptotics of the solutions at $\xi \to \pm\infty$, which is of the same structure for both Φ_v and η_σ, so the counting argument follows exactly the same lines in both cases.

(*ii*) Although the particle-on-a-hill analogy for Φ_v or the mapping onto the Schrödinger equation for η_σ are insightful and very efficient ways to arrive at our results for existence and stability of uniformly translating front solutions, the analysis by no means relies on these. In fact, much of the phase space analysis can easily be generalized to higher order equations as, e.g., Eq. (1.3) — see Section V.

(*iii*) In the stability analysis of non-monotonic fronts, the discrete set of solutions with $A_v = 0$ or $A_\sigma = 0$ plays a particular role. For equations like (1.3) – (1.8), monotonicity ceases to be a criterium, but conditions like $A_v = 0$ defining so-called strongly heteroclinic solutions continue to play a central role in the stability analysis, as is discussed in Appendix F to Sect. V.

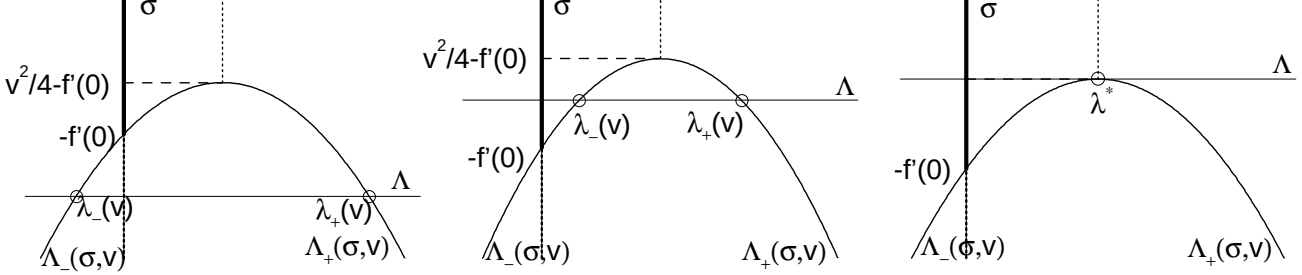

FIG. 4. Steepness $\Lambda(\sigma, v)$ (2.39) versus decay rate σ of linear perturbations η_σ (2.36), (2.37) of a given front Φ_v with velocity $v \geq v^*$. The solid curve denotes real Λ, the dotted curve the real part of complex Λ. $\lambda_\pm(v)$ and λ^* are the steepnesses of Φ_v and of the zero mode $\eta_0 = \partial_\xi \Phi_v$. They are marked by circles on the Λ axis. The generic steepness of a front Φ_v with $v > v^*$ is $\lambda_-(v)$, while in the particular case of $A_v = 0$, it is $\lambda_+(v)$. The continuous spectrum of σ is denoted by a fat solid line on the σ-axis, the interval in which there may be discrete eigenvalues σ by the fat dotted line. The continuous spectrum within the Hilbert space of $\mathcal{H}_v$ exists only at $v^2/4 - f'(0) \leq \sigma$. The continuous spectrum for $-f'(0) < \sigma < v^2/4 - f'(0)$ is on the Λ_--branch. There might be discrete solutions characterized by $A_\sigma = 0$. They lie on the Λ_+-branch, might exist for all $\sigma < v^2/4 - f'(0)$, and need to be constructed. *a*) The front Φ_v propagates into a metastable state ($f'(0) < 0$). Its steepness is $\lambda_+(v)$. It is stable against all linear perturbations with $\Lambda < \lambda_+(v)$. The discrete spectrum of steep perturbations with $\Lambda > \lambda_+(v)$ needs to be investigated. *b*) The front propagates into an unstable state ($f'(0) > 0$) with velocity $v > v^*$. It is stable against all linear perturbations with $\lambda_-(v) < \Lambda < \lambda_+(v)$, it is unstable against the continuous spectrum of very flat perturbations with $0 < \Lambda < \lambda_-(v)$, which might be excluded by the initial conditions. The discrete spectrum of steep perturbations with $\Lambda > \lambda_+(v)$ needs to be investigated. *c*) The front propagates into an unstable state ($f'(0) > 0$) with velocity $v = v^*$. The discussion is as for (*b*) after identifying $\lambda_\pm(v^*) = \lambda^*$.

D. Consequences of the stability analysis for selection and rate of convergence

Suppose now, that we insert an initial condition $\phi(x, 0)$ into the nonlinear diffusion equation (2.1) with a given nonlinearity $f(\phi)$, and then study the ensuing dynamics. In this Section, we address the question what the linear stability analysis tells us about the asymptotic ($t \to \infty$) state and the rate of convergence. To answer this question, we will need to complement the picture we developed so far — even after extending the analysis of linear perturbations beyond the Hilbert space — with a separate analysis of the leading edge dynamics. We will do this in Section II E, but here already anticipate one result from this Section, namely: *If initially at $t = 0$ the steepness λ defined in (2.6) is nonzero (finite or infinite), then at any finite time $t < \infty$ the steepness is conserved:*

$$\phi(x,0) \overset{x\to\infty}{\sim} e^{-\lambda x} \implies \phi(x,t) \overset{x\to\infty}{\sim} e^{-\lambda x} \text{ for all } t < \infty \ . \tag{2.44}$$

Note that the limits $x \to \infty$ and $t \to \infty$ do not commute. We characterize the initial condition by its steepness λ_{init} defined by

$$\phi(x, t = 0) \overset{x\to\infty}{\sim} e^{-\lambda_{init} x} \ . \tag{2.45}$$

As a consequence of (2.44), we can use λ_{init} to characterize not only the initial conditions but also the profile at any later time $0 \leq t < \infty$, when the front velocity might be already close to its asymptotic value.

We now study the temporal development of some initial condition $\phi(x, 0)$ under the nonlinear diffusion equation with some nonlinearity $f(\phi)$. Anticipating that $\phi(x, t)$ approaches a uniformly translating front solution $\Phi_v(\xi)$ for $t \to \infty$, we may wish to consider $\phi(x, t)$ as some asymptotic front profile Φ_v plus some decaying linear perturbation. If the initial condition has steepness λ_{init}, and we linearize it about an asymptotic front with steepness λ_{asympt}, the resulting perturbation $\eta(x, t) = \phi(x, t) - \Phi_v(x - vt)$ will in view of (2.44) then have steepness

$$\lambda_\eta = \min\left[\lambda_{init}, \lambda_{asympt}\right] \ . \tag{2.46}$$

Let us now explore what the stability analysis implies for the decay rate of the perturbation.

1. *Pushed regime: $v_c = v^\dagger$*

We first consider equations with the nonlinearity $f(\phi)$ such, that the slowest stable front is a strongly heteroclinic orbit in phase space with $A_{v^\dagger} = 0$ in (2.15). We have denoted this asymptotic front with $\Phi^\dagger$ and its velocity with $v^\dagger$. Its steepness is $\lambda_+(v^\dagger) = \lambda_0(v^\dagger) + \mu(v^\dagger)$, cf. (2.21). There is a continuous family of stable front solutions Φ_v with velocity $v > v^\dagger$ which are all flatter than $\lambda_-(v^\dagger) = \lambda_0(v^\dagger) - \mu(v^\dagger)$. Their steepness $\lambda = \lambda_-(v^\dagger)$ is related to their velocity v through

$$v(\lambda) = \lambda + \frac{1}{\lambda} \ , \tag{2.47}$$

as can be obtained by inverting (2.16).

CASE I: Consider an initial condition with steepness $\lambda_{init} > \lambda_0(v^\dagger)$. We let ϕ evolve some time, and then linearize it about $\Phi^\dagger$. According to (2.46), the perturbation η will have steepness $\lambda_\eta > \lambda_0(v^\dagger)$. It then is in the

Hilbert space analyzed in Section II C 1. We can decompose the perturbation into the known eigenperturbations. The spectrum of decay rates has no negative eigenvalues, one eigenvalue zero and then a gap above zero. A contribution from the zero mode can be made vanishing by adjusting the position of the subtracted asymptotic front Φ_v, by making use of the translational freedom of Φ_v. The perturbation then can be decomposed into Hilbert space functions η_σ with σ all positive and bounded away from zero. Thus, for large times, the perturbation will decay exponentially. This means, that an initial condition with $\lambda_{init} > \lambda_0(v^\dagger)$ will converge to $\Phi^\dagger$ exponentially in time, generically with $e^{-\sigma_1 t}$, where σ_1 is the smallest positive eigenvalue.

CASE II: If the initial steepness is $\lambda_-(v^\dagger) < \lambda_{init} \leq \lambda_0(v^\dagger)$, the perturbation of ϕ about $\Phi^\dagger$ will not be in the Hilbert space. However, we do know from the results illustrated in Fig. 4 that there is an eigenmode η_σ of the linear stability operator of $\Phi^\dagger$ with the proper steepness $\lambda_{init} = \lambda_\eta$, that will decay exponentially in time, see Section II C 2. The remaining linear perturbation $\eta - \eta_\sigma$ might lie in the Hilbert space, in which case we are back to Case I. If it does not, we have to identify the subleading λ, its corresponding eigenmode η_σ etc. The iteration of this construction leads us to conclude, that the perturbation indeed will decay exponentially in time. (Examples of exponential convergence towards pushed fronts which is dominated by such modes can be found in Fig. 19 of [65].) Another way of putting the argument is, that only perturbations with $\lambda < \lambda_-(v^\dagger)$ can grow in time, but these cannot be involved in the decomposition of a perturbation with $\lambda_\eta > \lambda_-(v^\dagger)$. A more elegant way of analyzing this case and the following ones will be discussed in Section II E.

CASE III: If the initial steepness is $\lambda_{init} < \lambda_-(v^\dagger)$, and we linearize ϕ about $\Phi^\dagger$, there is a perturbation η_σ with steepness $\lambda_\eta = \lambda_{init}$, that is growing in time ($\sigma < 0$). So such an initial condition cannot approach $\Phi^\dagger$ or any other asymptotic front Φ_v with steepness $\lambda_{asympt} > \lambda_{init}$. If we linearize ϕ about the asymptotic front Φ_v with the same steepness $\lambda_{init} = \lambda_{asympt}$, the remaining perturbation will be steeper, so contributions from the zero mode are excluded by construction, and the perturbation can be decomposed into eigenperturbations of Φ_v, which all decay in time.

Let us summarize so far: All initial conditions with $\lambda_{init} > \lambda_-(v^\dagger)$ converge exponentially in time to the "selected" front with velocity $v_{sel} = v^\dagger$ and steepness $\lambda_{sel} = \lambda_+(v^\dagger)$. Initial conditions with $\lambda_{init} < \lambda_-(v^\dagger)$ will converge to a quicker asymptotic front with steepness $\lambda_{asympt} = \lambda_{init}$ and velocity $v(\lambda_{init})$ given by (2.47).

In Section II A, we have termed an initial condition sufficiently steep ($\lambda_{init} > \lambda_{steep}$), if it approached the "selected" front for large times. We have denoted the steepness of the selected front with λ_{sel}. In the pushed regime, one can thus identify these parameters with

$$\lambda_{steep} = \lambda_-(v^\dagger) = \frac{v^\dagger}{2} - \mu(v^\dagger) \ , \tag{2.48}$$

$$\lambda_{sel} = \lambda_+(v^\dagger) = \frac{v^\dagger}{2} + \mu(v^\dagger) \ , \quad \mu(v^\dagger) = \sqrt{\frac{{v^\dagger}^2 - 4}{4}} \ ,$$

$$v_{sel} = v^\dagger \ .$$

2. Fronts into metastable states

The only difference between a pushed front propagating into an unstable state, i.e., with a nonlinearity f such that $f'(0) > 0$ and $v_c = v^\dagger > v^*$, and a front propagating into a metastable state, i.e., with $f'(0) < 0$, is the sign of $\lambda_-(v)$: For a front into a metastable state, we have

$$\mu(v) = \sqrt{\frac{v^2 - 4f'(0)}{4}} > \frac{v}{2} \quad \text{for} \quad f'(0) < 0 \ , \tag{2.49}$$

so $\lambda_-(v) < 0$ and $\lambda_+(v) > 0$ for all $v > 0$ (the sign of $\lambda_0(v)$ is the same as the sign of v). Suppose, that the selected front still travels with positive speed $v_{sel} = v^\dagger$ (otherwise reverse x). Because now $\lambda_-(v) < 0$,

$$\lambda_{steep} = 0 \ , \tag{2.50}$$

so all initial conditions are sufficiently steep and converge to $\Phi^\dagger$. The continuous spectrum of asymptotic solutions Φ_v with $\lambda_{asympt} < \lambda_{steep}$ ceases to exist, and the asymptotic front $\Phi^\dagger$ therefore now is unique.

For the convergence of an initial condition ϕ towards $\Phi^\dagger$ we still need to distinguish, whether λ_{init} is larger or smaller than $\lambda_0(v^\dagger) = v^\dagger/2$. If $\lambda_{init} > \lambda_0(v^\dagger)$, the perturbation about $\Phi^\dagger$ lies in the Hilbert space, while for $\lambda_{init} < \lambda_0(v^\dagger)$, it does not. This corresponds to the Cases I and II for $v_c = v^\dagger$ above, which apply literally, because the spectrum of eigenperturbations of $\Phi^\dagger$ is continuous and because the steepness of these modes extends down to $\lambda = 0$ — see Fig. 4. In both cases, the initial conditions converge to $\Phi^\dagger$ exponentially in time. Case III does not occur for fronts into metastable states.

3. Pulled regime: $v_c = v^*$

At the transition from fronts propagating into metastable towards fronts into unstable states, $f'(0)$ changes sign, and so does $\lambda_-(v)$. At this point a continuum of possible attractors Φ_v of the dynamics comes into existence, but the convergence behavior of sufficiently steep initial conditions is completely unchanged. In other words: Cases I and II are completely unchanged, and only Case III needs to be considered additionally for initial conditions with $\lambda_{init} < \lambda_{steep}$.

A qualitative change in the convergence behavior of sufficiently steep initial conditions $\lambda_{init} > \lambda_{steep}$ only takes place at the transition from the pushed to the pulled regime. This happens for f changing such that $v^\dagger$ approaches v^*. Then

$$\lambda_{steep} = \lambda_0(v^*) = \lambda_{sel} \ . \tag{2.51}$$

This transition leaves the multiplicity of possible attractors unchanged, but the resulting changes in the spectrum have deep consequences for the convergence behavior of sufficiently steep initial conditions.

We now need to distinguish but two Cases for the initial condition, namely $\lambda \geq \lambda^*$ and $\lambda < \lambda^*$, where we use the short hand notation $\lambda^* = \lambda_0(v^*) = \lambda_\pm(v^*) = v^*/2$.

For flat initial conditions $\lambda_{init} < \lambda^*$, the arguments from Case III above apply literally. Such an initial condition will approach a front Φ_v with velocity $v(\lambda_{init}) > v^*$ given by (2.47) and with steepness $\lambda_{asympt} = \lambda_{init}$. Sufficiently steep initial conditions, however exhibit a new behavior:

CASE IV: Consider a sufficiently steep initial condition with $\lambda > \lambda^*$. As before, we linearize the profile $\phi(x,t)$ after a sufficient evolution time about the selected front Φ^*. The corresponding perturbation $\eta = \phi - \Phi^*$ then decays like Φ^* (2.19), because the steepness of $\phi(x,t)$ remains larger than that of Φ^* at any finite time t, cf. Eq. (2.46). As a result, η is just outside the Hilbert space in the generic case of $\alpha \neq 0$ (2.15), just like the zero mode (2.33). The Hilbert space has a continuous spectrum for all decay rates $\sigma > 0$, and there are no growing perturbations with $\sigma < 0$. The perturbation η can be written as a multiple of the zero mode η_0 plus a remainder inside the Hilbert space. From this we might be tempted to argue, that the perturbation will decay, and that we only can not tell how quickly — probably non-exponential, because the spectrum is gapless. However, in contrast to Cases I – III, there is no way to get rid of the zero mode, because no matter at which position ξ_0 one places the subtracted $\Phi^*(\xi - \xi_0)$, Φ^* will always dominate the large ξ behavior, and therefore the coefficient of the zero mode in the decomposition of the perturbation will always be non-vanishing. A convergence argument based on simply neglecting the contribution from the zero mode is bound to be wrong: In the very same way we could argue, that a steep initial condition converges to Φ_v with just any $v \geq v^*$. Strictly speaking, the linear stability analysis does not even allow us to conclude, that sufficiently steep initial conditions approach Φ^* at all. We only can reason, that there is no steeper attractor than Φ^*, and that one therefore expects that the pulled front solution Φ^* is selected from steep initial conditions. The different analytical tools that we will develop in Section II E to analyze the convergence behavior, will confirm this.

E. The dynamics of the leading edge of a front

In this Section, we reconsider the dynamics in the leading edge in more detail, first to demonstrate the conservation of steepness expressed by (2.44), second to clarify the dynamics that ensues from flat initial conditions, and third to lay the basis for the quantitative analysis of Case IV in Section III.

1. Equation linearized about $\phi = 0$

When we analyze the leading edge region of the front, where $|\phi| \ll 1$, we to lowest order can neglect $o(\phi^2)$ in (2.9) and analyze

$$\partial_t \phi = \partial_x^2 \phi + \phi \ . \tag{2.52}$$

We first explore the predictions of this equation, before exploring the corrections due to the nonlinearity f in Section II E 2.

(2.52) is a linear equation, so the superposition of solutions again is a solution. A generic solution is, e.g., an exponential $e^{-\lambda x}$. It will conserve shape and propagate with velocity $v(\lambda) = \lambda + 1/\lambda$ (2.47):

$$\phi(x,t) \sim e^{-\lambda\,[x - v(\lambda)t]} \ . \tag{2.53}$$

The minimum of $v(\lambda)$ is given by $v^* = v(\lambda^* = 1) = 2$.

Consider now a superposition of two exponentials $c_1 \ e^{-\lambda_1 x} + c_2 \ e^{-\lambda_2 x}$. Without loss of generality, we can assume that the maximum velocity $v_{max} = \max[v(\lambda_1), v(\lambda_2)] = v(\lambda_1)$. In the coordinate system $\xi_1 = x - v(\lambda_1)t$ the temporal evolution then becomes

$$\phi(x,t) = c_1 \ e^{-\lambda_1 \xi_1} + c_2 \ e^{-\lambda_2 \xi_1} \ e^{-\sigma t} \ , \tag{2.54}$$

$$\sigma = \lambda_2 \Big(v(\lambda_1) - v(\lambda_2) \Big) > 0 \ . \tag{2.55}$$

Clearly, the contribution of λ_2 decays on the time scale $1/\sigma$, and so for large times $\gg 1/\sigma$, the velocity of a point where $\phi = const. > 0$ will approach $v(\lambda_1)$ and the profile will converge to $e^{-\lambda_1 \xi_1}$ (see [78] for a similar type of analysis). The steepness of the leading edge at $\xi \to \infty$, on the other hand, will be given by $\lambda_{min} = \min[\lambda_1, \lambda_2]$ for all times $t < \infty$.

This simple example already backs up much of our discussion of Cases II and III in Section II D:
1) The limits $\xi \to \infty$ and $t \to \infty$ do not commute.
2) The steepness $\lambda = \min_i[\lambda_i]$ is a conserved quantity at $x \to \infty$ and $t < \infty$.
3) The velocity of a constant amplitude $\phi = const. > 0$ will be governed by the quickest mode present $v = \max_i[v(\lambda_i)]$ at large times $t \gg 1$.

Let us now analyze initial conditions steeper than any exponential. Quite generally, an initial condition $\phi(x,0)$ evolves under (2.52) as[4]

[4]Eliminate the linear growth term by the transformation $\phi = e^t \bar{\phi}$, solve the diffusion equation $\partial_t \bar{\phi} = \partial_x^2 \bar{\phi}$, and transform back.

$$\phi(x,t) = \int_{-\infty}^{\infty} dy\ \phi(y,0)\ \frac{e^{-\left[(x-y)^2-4t^2\right]/(4t)}}{\sqrt{4\pi\ t}}\ . \quad (2.56)$$

Assume for simplicity, that the initial condition $\phi(y,0)$ is strongly peaked about $y=0$, so that for large times, we can neglect the spatial extent of the region where $\phi(y,0) \neq 0$ initially. Upon introducing the coordinate $\xi = x \mp 2t$ moving either to the left or to the right, we get

$$\phi(x,t) \propto \frac{e^{\mp\xi-\xi^2/(4t)}}{\sqrt{t}} \quad \text{for } t \gg 1\ . \quad (2.57)$$

This general expression leads to three important observations:
1) The steepness of the leading edge characterized by $\lambda = \infty$ at $\xi \to \infty$ indeed is conserved for all finite times $t < \infty$.
2) At finite amplitudes $\phi = const. > 0$ and large times t, the steepness of the front propagating towards $\xi \to \infty$ approaches $\lambda^* = 1$ and the velocity approaches $v^* = 2$.
3) Eq. (2.57) furthermore implies, that a steep initial condition like $\phi(y,0)$ approaches the asymptotic velocity v^* as

$$v(t)_{lin} = v^* + \dot{\xi}_h = 2 - \frac{1}{2t} + O\left(\frac{1}{t^{3/2}}\right)\ , \quad (2.58)$$

where we defined the position $\xi_h(t)$ of the amplitude h in the comoving frame $\xi = x - 2t$ as $\phi(\xi_h(t),t) = h$.

This algebraic convergence is consistent with the gapless spectrum of linear perturbations, and as such it identifies the missing part in the discussion of Case IV in Section II D. However, Bramson's work [77] shows, that the qualitative prediction of convergence as $1/t$ is right, but the coefficient of $1/t$ is wrong. In fact, the mathematical literature [52] has established (2.58) as an upper bound for the velocity of a pulled front in a nonlinear diffusion equation. The algebraic convergence clearly comes from the $1/\sqrt{t}$ prefactor characteristic of the fundamental Gaussian solution of the diffusion equation — this qualitative mechanism will be found to be right in Section III.

We finish our discussion of solutions of the linearized equation (2.52) with another example, that we find illustrative. After the discussion of the solution (2.53) one might be worried about initial conditions with $\lambda \gg 1$. Such an initial condition is steep according to our definition, so it should approach the velocity v^*. But according to (2.53), it approaches the larger velocity $v(\lambda)$. However, even in the framework of the linearized equation, this paradox can be resolved: An initial condition $e^{-\lambda x}$ on the whole real axis is, of course, unphysical, and we in fact only want this behavior at $x \gg 1$, where ϕ is small. Let us therefore truncate the exponential for small x by writing, e.g., $\phi(x,0) = \theta(x)\ e^{-\lambda x}$, with θ the step function. Insertion into (2.56) yields the evolution

$$\phi(x,t) = e^{-\lambda[x-v(\lambda)t]}\ \frac{1+\mathrm{erf}\ \frac{x-2\lambda t}{\sqrt{4t}}}{2}\ , \quad (2.59)$$

where $\mathrm{erf}\ x = 2\pi^{-1/2}\int_0^x dt\ e^{-t^2}$ is the errorfunction. For $t \gg 1$, the crossover region where $x \approx 2\lambda t$ separates two different asymptotic types of behavior:

$$\phi(x,t) \approx \begin{cases} e^{-\lambda[x-v(\lambda)t]} & \text{for } x \gg 2\lambda t \\ \frac{e^{-(x-2t)-(x-2t)^2/4t}}{\sqrt{4\pi t}\ \lambda(1-x/(2\lambda t))} & \text{for } x \ll 2\lambda t \end{cases} \quad (2.60)$$

In the region of $x \gg 2\lambda t$, we find our previous solution (2.53) with conserved leading edge steepness and velocity $v(\lambda)$, while in the region of $x \ll 2\lambda t$, we essentially recover (2.57), with $\xi = x - 2t$.

Considering the three different velocities — $v(\lambda)$ for the leading edge region, $v^* = 2$ for the "Gaussian" region behind, and 2λ for the crossover region between the two asymptotes — the distinction between flat and steep initial conditions now comes about quite naturally:
a) For flat initial conditions, we have $\lambda < 1$, and an ordening of velocities as $2\lambda < v^* < v(\lambda)$. The crossover region then moves slower than both asymptotic regions, so for large times the region of finite ϕ will be dominated by $e^{-\lambda[x-v(\lambda)t]}$.
b) For steep initial conditions, we have $\lambda > 1$, and the velocities order as $v^* < v(\lambda) < 2\lambda$. The crossover region then will move quicker than both asymptotic regions, and the region of finite ϕ will be dominated by $e^{-\xi-\xi^2/4t}/\sqrt{t}$, where $\xi = x - 2t$.

We finally note that the above results can also be reinterpreted in terms of the intuitive picture advocated in [63,65]: The group velocity $v_{gr}(\lambda) = dv(\lambda)/d\lambda$ of a near exponential profile in the leading edge is, according to (2.47), negative for $\lambda < 1$ and positive for $\lambda > 1$. In this way of thinking, the region with steepness λ in the case considered above expands when $\lambda < 1$ since the crossover region moves back in the comoving frame [case (*a*)], and it moves out of sight towards $\xi \to \infty$ for $\lambda > 1$ [case (*b*)], since the crossover region moves faster than the local comoving frame.

2. Leading edge representation of the full equation

Just as the linear stability analysis of the front was insufficient to cover the full dynamical behavior of the nonlinear diffusion equation (2.1), and in particular the dynamics of the leading edge, so is the linearized equation (2.52). In Section III we will see, that only through joining these complementary approaches, we can gain a quantitative understanding of the convergence of steep initial conditions towards a pulled front Φ^*, the Case IV.

The shortcomings of the linearized equation (2.52) become quite clear by confronting it with what we will call the leading edge representation of the full equation (2.1):

$$\partial_t \psi = \partial_\xi^2 \psi + \bar{f}(\psi,\xi)\ , \quad (2.61)$$

where we transformed with

$$\psi = \phi \, e^{\lambda^* \xi} \quad , \quad \xi = x - v^* t \; . \tag{2.62}$$

The parameters are $\lambda^* = v^*/2 = \sqrt{f'(0)}$. This transformation eliminates the terms of order ψ and $\partial_\xi \psi$ from the linear part of the equation. The nonlinearity is

$$\begin{aligned} \bar{f}(\psi, \xi) &= e^{\lambda^* \xi} \, \left(f\left(\psi \, e^{-\lambda^* \xi} \right) - f(0) - f'(0) \, \psi \, e^{-\lambda^* \xi} \right) \\ &= O\left(\psi^2 \, e^{-\lambda^* \xi} \right) \; . \end{aligned} \tag{2.63}$$

This transformation is quite comparable to the transformation of a linear perturbation η into the Schrödinger picture as in (2.25), (2.26). However, we here transform the full nonlinear equation, and not only the linearization about some asymptotic solution.

For, e.g., $f(\phi) = \phi - \phi^3$ we have $\bar{f} = -\psi^3 \, e^{-2\xi}$. When we neglect $\bar{f}$ in (2.61), the equation is equivalent to the linearization about $\phi = 0$ (2.52). The linearization is correct for $\xi \gg 1$, but the presence of the crossover towards a different behavior for smaller ξ has important consequences for the solutions of the full nonlinear diffusion equation.

Let us illustrate this on the fact, that for the leading edge of a pulled front $\Phi^* \sim (\alpha \xi + \beta) \, e^{-\xi}$ (2.15), we generically find $\alpha \neq 0$ and accordingly the leading edge behavior (2.19). This leading edge behavior will play a central role in Section III. In Section II B we derived $\alpha \neq 0$ from the uniqueness of the trajectory in phase space, i.e., from the construction of the whole front from $\phi = 0$ up to $\phi = 1$. We now will give a different argument for $\alpha \neq 0$ from the analysis of (2.61), that does not rely on constructing the whole solution up to $\phi = 1$.

The front Φ^* propagates uniformly with velocity $v^* = 2$, so in the frame $\xi = x - 2t$ it is stationary. $\Psi^* = \Phi^* e^{\xi}$ then solves

$$\partial_\xi^2 \Psi^* + \bar{f}(\Psi^*, \xi) = 0 \; . \tag{2.64}$$

The boundary conditions (2.12) for Φ^* become for Ψ^*:

$$\Psi^*(\xi) \sim \begin{cases} \alpha \xi + \beta & \text{for } \xi \to \infty \\ 0 & \text{for } \xi \to -\infty \end{cases} \tag{2.65}$$

The solution $\Psi^* = \alpha \xi + \beta$ for $\xi \to \infty$ can directly be derived from (2.64) and the condition, that Φ^* vanishes at $\xi \to \infty$. Now integrate (2.64) over the real ξ axis, and find

$$\alpha = - \int_{-\infty}^{\infty} d\xi \; \bar{f} \left(\Psi^*, \xi \right) \; . \tag{2.66}$$

The integral on the right hand side is well-defined, since $\bar{f}$ vanishes exponentially, both for $\xi \to -\infty$ and for $\xi \to \infty$. Clearly, a nonlinearity $\bar{f} \neq 0$ generically implies $\alpha \neq 0$ and hence the leading edge behavior (2.19) for a pulled Φ^* front. Only for particular nonlinearities f, we occasionally find $\alpha = 0$ (see (3.67) and Appendix C). Having $\alpha = 0$ is obviously only possible if $\bar{f}$ has terms of opposite sign, so that its spatial average vanishes. For the nonlinearity of form $f = \phi - \phi^k$ with $k > 1$ (1.2), we find $\alpha \neq 0$ always, and in this case the term $\bar{f}$ acts like a localized sink term in the diffusion equation (2.64) for ψ. This interpretation is especially useful for the discussion of the non-uniformly translating fronts [74,76].

F. Summary of selection and relaxation mechanism; "Marginal stability"; interior and edge dominated dynamics

With the analysis and discussion in this Section, we have attempted to bring out the connection between the stability properties of the uniformly translating solutions and the selection mechanism. In addition, we emphasized the role that the conservation of steepness plays in this. The main results from our discussion are summarized in Table III.

Our analysis confirms the idea that the selected front — the one which emerges under the dynamics starting from sufficiently steep initial conditions — is the steepest front which is not unstable. When the front solutions Φ_v are viewed as a function of the steepness λ, (2.6) there is always a change in stability at the selected front ($v^\dagger$ in the pushed regime, v^* in the pulled regime) so the selected front is also *marginally stable*. This is the reason that the selection mechanism was refered to as the marginal stability selection mechanism in [61,63,65].

With our present discussion we have put more emphasis than in earlier formulations on the central role of the steepness and its conservation, and we have been much more precise and detailed about the stability properties of the front solutions. This discussion also leads us to distinguish between *interior dominated dynamics* and *leading edge dominated dynamics*: The relaxation of pushed fronts is typically dominated by modes with such a large weight in the interior front region that they are localized in the front interior region in the leading edge representation ψ. The relaxation of pulled fronts, on the other hand, is dominated by the dynamics in the leading edge — the relevant stability modes are extended in the leading edge representation. Note that the dynamics associated with fronts emerging from "*flat*" initial conditions is always *leading edge dominated*, but we reserve the terms *pushed* and *pulled* for the front selection associated with steep initial conditions, as the selected front speeds $v^\dagger$ and v^* are defined intrinsically by the partial differential equation under study.

The "marginal stability" viewpoint also has an important shortcoming, however. In line with the fact that the rate of convergence to the pulled velocity is difficult to understand in terms of the linear stability spectrum, it does not give much insight into the dynamics that actually leads to the selection of v^*. The leading edge dominated dynamics that underlies the pulling mechanism is actually much better understood by the analysis of Section III, which builds rather on exploiting the leading edge representation than on stability considerations of the asymptotic profile.

INITIAL CONDITION $\phi(x,0) \sim e^{-\lambda_{init} x}$ as $x \to \infty$	*NONLINEARITY* $f(\phi)$ metastable ($f'(0) < 0$): $v_{sel} = v^\dagger > 0$	unstable ($f'(0) > 0$), *pushed* regime: $v_{sel} = v^\dagger > v^*$ $v^* = 2\sqrt{f'(0)} > 0$	unstable ($f'(0) > 0$), *pulled* regime: $v_{sel} = v^*$ $v^* = 2\sqrt{f'(0)} > 0$
steep: $\lambda_{init} > \lambda_0(v_{sel})$ (including $\lambda = \infty$)	Case I: pushed dynamics, $\lambda \longrightarrow \lambda_+(v^\dagger)$ $v(t) = v^\dagger + O(e^{-\sigma t})$	Case I: pushed dynamics, $\lambda \longrightarrow \lambda_+(v^\dagger)$ $v(t) = v^\dagger + O(e^{-\sigma t})$	Case IV: pulled dynamics, $\lambda \longrightarrow \lambda^*$ $v(t) = v^* + O(1/t)$
steep: $\lambda_-(v_{sel}) < \lambda_{init} < \lambda_0(v_{sel})$	Case II: pushed dynamics, $\lambda \longrightarrow \lambda_+(v^\dagger)$ $v \longrightarrow v^\dagger$ generically: $v(t) = v^\dagger + O(e^{-\sigma t})$	Case II: pushed dynamics, $\lambda \longrightarrow \lambda_+(v^\dagger)$ $v \longrightarrow v^\dagger$ generically: $v(t) = v^\dagger + O(e^{-\sigma t})$	not applicable, since $\lambda_\pm(v^*) = \lambda_0(v^*) = \lambda^*$
flat: $0 < \lambda_{init} < \lambda_-(v_{sel})$	not applicable, since $\lambda_-(v^\dagger) < 0$	Case III: leading edge dominated dynamics, $\lambda \longrightarrow \lambda < \lambda_-(v^\dagger)$ $v \longrightarrow v(\lambda) > v^\dagger$ generically: $v(t) = v(\lambda) + O(e^{-\sigma t})$	Case III: leading edge dominated dynamics, $\lambda \longrightarrow \lambda < \lambda^*$ $v \longrightarrow v(\lambda) > v^*$ generically: $v(t) = v(\lambda) + O(e^{-\sigma t})$

Table III: Table of initial conditions and nonlinearities, resulting in relaxation cases I – IV from Section II D. Fronts at all times t are characterized by their steepness λ (2.6) in the leading edge, and an arrow $\longrightarrow$ indicates the evaluation of the quantity for $t \to \infty$. The nonlinearity only enters through the existence of a strongly heteroclinic orbit $\Phi_v(x - vt)$ with $v_{sel} = v^\dagger > v^*$ (see Section II B) or its non-existence (then $v_{sel} = v^*$). v_{sel} determines $\lambda_{\pm,0}(v_{sel})$ as in (2.16), which in turn classifies the initial conditions. Pushed or pulled dynamics are special cases of interior or leading edge dominated dynamics for steep initial conditions. Cases I – III are treated in Section II with stability analysis methods and generically show exponential relaxation. Case IV is not amenable to stability analysis methods. It shows algebraic relaxation and is treated from Section III on.

III. UNIVERSAL PULLED CONVERGENCE OF STEEP INITIAL CONDITIONS IN THE NONLINEAR DIFFUSION EQUATION

In the previous Section, we successfully analyzed the basins of attraction of the asymptotic fronts in the space of initial conditions, and we calculated the rate of convergence of the initial conditions towards the attractors in Cases I, II, and III. For Case IV of sufficiently steep initial conditions ($\phi(x, t = 0) < e^{-\lambda^* x}$ as $x \to \infty$) evolving under an equation of motion with an f such that $v_c = v^*$, we have seen, however, that neither the linear stability analysis nor the leading edge representation alone are able to give us the convergence rate of such pulled fronts. In fact, Section II does not even contain a precise argument, that such an initial condition does converge towards the solution $\Phi^* = \phi(x - v^* t)$ with asymptotic velocity v^* at all.

In the present Section, we will combine our understanding of the dynamics of the leading edge and of the interior of a front into one consistent analytical frame, that allows us to deal with Case IV of steep initial conditions converging to a pulled front. The different dynamical regions of such a front are sketched in Fig. 2. We match an expansion in the interior, that resembles features of the linear stability analysis, to an expansion of the leading edge. Both expansions are asymptotic expansions in $1/\sqrt{t}$. This approach not only shows the convergence of steep initial conditions towards a pulled front with velocity v^*, but it even allows us to derive the ensuing power law convergence towards Φ^*. This convergence is universal in leading and subleading order, and we calculate all universal convergence terms analytically. For clarity, we present the detailed calculation for the nonlinear diffusion equation in this Section first, and then discuss the generalization — the result of which was summarized in Section I C — in Section V.

A. Observations which motivate our approach

1. *Asymptotic steepness of leading edge determines rate of convergence*

Our calculation of the spreading of the leading edge under the linearized equation in Section II E gave qualitatively the right results, but failed to reproduce the quantitative results for the nonlinear equation: Inserting sufficiently steep initial conditions (2.7) into the *linearized* equation (2.9), we found that the asymptotic shape (2.57) approaches $e^{-\xi}$ times a Gaussian for $t \to \infty$ and $\xi \gg 1$ and that this implies for the asymptotic convergence that $v(t)_{lin} = 2 - 1/(2t) + \dots$ (2.58). For the *nonlinear* equation, we know, that the asymptotic front profile Φ^* behaves as $\Phi^* \sim \xi\, e^{-\xi}$ for $\xi \gg 1$ (2.19) and Bramson has derived with probabilistic methods, that $v(t) = 2 - 3/(2t) + \dots$ independent of the height at which the velocity is measured [77]. Thus the actual front is slightly flatter for $t \to \infty$, and convergence is slower than in the linearized equation. We will argue below, that the shape Φ^* in the leading edge and the quantitative rate of convergence are intimately related. It is intuitively quite reasonable, that a leading edge pulling the interior part of the front along has a flatter shape Φ^* which, of course, needs to be consistent with its *o.d.e.* (2.11), so it has $\alpha \neq 0$ in (2.15). In fact, this idea can be made mathematically sound at least for nonlinearities, which obey (2.10), as we showed in Section II E. This argument can be generalized to higher order equations [74,75].

How the exact result of Bramson [77] comes out naturally and generally, is brought out quite clearly by rephrasing an argument of [65] as follows (see also [72,85]).

Let us work in the leading edge representation (2.61), (2.62), and let us from here on use the co-moving variable ξ specifically for the frame moving with the pulled velocity $v^* = 2$,

$$\xi = x - v^* t = x - 2t \ . \tag{3.1}$$

The fundamental similarity solution of (2.61) in the region, where the nonlinearity can be neglected, is, of course, the Gaussian

$$\psi_0(\xi, t) = \frac{e^{-\xi^2/(4t)}}{\sqrt{4\pi t}} \ . \tag{3.2}$$

It reproduces our solution (2.57) for ϕ. But also any derivative of the Gaussian $\psi_n = \partial_\xi^n \psi_0$ solves (2.61) for $\xi \gg 1$. The ψ_n/ψ_0 are simply Hermite polynomials [102,103]. In particular, the dipole solution

$$\psi_1(\xi, t) = \partial_\xi \psi_0 \propto \frac{\xi\, e^{-\xi^2/(4t)}}{t^{3/2}} \tag{3.3}$$

also solves the diffusion equation (2.61) for $\xi \gg 1$ and has the proper asymptotics $\Phi\, e^{\xi} \propto \xi$ for $t \to \infty$. Transforming (3.3) back to ϕ, we find

$$\phi(x, t) \propto (x - 2t)\, e^{-[x - 2t + (3/2)\ln t]}\, e^{-(x-2t)^2/(4t)} \ . \tag{3.4}$$

If we now trace the position $2t + X_h(t)$ of the point where ϕ reaches the amplitude h, we find by solving $\phi(2t + X_h, t) = h$ from (3.4) for $X_h(t) \ll \sqrt{4t}$

$$v(t) = 2 + \dot{X}_h = 2 - \frac{3}{2t} + \dots \ , \tag{3.5}$$

in agreement with Bramson's result. This indicates that for large times $t \gg 1$ and far in the leading edge $\xi \gg 1$, the converging front is approximately given by (3.3), if $\alpha \neq 0$ in (2.15). We will see indeed that (3.3) does emerge as the dominant term in a systematic asymptotic expansion in the leading edge region. For reasons explained below, it is, however, more convenient to formulate this expansion in a slightly different frame.

2. Interior follows leading edge: uniform convergence

The above argument shows that the leading $-3/(2t)$ velocity correction is due to the diffusion-type dynamics in the leading edge. Why would the convergence to the asymptotic profile be *uniform*, i.e., be independent of the height h whose position is tracked? The answer to this question is intuitively quite simple. As $\dot{X}_h \simeq -3/(2t)$, $X_h \simeq -3/2 \ln t$. Now, if we compare the position X_{h_1} of a height h_1 in the leading edge ($h_1 \ll 1$) with a position X_{h_2} of a height h_2 in the interior ($h_2 = O(1)$) where the dynamics of ϕ is described by the nonlinear equation, we will have $X_{h_2} = X_{h_1} - W(h_1, h_2)$, where W is the width of the front between these two heights. Now, if W approaches a finite value for long times, we need to have also $X_{h_2} \simeq 3/2 \ln t$ in dominant order as $t \to \infty$, and hence also $\dot{X}_{h_2} = -3/(2t) + \cdots$. But that $W = O(1)$ for large times, is quite evident from the equation of motion (1.1), and our analysis will confirm this expectation. In other words, the leading order velocity correction as $-3/(2t)$ is set by the dynamics of the leading edge, and because of the finite asymptotic width of the front, the convergence is *uniform*, i.e., independent of h.

3. Choose proper frame and subtraction for the interior

The above observations have another important consequence. After the front has evolved for some time, we will find it selfconsistent to assume, that its shape will resemble the asymptotic shape Φ^*. If we want to understand the interior part of the front, it might at first sight seem appropriate to linearize the converging front ϕ about the asymptotic front Φ^*. However, the profile Φ^* propagates uniformly with velocity 2, while as we saw above, the transient profile ϕ propagates with velocity $v^* - 3/(2t)$. Thus, if the interior regions of the ϕ- and the Φ^*-fronts are at about the same part of space at time t_0, their distance will *diverge* as $(3/2)\ln(t/t_0)$ as t grows! This was already illustrated in Fig. 1. Hence, linearization of ϕ about the asymptotic profile Φ^* during the whole time evolution requires to move Φ^* along with the velocity $2 - 3/(2t) + \ldots$ of ϕ and *not* with its proper velocity 2. Our expansion is therefore based on writing ϕ as

$$\phi(\xi, t) = \Phi^*(\xi_X) + \eta(\xi_X, t) \ , \tag{3.6}$$

where

$$\xi_X = \xi - X(t) = x - 2t - X(t) \ . \tag{3.7}$$

With this Ansatz, we anticipate that we need to shift the profile Φ^* an appropriate "collective coordinate" $X(t) \propto \ln t$ of the front, and that with a proper choice of $X(t)$, η becomes a small and decaying perturbation.

4. Choose proper expansions and match leading edge to interior

We will need two different expansions for the leading edge and for the interior, which will have to be matched together. The expansions have to be chosen such that they can be matched in overlapping intervals through resummation of the expansions.

Since we use the coordinate system (3.7) in the interior, we also should use it in the leading edge. The leading $1/t$ contribution from the leading edge suggests to expand the interior in powers of $1/t$ times functions of ξ_X, and we shall see indeed that such a form emerges automatically from the ansatz (3.6). The appropriate variable for $\xi_X \gg \sqrt{t}$ in the leading edge, on the other hand, is the similarity variable of the diffusion equation

$$z = \frac{\xi_X^2}{4t} \ , \tag{3.8}$$

as suggested by (3.2) – (3.4). Expressing ξ_X by z and t introduces a dependence on $1/\sqrt{t}$. We find, that it is actually consistent to expand the interior in powers of $1/\sqrt{t}$ (instead of $1/t$) times functions of ξ_X, and the leading edge also in powers of $1/\sqrt{t}$ times functions of z.

The structure of these expansions is essentially our only input. Given this structure, the leading and subleading order universal terms of the expansions then are uniquely determined.

B. Expansion in the interior region

We first analyze the interior part of the front, where ϕ varies from close to 0 to close to 1. We work in the comoving frame $\xi_X = x - v^* t - X(t)$ of (3.7), where X will have to be determined. We expand ϕ about $\Phi^*(\xi_X)$ (3.6). Because of translation invariance, we have the freedom to fix the position of Φ^* and the zero of the coordinate system by imposing

$$\phi(0,t) = \frac{1}{2} \ \text{ and } \ \Phi^*(0) = \frac{1}{2} \ \Rightarrow \ \eta(0,t) = 0 \ . \tag{3.9}$$

Furthermore Φ^* is defined as $\lim_{\xi \to -\infty} \Phi^*(\xi_X) = 1$. We assume, that also ϕ approaches 1 for $\xi_X \to -\infty$. This results in the second condition on η

$$\lim_{\xi_X \to -\infty} \eta(\xi_X, t) = 0 \ . \tag{3.10}$$

---

[5] Throughout this paper, we shall suppress the index X on partial derivatives with respect to ξ_X for notational convenience. Since $\partial_{\xi_X}|_t = \partial_\xi|_t$, this does not lead to any ambiguities.

We insert ϕ into the equation of motion (1.1), transform x to the coordinate ξ (3.7) and find for η the equation[5]

$$\partial_t \eta = \partial_\xi^2 \eta + v^* \partial_\xi \eta + \dot{X} \partial_\xi \Phi^* + f(\Phi^* + \eta) - f(\Phi^*) \ . \tag{3.11}$$

If η is small enough, because time has evolved sufficiently long, $f(\Phi^* + \eta)$ can be expanded in η and we find

$$\partial_t \eta = \mathcal{L}^* \eta + \dot{X} \ \partial_\xi \Phi^* + \dot{X} \ \partial_\xi \eta + \frac{f''(\Phi^*)}{2} \ \eta^2 + O(\eta^3) \ , \tag{3.12}$$

where

$$\mathcal{L}^* = \partial_\xi^2 + v^* \partial_\xi + f'(\Phi^*(\xi_X)) \tag{3.13}$$

is the linearization operator (2.25) for $v = v^*$.

In Sections II E 1 and III A 1 we have argued, that one expects $\dot{X}(t) = O(t^{-1})$. Asymptotic balancing in (3.12) then requires, that the leading order term of η is of the same order $\eta = O(t^{-1})$. We therefore try to expand as $\eta = \eta_1(\xi_X)/t + \ldots$. We have argued, that connecting the interior expansion to the leading edge expansion requires an ordening in powers of $1/\sqrt{t}$. So we make the ansatz

$$\dot{X} = \frac{c_1}{t} + \frac{c_{3/2}}{t^{3/2}} + \frac{c_2}{t^2} + \ldots \ , \tag{3.14}$$

$$\eta(\xi_X, t) = \frac{\eta_1(\xi_X)}{t} + \frac{\eta_{3/2}(\xi_X)}{t^{3/2}} + \ldots \ . \tag{3.15}$$

Substitution of the above expansions into (3.13) and ordering in powers of $1/\sqrt{t}$ yields a hierarchy of *o.d.e.*'s of second order:

$$\mathcal{L}^* \eta_1 = -c_1 \partial_\xi \Phi^* \ , \tag{3.16}$$

$$\mathcal{L}^* \eta_{\frac{3}{2}} = -c_{\frac{3}{2}} \partial_\xi \Phi^* \ , \tag{3.17}$$

$$\mathcal{L}^* \eta_2 = -\eta_1 - c_1 \partial_\xi \eta_1 - c_2 \partial_\xi \Phi^* - f''(\Phi^*) \eta_1^2 / 2 \ , \tag{3.18}$$

$$\mathcal{L}^* \eta_{\frac{5}{2}} = -\tfrac{3}{2} \eta_{\frac{3}{2}} - c_1 \partial_\xi \eta_{\frac{3}{2}} - c_{\frac{3}{2}} \partial_\xi \eta_1 - c_{\frac{5}{2}} \partial_\xi \Phi^* - f''(\Phi^*) \eta_1 \eta_{\frac{3}{2}} \qquad \text{etc., generally:} \tag{3.19}$$

$$\mathcal{L}^* \eta_{\frac{n}{2}} = -\frac{n-2}{2} \ \eta_{\frac{n-2}{2}} - \sum_{m=2}^{n-2} c_{\frac{m}{2}} \partial_\xi \eta_{\frac{n-m}{2}} - c_{\frac{n}{2}} \partial_\xi \Phi^* - \sum_{k=2}^{\infty} \frac{f^{(k)}(\Phi^*)}{k!} \left(\sum_{m_k} \eta_{m_k} \right)^k \Bigg|_{\sum_k m_k = \frac{n}{2}} \ . \tag{3.20}$$

It is important to realize that we do not need to drop nonlinear terms, but that the expansion of $f(\Phi^* + \eta)$ in powers of η is also ordered in powers of $1/\sqrt{t}$. So the higher order terms η^n find their natural place as inhomogeneities in the equations for η_i for $i \geq 2$. The hierarchy of *o.d.e.*'s is such, that the differential equation for η_i contains inhomogeneities, that depend only on η_j with $j < i$. The equations therefore can be solved successively by going up in the hierarchy. Each η_i solves a second order differential equation, and the two constants of integration are fixed by the two conditions (3.9) and (3.10)[6].

Note also, that the time dependent collective coordinate $X(t)$ in $\xi_X = \xi - X(t)$ only enters Eqs. (3.16)-(3.20) in the form of the constants $c_{n/2}$, which at this point are still undetermined, and that the functions $\eta_{n/2}$ obey *o.d.e.*'s.

Let us now compare $\eta = \phi - \Phi^*$ to the variations of the profile shape with velocity v,

$$\delta = \Phi_{v^* + \dot{X}} - \Phi^* = \dot{X} \ \eta_{\rm sh} + \frac{\dot{X}^2}{2} \ \eta_{\rm sh}^{(2)} + \ldots \ , \tag{3.21}$$

where $\eta_{\rm sh} \equiv \delta \Phi_v / \delta v|_{v^*}$ is a "shape mode", which gives the change in the profile under a change in v. By considering variations of v in the *o.d.e.* for the profile Φ_v, we find that $\eta_{\rm sh}$ and $\eta_{\rm sh}^{(2)}$ obey

$$\mathcal{L}^* \eta_{\rm sh} + \partial_\xi \Phi^* = 0 \ , \tag{3.22}$$

$$\mathcal{L}^* \eta_{\rm sh}^{(2)} + 2 \partial_\xi \eta_{\rm sh} + f''(\Phi^*) \ (\eta_{\rm sh})^2 = 0 \ . \tag{3.23}$$

Upon comparing (3.22) – (3.23) with (3.16) – (3.18), we can identify

$$\eta_1 = c_1 \eta_{\rm sh} \ , \tag{3.24}$$

$$\eta_{3/2} = c_{3/2} \eta_{\rm sh} \ , \tag{3.25}$$

$$\eta_2 = c_2 \eta_{\rm sh} + \frac{c_1^2}{2} \eta_{\rm sh}^{(2)} + c_1 \rho \ , \tag{3.26}$$

with ρ a correction term, that solves the equation

$$\mathcal{L}^* \rho + \eta_{\rm sh} = 0 \ . \tag{3.27}$$

In these differential equations, $\eta_{\rm sh}$, $\eta_{\rm sh}^{(2)}$ and ρ obey the conditions

$$\eta_{\rm sh}(0) = 0 \ , \quad \eta_{\rm sh}^{(2)}(0) = 0 \ , \quad \rho(0) = 0 \ , \tag{3.28}$$

$$\eta_{\rm sh}(-\infty) = 0 \ , \ \eta_{\rm sh}^{(2)}(-\infty) = 0 \ , \ \rho(-\infty) = 0 \ , \tag{3.29}$$

cf. (3.9) and (3.10).

ρ_v is the first nonvanishing term that indicates the difference between the transient profile $\phi(x,t)$ and the uniformly translating front solution with the instantaneous velocity

$$v(t) = v^* + \dot{X} \ . \tag{3.30}$$

as resummation of ϕ yields

[6] Had we introduced an $\eta_{1/2}$, we had found the equation $\mathcal{L}^* \eta_{1/2} = 0$ with the unique solution $\eta_{1/2} = 0$.

$$\phi(\xi_X,t) = \Phi_{v(t)}(\xi_X) + \frac{c_1}{t^2}\,\rho(\xi_X) + \qquad (3.31)$$
$$+ \frac{t_0}{t^2}\,\eta_{\rm sh}(\xi_X) + O\left(\frac{1}{t^{5/2}}\right)\ .$$

This equation confirms that up to order $1/t^2$, the profile shape is given by the solution $\Phi_{v(t)}$ of the *o.d.e.* with the instantaneous velocity $v(t)$.

Now some remarks on these results are in place:

1) We see, that the dynamics in the front interior is slaved to the evolution of $v(t)$ imposed by the leading edge, as we anticipated in Section III A 3.

2) Based on numerical data, Powell et al. [67] have conjectured, that ϕ converges along the trajectory in function space formed by the Φ_v's with $v < v^*$. We here have derived this result analytically, and identify the velocity v of the transients Φ_v with the actual instantaneous velocity $v = v^* + \dot{X}$ of the front. We find a non-vanishing correction of order $1/t^2$ to $\phi \approx \Phi_{v^*+\dot{X}}$.

3) The transients Φ_v have always $v < v^*$ at late times, since we will find that $c_1 = -3/2$, in accord with the discussion of Section III A 1. Note that as discussed in Section II B, such Φ_v are positive from $\xi_X \to -\infty$ up to a finite value of ξ_X only (How they continue for larger ξ_X, where they go negative, depends on the definition of $f(\phi)$ for negative arguments). For the transient (3.31) we need only the positive part of Φ_v. The transient (3.31) crosses over to a different functional form, before Φ_v goes negative.

4) There is a non-universal contribution of order $1/t^2$ to (3.31). It is non-universal, because it depends on initial conditions: The structure of our expansion (3.14), (3.15) is an asymptotic expansion about $t \to \infty$, that does not fix $t = 0$. We thus can expand in $1/(t-t_0) = 1/t + t_0/t^2 + O(1/t^3)$ just as well as in $1/t$. This allows us to add an arbitrary multiple of $\eta_{\rm sh}/t^2$ to ϕ in Eq. (3.31). The order $1/t^2$ term in (3.31) is thus always non-zero, because ρ in (3.32) is non-vanishing, but its precise value will depend on initial conditions.

5) The expansion is an asymptotic expansion [105]. Thus, when we will have determined the coefficients c_1 and $c_{3/2}$ in (3.14) later, these are the *exact* prefactors if we expand the velocity and shape in inverse powers of t in the limit $t \to \infty$, but the expansion will not have a finite radius of convergence in $1/\sqrt{t}$.

C. Interior shape expanded towards the leading edge

We now will see, that for $\xi_X \geq O(\sqrt{t})$ the structure of our expansion (3.15) breaks down. We then have to resum the terms and use a different expansion[7].

Let us calculate the contributions η_i from (3.16) – (3.20) explicitly in the leading edge region, where $\xi_X \gg 1$ and $\phi, \Phi^* \ll 1$. In this region $\mathcal{L}^*$ (3.13) and Φ^* (2.15) are

$$\mathcal{L}^* = \partial_\xi^2 + 2\partial_\xi + 1 \quad , \quad \Phi^* = (\alpha\xi_X + \beta)\, e^{-\xi_X}\ . \qquad (3.32)$$

Again we transform the exponential away through

$$\mathcal{L}^* = e^{-\xi_X}\,\partial_\xi^2\,e^{\xi_X} \quad , \quad \eta_{\frac{n}{2}} = e^{-\xi_X}\,\psi_{\frac{n}{2}} \quad , \quad \phi = e^{-\xi_X}\,\psi\ . \qquad (3.33)$$

The differential equations determining the $\psi_{\frac{n}{2}}$ are explicitly

$$\begin{aligned}
\partial_\xi^2\psi_1 &= c_1(\alpha\xi_X + \gamma) \quad , \quad \gamma = \beta - \alpha\ , \qquad (3.34)\\
\partial_\xi^2\psi_{\frac{3}{2}} &= c_{\frac{3}{2}}(\alpha\xi_X + \gamma)\ ,\\
\partial_\xi^2\psi_2 &= [-1 + c_1(1-\partial_\xi)]\psi_1 + c_2(\alpha\xi_X + \gamma)\ ,\\
\partial_\xi^2\psi_{\frac{5}{2}} &= [-\tfrac{3}{2} + c_1(1-\partial_\xi)]\psi_{\frac{3}{2}} + c_{\frac{3}{2}}(1-\partial_\xi)\psi_1 +\\
&\qquad + c_{\frac{5}{2}}(\alpha\xi_X + \gamma)\ ,\\
&\qquad \text{etc., generally:}\\
\partial_\xi^2\psi_{\frac{n}{2}} &= [-\tfrac{n-2}{2} + c_1(1-\partial_\xi)]\psi_{\frac{n-2}{2}}\\
&\quad + \sum_{m=3}^{n-2} c_{\frac{m}{2}}(1-\partial_\xi)\psi_{\frac{n-m}{2}} + c_{\frac{n}{2}}(\alpha\xi_X + \gamma)\ ,
\end{aligned}$$

where we have omitted exponentially small corrections of order $e^{-\xi_X}$ in the inhomogeneities on the r.h.s. of the equations. The conditions (3.9) and (3.10) on η do not influence the solution in the leading edge.

The equations (3.34) are easily solved. For $\psi = e^{\xi_X}\phi$ we find in the region $\xi_X \gg 1$

$$\begin{aligned}
\psi = e^{\xi_X}\Phi^* + \sum_{n=2}^{\infty}\frac{\psi_{\frac{n}{2}}}{t^{n/2}} = \qquad (3.35)\\
\alpha\,\xi_X + \beta +\\
+\frac{c_1\alpha\,\xi_X^3}{3!\,t} + \frac{c_1\gamma\,\xi_X^2}{2!\,t} + O\left(\frac{\xi_X}{t}\right)\\
+ \frac{c_{\frac{3}{2}}\alpha\,\xi_X^3}{3!\,t^{3/2}} + O\left(\frac{\xi_X^2}{t^{3/2}}\right)\\
+\frac{c_1(c_1-1)\alpha\,\xi_X^5}{5!\,t^2} + \frac{c_1[(c_1-1)\gamma - c_1\alpha]\,\xi_X^4}{4!\,t^2} + \dots\\
+ \frac{c_{\frac{3}{2}}(2c_1 - \frac{3}{2})\alpha\,\xi_X^5}{5!\,t^{5/2}} + \dots\\
+\frac{c_1(c_1-1)(c_1-2)\alpha\,\xi_X^7}{7!\,t^3} + \dots
\end{aligned}$$

[7] Actually, the interior expansion also breaks down for $\xi_X \to -\infty$. There too, a different expansion can be used, and this expansion can be matched to the one we introduced for the interior region. We will not discuss this further here, as it is of no further consequence.

Obviously, for $\xi_X \geq \sqrt{t}$, the expansion is not properly ordered in powers of $1/\sqrt{t}$ anymore, since, e.g., ξ_X^3/t eventually will become larger than ξ_X. A quick inspection of (3.35) shows, that we can continue to work in an $1/\sqrt{t}$ expansion, if we use the variable $z = \frac{\xi_X^2}{4t}$ (3.8) instead of ξ_X. (3.35) can be identified with

$$\psi = \sqrt{t}\,\alpha\left((4z)^{1/2} + \frac{c_1(4z)^{3/2}}{3!} + \frac{c_1(c_1-1)(4z)^{5/2}}{5!} + \frac{c_1(c_1-1)(c_1-2)(4z)^{7/2}}{7!} + \cdots\right) + t^0\left(\beta + \frac{c_1(\beta-\alpha)(4z)}{2!} + \frac{c_{\frac{3}{2}}\alpha(4z)^{3/2}}{3!} + O(z^2)\right) + O(1/\sqrt{t}) \tag{3.36}$$

Already this expansion hints at the fact that this resummed expansion crosses over to a different expansion for $\xi_X, t \gg 1$, $z = \xi_X^2/4t = O(1)$, and that the requirement that this latter expansion is well behaved for large z, fixes the coefficients c_1, etc. To see this, note that if we take $c_1 = -3/2$, then the first combination of terms reduces to $\alpha\sqrt{4zt}\; e^{-z} = \xi_X e^{-\xi_X^2/4t}$, which is, in dominant order, the behavior already anticipated in Section III A 1.

Instead of resumming the interior expansion explicitly, it turns out to be much more transparent to write an expansion directly in terms of powers of $1/\sqrt{t}$ and the similarity variable of the diffusion equation, z. This approach, which amounts to a matching procedure, is the subject of the next subsection.

D. Analysis of the leading edge

We now take up the analysis of the leading edge region in the case that the initial conditions are sufficiently steep, so that, for $\psi = \phi\, e^{\xi_X}$

$$\lim_{\xi_X \to \infty} \psi(\xi_X, t) = 0\ . \tag{3.37}$$

Note that according to the discussion of Section II E, this condition holds at any finite time, if it is obeyed initially at $t = 0$.

We have already argued in Sections II E and III A 1 that the asymptotic profile of the leading edge might be expected to be somewhat like a Gaussian in ξ_X and t times a Hermite polynomial. Also the resummation of the interior front solution suggests such a form for large ξ_X. We now investigate this expansion more systematically, and will show that it actually takes the form of a Gaussian times a generalization of Hermite polynomials, namely confluent hypergeometric functions [103].

In passing, we stress that only to lowest order the arguments from III A 1 can be compared directly to our calculation here, because we now work with the coordinate $z = (x - 2t - X(t))^2/(4t)$, while we presented our earlier intuitive arguments in the coordinate $z^* = (x-2t)^2/(4t)$. Of course, one can also set up a systematic expansion in the latter coordinate z^*, but this requires the introduction of logarithmic terms for a proper matching to the interior part of the front. Working throughout in the shifted frames $\xi_X = x - 2t - X(t)$ or z, resp., avoids this altogether.

In the coordinates ξ_X and t, the equation of motion for ψ in the leading edge region is (Recall that the earlier leading edge representation in (2.61) was in the frame $\xi = x - 2t$)

$$\partial_t\psi = \partial_\xi^2\psi + \dot{X}(\partial_\xi - 1)\psi + o(e^{-\xi_X})\ . \tag{3.38}$$

The differential operators transform under change of coordinates to $z = \xi_X^2/(4t)$ and t as

$$\partial_t\big|_\xi = \partial_t\big|_z - \frac{z}{t}\partial_z\big|_t\ ,\ \partial_\xi\big|_t = \sqrt{\frac{z}{t}}\,\partial_z\big|_t\ . \tag{3.39}$$

Motivated by the form (2.57) and the discussion of Section III A 1, we extract the Gaussian $e^{-\xi_X^2/(4t)} = e^{-z}$ from ψ:

$$\psi(\xi, t) = e^{-z}\, G(z, t)\quad ,\quad z = \frac{\xi_X^2}{4t}\ . \tag{3.40}$$

This extraction also allows us to make contact later with functions tabulated in [103]. The dynamical equation (3.38) is equivalent to the equation for G:

$$\left[z\partial_z^2 + \left(\frac{1}{2} - z\right)\partial_z - \frac{1}{2} - t\partial_t - c_1\right]\, G = \\ = \left[(\dot{X}t - c_1) + \dot{X}\sqrt{t}\sqrt{z}(1 - \partial_z)\right]\, G\ . \tag{3.41}$$

The equation is organized such, that the differential operators of order t^0 are on the l.h.s. of the equation, while the r.h.s. has the operators of order $t^{-1/2}$ and smaller.

In analogy to our earlier expansion (3.15), we now make an ansatz for G in powers of $1/\sqrt{t}$ times functions of z. A glimpse at the form of the interior shape expanded towards the leading edge (3.36) tells us, that the expansion should start with the order $\sqrt{t}$. We write

$$G(z, t) = \sqrt{t}\, g_{\frac{-1}{2}}(z) + g_0(z) + \frac{g_{\frac{1}{2}}(z)}{\sqrt{t}} + \dots\ . \tag{3.42}$$

Insertion of this ansatz into (3.41) again results in a hierarchy of ordinary differential equations, that can be solved successively:

$$\left[z\partial_z^2 + \left(\frac{1}{2} - z\right)\partial_z - 1 - c_1\right]\, g_{\frac{-1}{2}} = 0\ , \tag{3.43}$$

$$\left[z\partial_z^2 + \left(\frac{1}{2} - z\right)\partial_z - \frac{1}{2} - c_1\right]\, g_0 = \\ = \left[c_{\frac{3}{2}} + c_1\sqrt{z}(1 - \partial_z)\right]\, g_{\frac{-1}{2}}\ , \tag{3.44}$$

$$\left[z\partial_z^2 + \left(\frac{1}{2} - z\right)\partial_z - c_1\right]\ g_{\frac{1}{2}} = \tag{3.45}$$
$$= \left[c_2 + c_{\frac{3}{2}}\sqrt{z}(1-\partial_z)\right]\ g_{\frac{-1}{2}} + \left[c_{\frac{3}{2}} + c_1\sqrt{z}(1-\partial_z)\right]\ g_0\ ,$$

etc. The general solution of the homogeneous equations with two constants of integration $k_{\frac{n}{2}}$ and $l_{\frac{n}{2}}$ can be found in [103], they are confluent hypergeometric functions. How to find a special solution $g^{sp}_{\frac{n}{2}}$ of the inhomogeneous equation is discussed in general in Appendix D. The approach of the appendix leads to integral expressions for the special solutions, rather than to the series expansions used here. We write the general solution as

$$g_{\frac{n}{2}}(z) = g^{sp}_{\frac{n}{2}}(z) + k_{\frac{n}{2}}\ M\left(c_1 + \frac{1-n}{2}, \frac{1}{2}, z\right) + \ l_{\frac{n}{2}}\ \sqrt{z}\ M\left(c_1 + \frac{2-n}{2}, \frac{3}{2}, z\right)\ , \tag{3.46}$$

where the functions $M(a,b,z)$ can be expressed by the Kummer series [103]

$$M(a,b,z) = 1 + \frac{a\ z}{b} + \frac{a(a+1)\ z^2}{b(b+1)\ 2!} + \ldots + \frac{(a)_n z^n}{(b)_n n!} + \cdots\ ,$$
$$\text{with} \quad (a)_n = \prod_{k=1}^{n}(a+k-1) = \frac{\Gamma(a+n)}{\Gamma(a)}\ . \tag{3.47}$$

Just as in the integration of the interior shape in Section III B, there are two constants of integration to be determined in every solution $g_{\frac{n}{2}}$. In addition, however, the c_i are not just parameters of the equations as in Section III B, but they now have to be determined also. The conditions we use to determine these three constants per equation, are now (3.36) and (3.37) in analogy to the two conditions (3.9) and (3.10) for the $\eta_{\frac{n}{2}}$: (i) The solution $g_{\frac{n}{2}}$ has to agree with the expansion of the interior towards the leading edge (3.36) for small z. Then the coefficients of z^0 and $z^{1/2}$ in (3.36) determine the constants of integration $k_{\frac{n}{2}}$ and $l_{\frac{n}{2}}$. (ii) The transients at any finite time have to be sufficiently steep in the sense that they obey (3.37) at any finite time t. Because of the form the expansions (3.41) and (3.43), we require that each term g in the expansion diverges for large z at most as a power law of z, *not* exponentially as e^z. In addition, they have to stay consistent with the structure of the expansion (3.15) for η. This gives another condition on the constants of integration, that can be obeyed only for a particular choice of $c_{\frac{n+3}{2}}$. With these choices of the constants, the small z expansion of $\psi = e^{-z}G$ from (3.40) and (3.42) becomes identical with the interior shape expanded towards the leading edge (3.36).

We will solve the first two equations (3.43) and (3.44) explicitly, since they determine the universal terms of the velocity correction $\dot{X}$. In particular, the solution for $g_{\frac{-1}{2}}$ (3.43) will connect to our qualitative discussion of the leading $1/t$ velocity convergence term (3.5) in Section III A 1. Eq. (3.44) will give the universal subleading term[8] of order $1/t^{-3/2}$.

Let us now start with the solution of the homogeneous leading order equation (3.43), where $g^{sp}_{\frac{-1}{2}}(z) = 0$. The constants of integration are fixed by (3.36) as $k_{\frac{-1}{2}} = 0$ and $l_{\frac{-1}{2}} = 2\alpha$. Therefore $g_{\frac{-1}{2}}(z)$ is after matching to the interior

$$g_{\frac{-1}{2}}(z) = 2\alpha\ \sqrt{z}\ M\left(c_1 + \frac{3}{2}, \frac{3}{2}, z\right)\ . \tag{3.48}$$

In order to analyze, how c_1 is determined by the matching and the requirement that all transients are steeper for $\xi_X \to \infty$ than the asymptotic profile, we first recall the large z behavior of Kummer functions $M(a,b,z)$ [103]: For b not zero nor a negative integer ($-b \notin \mathcal{N}_0$), each term of the series (3.47) is finite. For a not zero nor a negative integer, the series is infinite. For a zero or a negative integer $a = -n$, the series is finite, since all terms from order z^{n+1} on contain the factor $(a+n) = 0$. For $b = 1/2$ or $3/2$, these finite polynomials are Hermite polynomials. The large z asymptotics for the two cases of a's and for $-b \notin \mathcal{N}_0$ is:

$$M(a,b,z) \overset{z\to\infty}{\sim} \begin{cases} \frac{\Gamma(b)}{\Gamma(a)}\ z^{a-b}\ e^z & \text{for } -a \notin \mathcal{N}_0\ , \\ \frac{(a)_{|a|}\, z^{|a|}}{(b)_{|a|}(|a|)!} & \text{for } -a \in \mathcal{N}_0\ . \end{cases} \tag{3.49}$$

Now insert (3.48) into (3.49) and find for $\xi_X \gg \sqrt{t}$

$$\phi \propto e^{-\xi_X} \begin{cases} \xi_X^{2c_1+1}\ t^{-c_1} & -c_1 - 3/2 \notin \mathcal{N}_0 \\ \xi_X^{-2c_1-2}\ t^{c_1+3/2}\ e^{-\xi_X^2/(4t)} & -c_1 - 3/2 \in \mathcal{N}_0 \end{cases}\ . \tag{3.50}$$

For $c_1 + 3/2$ not zero nor a negative integer, we need $c_1 \le 0$ to make the transient profile steeper than Φ^* at any finite time t. Then the exponent $-c_1$ of t becomes positive and our ordering in powers of $1/\sqrt{t}$ from (3.15) is destroyed. (For $c_1 = 0$, ϕ has the asymptotic profile already and no convergence takes place.) Accordingly, as explained above, for sufficiently steep initial conditions that obey (3.37) for and consistency with (3.15), $c_1 + 3/2$ has to be zero or a negative integer. Possible solutions consistent with (3.37) and (3.15) are

[8] Don't confuse the expansion in $1/\sqrt{t}$ of the velocity in (3.5) or (3.14) with the denominators in (3.2) and (3.3). These powers of $1/\sqrt{t}$ in the ξ^*-representation are absorbed into the $X(t)$ of ξ in the ξ-representation, as is sketched in (3.4).

$$\begin{aligned} c_1 &= \tfrac{-3}{2} \quad , \quad g_{\frac{-1}{2}}(z) = 2\alpha\,\sqrt{z}\ , \\ c_1 &= \tfrac{-5}{2} \quad , \quad g_{\frac{-1}{2}}(z) = 2\alpha\,\sqrt{z}\,\left(1-\tfrac{2z}{3}\right)\ , \\ c_1 &= \tfrac{-7}{2} \quad , \quad g_{\frac{-1}{2}}(z) = 2\alpha\,\sqrt{z}\,\left(1-\tfrac{4z}{3}+\tfrac{4z^2}{15}\right)\ , \end{aligned} \tag{3.51}$$

etc., with the $g_{\frac{-1}{2}}$ given by Hermite polynomials. Now, there are two ways to argue, why generically $c_1 = -3/2$ will be observed, one for non-negative initial conditions and one for more general initial conditions. (*a*) If the initial condition is always non-negative, e.g., because ϕ is a density, the transient may not have nodes, so $c_1 = -3/2$ is the only possible solution. (*b*) Starting from an initial condition with nodes, the general solution will be a superposition of the solutions (3.51). The solution with $c_1 = -3/2$ propagates quickest, so the other contributions will be convected to the back, and $c_1 = -3/2$ will dominate at large times [106]. This argument coincides with the argument from Section II C, that fronts with nodes generically are not attractors for the long time dynamics for the nonlinear diffusion equation (1.1). Furthermore we have checked various initial conditions with nodes numerically and we have found, that either the node gets stuck behind the evolving front or moves away to $\xi \to \infty$ with higher velocity than v^*, leaving in both cases a leading edge of the front behind, that develops with $c_1 = -3/2$. We thus find for initial conditions (3.37) steeper than Φ^* generically

$$c_1 = \frac{-3}{2} \quad , \quad g_{\frac{-1}{2}}(z) = 2\alpha\,\sqrt{z}\ . \tag{3.52}$$

This solution is identical with the order $\sqrt{t}$ of ψe^z with ψ from (3.36). For ϕ we find in the region $\xi_X \gg 1$ linearizable about the unstable state in leading order

$$\phi = \alpha\xi_X\ e^{-\xi_X-\xi_X^2/(4t)}\left(1+O(\xi_X^{-1})+O(t^{-1/2})\right) \tag{3.53}$$

$$\xi_X = x - v^*t + \frac{3}{2}\,\ln t + O(1/\sqrt{t})\ , \tag{3.54}$$

consistent with the arguments from Section III A 1.

Integration of g_0 now gives the subleading universal terms, which are $O(1/\sqrt{t})$ in (3.53) and (3.54). Insertion of (3.52) into (3.44) results in

$$\left[z\partial_z^2 + \left(\frac{1}{2}-z\right)\partial_z + 1\right] g_0 = 2\alpha\left(\frac{3}{4} + c_{\frac{3}{2}}\sqrt{z} - \frac{3}{2}\,z\right)\ . \tag{3.55}$$

We now can follow Appendix D for the general solution of the inhomogeneous equation, or we rather can guess a special solution of the inhomogeneous equation by noting that the function

$$F_N(z) = \sum_{n=N}^{\infty} \frac{(1)_{n-2}\ z^n}{\left(\frac{1}{2}\right)_n\ n!} \tag{3.56}$$

is proportional to a truncated Kummer series $M(-1,\frac{1}{2},z)$ (3.47) and solves

$$\left[z\partial_z^2 + \left(\frac{1}{2}-z\right)\partial_z + 1\right] F_N(z) = \frac{z^{N-1}}{\left(\frac{1}{2}\right)_{N-1}\ (N-1)}\ , \tag{3.57}$$

By further inspection, we find the special solution of the inhomogeneous equation (3.55)

$$g_0^{sp}(z) = 2\alpha\ \left(\frac{3}{4} + 2c_{\frac{3}{2}}\sqrt{z} - \frac{3}{4}\ F_2(z)\right)\ . \tag{3.58}$$

Upon comparing (3.56) to (3.47) and (3.49), one finds

$$g_0^{sp}(z) \overset{z\to\infty}{\sim} -\frac{3}{2}\ \alpha\ \sqrt{\pi}\ z^{-3/2}\ e^z\ . \tag{3.59}$$

The general solution (3.46) of (3.55) is thus

$$\begin{aligned} g_0(z) &= g_0^{sp}(z) + k_0\ (1-2z) + l_0\ \sqrt{z}\ M\left(\frac{-1}{2},\frac{3}{2},z\right) \\ &\overset{z\ll 1}{=} \left(\frac{3\alpha}{2}+k_0\right) + \left(4\alpha c_{\frac{3}{2}} + l_0\right)\sqrt{z} + O(z) \qquad (3.60) \\ &\overset{z\to\infty}{\sim} -\left(\frac{3}{2}\ \alpha\ \sqrt{\pi} + \frac{l_0}{4}\right)\ z^{-3/2}\ e^z\ , \qquad (3.61) \end{aligned}$$

where we have used (3.49) and (3.59) for the large z asymptotics. Compare now the small z expansion (3.60) to (3.36). One obviously has to identify

$$\frac{3\alpha}{2} + k_0 = \beta \quad , \quad 4\alpha c_{\frac{3}{2}} + l_0 = 0\ . \tag{3.62}$$

If g_0 would decay asymptotically as $z^{-3/2}\ e^z$ for large z (3.61), the subleading contribution of order $1/\sqrt{t}$ in ϕ (3.53) would not decay like a Gaussian $e^{-\xi_X^2/(4t)}$ as the leading order term does, but it would decay algebraically like $\xi_X^{-3}(4t)^{3/2}$. This would destroy the ordering of our expansion (3.42) as well as the structure of the expansion (3.15). We therefore have to make the coefficient of the leading order term $z^{-3/2}\ e^z$ in g_0 (3.61) vanish:

$$\frac{3}{2}\ \alpha\ \sqrt{\pi} + \frac{l_0}{4} = 0\ . \tag{3.63}$$

(3.62) and (3.63) fix all constants k_0, l_0 and $c_{\frac{3}{2}}$. The velocity correction of order $1/t^{3/2}$ is

$$c_{\frac{3}{2}} = \frac{3\sqrt{\pi}}{2}\ , \tag{3.64}$$

and the analytic solution for $g_0(z)$ is

$$\begin{aligned} g_0(z) = \beta\ (1-2z) + 3\alpha\ &\left(z - \frac{F_2(z)}{2}\right) \qquad (3.65) \\ &+ 6\alpha\ \sqrt{\pi\,z}\ \left(1 - M\left(\frac{-1}{2},\frac{3}{2},z\right)\right)\ , \end{aligned}$$

with α and β the coefficients of the asymptotic leading edge shape $\Phi^*(\xi) = (\alpha\xi+\beta)\ e^{-\xi}$ for $\Phi^* \ll 1$. Note, that

the subleading term β contributes only the rather trivial $(1-2z)$ term, while the coefficient of the leading α contains all nontrivial terms. The result (3.64) and (3.65) reproduces the order t^0 in (3.36) identically.

We summarize the results obtained from the analysis of the leading edge: The appropriate coordinate system is $\xi_X = x - v^* t - X(t)$, and the universal velocity correction is given by

$$\dot{X} = -\frac{3}{2t}\left(1-\sqrt{\frac{\pi}{t}}\right) + O\left(\frac{1}{t^2}\right) . \tag{3.66}$$

The shape in the leading edge, where $\phi \ll 1$, is given in terms of the variables ξ_X and t by

$$\phi(\xi_X, t) = e^{-\xi_X - \xi_X^2/(4t)}\, G\left(\frac{\xi_X^2}{4t}, t\right) \tag{3.67}$$

$$= e^{-\xi_X - \xi_X^2/(4t)} \left(\alpha\xi_X + g_0\left(\frac{\xi_X^2}{4t}\right) + \right. \tag{3.68}$$

$$\left. + \frac{1}{\sqrt{t}}\, g_{\frac{1}{2}}\left(\frac{\xi_X^2}{4t}\right) + \dots\right) ,$$

with $g_0(z)$ from (3.65).

Eqs. (3.65) – (3.67) is the second part of our final result, valid in the leading edge of the front, where $\phi \ll 1$. It complements our earlier result (3.31), valid in the interior of the front, with functions κ_v from (3.22) and ρ_v from (3.27).

Let us end this section by putting these analytical results into perspective:

1) The requirement that the leading edge remains steeper than the asymptotic profile Φ^* at any finite time, together with the requirement of consistency with our interior expansion (3.15), determines the velocity convergence constants $c_{\frac{n}{2}}$. These constants are thus determined in the leading edge by the initial conditions. They are just parameters in the equations for the interior (3.16) – (3.20).

2) The leading order velocity correction c_1 reproduces Bramson's result [77], which he derived through solving the (nonlinear) diffusion equation with probabilistic methods. The universal subdominant $1/t^{3/2}$ is new, however.

3) According to our discussion in connection with the interior expansion, $g_{\frac{1}{2}}$ and c_2 should be termed non-universal, because the change from $1/\sqrt{t}$ to $1/\sqrt{t-t_0}$ in the asymptotic expansion about $t \to \infty$ changes these terms. As for (3.31), we conclude, that at least parts of these terms depend on initial conditions and are therefore non-universal.

4) Again, the expansion is only asymptotic in $1/\sqrt{t}$: the results of the prefactors of the $1/t$ and the $1/t^{3/2}$ terms are exact, but as the expansion will not converge at any finite time, there should in principle be an optimal truncation of the expansion for every t.

5) The leading edge expansion is an intermediate asymptotics in z, valid for $1 \ll z \ll \sqrt{t}$ or $\sqrt{t} \ll \xi_X \ll t$, resp. Above, we extensively made use of the cross-over to the interior expansion for $z \ll 1$. Let us now look into the break-down for $z \geq O(\sqrt{t})$, i.e., for $\xi_X \geq O(t)$. This second break down immediately follows from inserting into (3.42) our results $g_{\frac{-1}{2}}(z) = O(\sqrt{z})$ and $g_0(z) \geq O(z)$ (in fact $g_0(z) = O(z \ln z)$ according to Appendix D). This new crossover actually needs to exist in view of our discussion in Section II E 1: The steepness λ is conserved for $x \to \infty$ for all times $t < \infty$. It will retain the information about the precise initial condition. This region of conserved steepness at $\xi_X > O(t)$ crosses over to the universal Gaussian leading edge region for $\xi_X < O(t)$, which determines the universal relaxation behavior as discussed above. The region of conserved stepness λ at $\xi_X > O(t)$ has no further consequence for the dynamics, if the initial steepness is only $\lambda > \lambda^*$. It will disappear towards $\xi_X \to \infty$ by outrunning the leading edge region with an approximately constant speed. This scenario is sketched in Fig. 2.

6) Our result is valid in the pulled regime but it does not apply at the bifurcation point from the pulled to the pushed regime. For nonlinearity (1.11) this means, that the analysis applies for $\epsilon > 3/4$ [65]. Only then $\Phi^*(\xi) \propto \xi\ e^{-\xi}$, which is one of the essential ingredients of our asymptotic analysis. For $\epsilon < 3/4$, the front is pushed, and convergence is exponential, as discussed in Sections II C and II D. For $\epsilon = 3/4$, precisely at the pushed/pulled transition, $\Phi^*(\xi) \propto e^{-\xi}$. In this case, convergence is still algebraic, but the analysis of this chapter does not apply exactly. The convergence analysis, however, can be set up along the same lines. As shown in Appendix E we then get instead of (3.66)

$$\dot{X} = -\frac{1}{2t}\left(1-\frac{1}{2}\sqrt{\frac{\pi}{t}}\right) + O\left(\frac{1}{t^2}\right) . \tag{3.69}$$

Note that the factor $3/2$ of the $1/t$ term is replaced by $1/2$ at the bifurcation point. Along the lines of the arguments of Section III A 1 this can be understood simply from the fact that at the bifurcation point the asymptotic behavior of Φ^* is as $\Phi^*(\xi) \sim e^{-\xi}$, *not* as $\xi e^{-\xi}$, and hence that the simple Gaussian leading edge solution $t^{-1/2} e^{-\xi - (\xi)^2/4t}$ matches to the asymptotic front profile in leading order.

IV. SIMULATIONS OF PULLED FRONTS IN THE NONLINEAR DIFFUSION EQUATION

In the previous section we analyzed the relaxation of steep initial conditions towards a pulled uniformly translating front (Case IV in Table III) in the nonlinear diffusion equation

$$\partial_t \phi = \partial_x^2 \phi + f(\phi) \ . \tag{4.1}$$

The results are summarized in Table I, where we have to take $v^* = 2$, and $\lambda^* = 1 = D$. If the initial condition has a finite steepness $\lambda^* < \lambda_{init} < \infty$, the Gaussian region is preceeded by a dynamically unimportant region of conserved steepness λ_{init} for all times $t < \infty$, as is discussed in Section II E 1 and sketched in Figure 2.

In this section, we present simulation data for the nonlinear diffusion equation, and compare these with our analytical predictions. In particular, we thoroughly investigate fronts with the nonlinearity

$$f(\phi) = \phi - \phi^3 \ , \tag{4.2}$$

which are certainly pulled. As an example of a nonlinearity allowing for both pushed and pulled fronts, we also present data for

$$f(\phi) = \epsilon\phi + \phi^3 - \phi^5 \ . \tag{4.3}$$

According to Appendix C, these fronts are pushed for $\epsilon < 3/4$ and pulled for $\epsilon > 3/4$.

As an initial condition, we here always choose

$$\phi(x,0) = \frac{1}{1+e^{\lambda_{init}(x-x_0)}} \to \begin{cases} e^{-\lambda_{init}(x-x_0)} & x \to \infty \\ 1 & x \to -\infty \end{cases} \ . \tag{4.4}$$

According to our analytical results, all initial conditions with initial steepness $\lambda_{init} > \lambda^* = 1$ exhibit the same universal relaxation behavior asymptotically as $t \to \infty$, and this we indeed do find in our simulations. We therefore only present simulations for the representative value $\lambda_{init} = 10$ below.

The section is organized into a discussion of the numerical features of pulled fronts (Section IV A), the presentation of the raw simulation data for nonlinearities (4.2) and (4.3) (Section IV B), and a detailed comparison of the simulations for nonlinearity (4.2) with the analytical predictions (Section IV C).

A. Numerical features specific to pulled fronts

To integrate a given initial condition $\phi(x,0)$ forward in time t according to the equation of motion (4.1), we use a semi-implicit algorithm, as explained in Section V F 6, Eq. (5.114). When running the program, we have to choose a spatial and temporal discretization Δx and Δt, a system size $0 \le x \le L$, and a position x_0 of the initial condition within the system. Comparing results for different parameters Δx, Δt, L, and x_0 to each other and to the analytical predictions in the extreme precision of often better than 6 significant figures, we find two features specific to the particular dynamic mechanism of pulled fronts:

1. Effect of finite difference code

The numerical results of the simulation depend, of course, on the step sizes Δx and Δt of the finite difference code. In fact, in Section V F 6 we will have collected all analytical tools to calculate the corrections to $v^* = 2$, $\lambda^* = 1$ and $D = 1$, that depend on the numerical integration scheme and on the parameters Δx and Δt. All data presented here are derived for $\Delta x = 0.01 = \Delta t$. For a pulled front in a nonlinear diffusion equation solved with a semi-implicit scheme, we find according to Eq. (5.116), that $v^* = 2.000075$, $\lambda^* = 0.999954$, and $D = 1.00035$.

2. Effect of finite system size

In contrast to a pushed front, the final $t \to \infty$ relaxation of a pulled front very sensitively depends on system size L and front position x_0. This effect is closely related to the different pulled mode of propagation and the breakdown of the linear stability analysis. Because the half-infinite space $x \gg 1$ of the leading edge dominates the dynamics, the very long time dynamics of the front is sensitive to the region at $x \gg 1$, even if there always $\phi \ll 1$. More precisely, the diffusive spreading of the linear perturbation as in Eq. (3.3) or (3.67), that determines the speed, strongly depends on the boundary conditions at $\xi_X = x - v^*t - X(t) = O(\sqrt{4Dt}\,)$.

For this reason, we shift the front back to its original position x_0 within the system after every time step $t_2 - t_1 = 1$. This eliminates the x-interval $0 \le x \le x_{shift} \approx v^*$ on the back side of the front from our data, while a new x-interval $L - x_{shift} \le x \le L$ has to be created. One might assume, that this procedure yields good results for integration times T up $T = O\left((L-x_0)^2/(4D)\right)$ because of the diffusive nature of the spreading. However, the precision noticeably breaks down earlier because of the arbitrariness of the newly created x-interval $L - x_{shift} \le x \le L$ in the shift process. Filling this region with the constant $\phi(x) = \phi(L - x_{shift})$ creates a flat initial condition, and the front accelerates beyond v^* for sufficiently long times. We therefore use $\phi(x) \equiv 0$ in this region. The observed velocities $v_\phi(t)$ for $L < \infty$ then always will stay below those in the infinite system $L \to \infty$. The simulations in the finite system are close to those in the infinite system up to times $T = O\Big((L-x_0)/v^*\Big)$.

B. Simulation data

1. $f(\phi) = \phi - \phi^3$: *pulled fronts*

As an example, we will extensively discuss simulations with the nonlinearity (4.2). We present data with initial conditions (4.4) and $\lambda = 10$, where the initial condition is located at $x_0 = 100$ in a system of size $L = 1000$. According to our estimate above, the simulations then should be reliable up to times t of order $(L - x_0)/2 = 450$. We present data up to $t = 400$. The data from this simulation is evaluated in a sequence of figures showing increasing detail and precision.

Fig. 1 already showed the temporal evolution of a steep initial condition $\lambda > \lambda^*$ under the equation of motion (4.1) and (4.2). It shows both, the total displacement of the front, and the evolution of the front shape. We now choose different presentations, that show these two different aspects of the dynamics separately and more clearly.

Let us first study the evolution of the front shape: In Fig. 5, we present $\phi(\xi_X, t)$ as a function of ξ_X, where $\xi_X = x - v^*t - X(t)$, Eq. (3.7), is adjusted such that $\phi(0, t) = 1/2$ (3.9) for all times t. The remaining dynamics in this frame is then the pure evolution of the shape from its steep initial profile $\phi(\xi_X, 0)$ towards its flatter asymptotic profile $\phi \to \Phi^*(\xi_X)$ as $t \to \infty$. Fig. 5(a) shows ϕ as a function of ξ_X on the interval $-5 < \xi_X < 5$. One sees the interior or nonlinear part of the front. Fig. 5(b) shows $\log \phi$ in the range $10^{-90} < \phi < 1$. This plot is appropriate to show the development of the leading edge, which here essentially determines the dynamics. Accordingly, a very different range of ξ_X has to be plotted, namely $0 < \xi_X < 190$. As is sketched already in Fig. 2, the leading edge here again consists of two regions, namely the "Gaussian" region, through which the asymptotic steepness λ^* spreads in time towards larger ξ_X, and the region of conserved steeness $\lambda = \lambda_{init}$ in front of it. In fact, Fig. 5(b) shows, that the initial $\lambda_{init} = 10$ on the level $\phi = 10^{-90}$ is still fully present for times $t = 1$ and 2, while at later times it gradually approaches $\lambda^* = 1$. At higher levels, $\phi = 10^{-10}$ say, this process of replacement of one steepness by the other is essentially completed at time $t = 70$, while at level 10^{-90}, it is not completed even at time $t = 400$, where the simulation stops.

In Fig. 6, we now focus on the second feature, namely the displacement of the front. We here plot the velocity $v_\phi(t)$ of various amplitudes ϕ as a function of t. According to our previous definition, we identify $v_{1/2}(t) = v^* + \dot{X}(t)$. For comparison, the predicted asymptotic value v^* is plotted as a dashed line. In Fig. 6(a), the nonuniversal initial transients up to time $t = 20$ are shown, which exceed even the large velocity range $0 < v < 3$ plotted. In Fig. 6(b), the velocities are plotted up to time $t = 400$ on the velocity interval $1.97 < v < 2$. We observe,

— that for fixed t, the velocity $v_\phi(t)$ is the smaller, the larger ϕ is. This is an immediate consequence of the fronts becoming flatter in time, cf. Fig. 5.

— that the $v_\phi(t)$ for large t approach a value largely independent of ϕ, that is still far from the asymptotic value v^*. We will see below, that this is the signature of the shape relaxation being $v_{\phi_1}(t) - v_{\phi_2}(t) \propto 1/t^2$ as $t \to \infty$, while the overall relaxation is $v_\phi(t) - v^* \propto 1/t$.

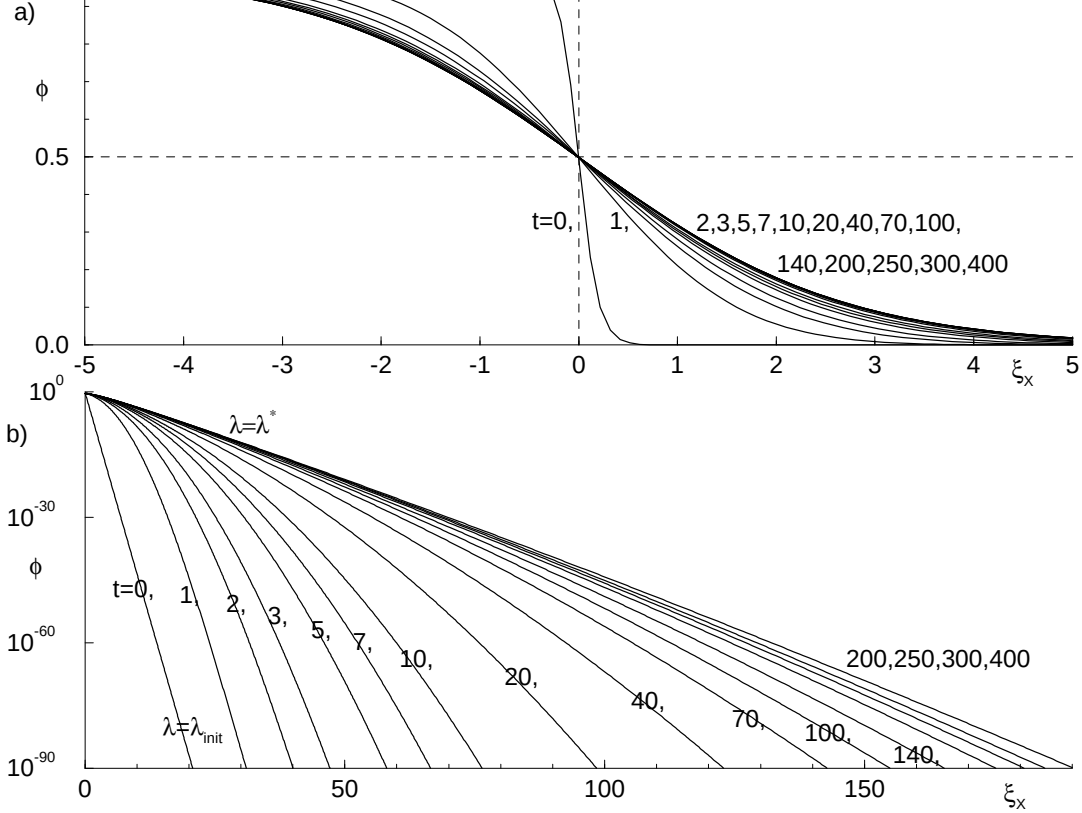

FIG. 5. Simulation of the evolution of the shape of a front under (4.1), (4.2) at the times denoted in the figure. The initial condition is (4.4) with $\lambda = \lambda_{init} = 10$. The comoving frame ξ_X is chosen such, that $\phi(\xi_X = 0, t) = 1/2$ for all t. *a*) A plot of ϕ versus ξ_X shows mainly the interior of the front. *b*) A plot of $\log \phi$ versus ξ_X for sufficiently large ξ_X shows mainly the leading edge of the front. Note the different scales of ξ_X.

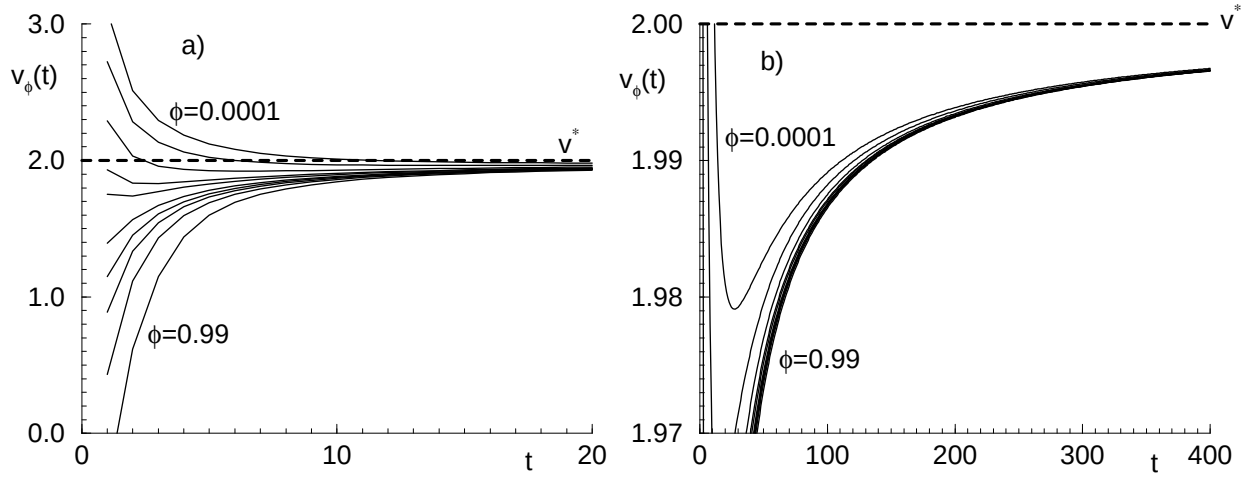

FIG. 6. The same simulation as in Fig. 5. Now the velocities $v_\phi(t)$ of amplitudes $\phi = 0.99$, 0.9, 0.7, 0.5, 0.3, 0.1, 0.05, 0.01, 0.001, and 0.0001 (solid lines) are shown as a function of time t. The asymptotic velocity v^* is marked by the dashed line. *a*) Initial transients for times $0 \le t \le 20$. *b*) The same data plotted for longer times $0 \le t \le 400$ and an enlarged scale of v. The velocities $v_\phi(t)$ become largely independent of the "height" ϕ, and together slowly approach v^*. We will explain this behavior by universal algebraic relaxation.

2. $f(\phi) = \epsilon\phi + \phi^3 - \phi^5$: pushed versus pulled fronts

A well-known example of a nonlinear diffusion equation (4.1) exhibiting both pushed and pulled fronts is given by the nonlinearity (4.3):

$$\partial_\tau \varphi = \partial_y^2 \varphi + \epsilon\varphi + \varphi^3 - \varphi^5 \ . \tag{4.5}$$

This equation for $\epsilon < 0$ is often used as a phenomenological (Ginzburg-Landau type) mean field model for a first order transition. Likewise, its extension to a complex field is often used to model a subcritical bifurcation in pattern forming systems. According to arguments recalled in Appendix C, fronts of (4.5) are pushed for $\epsilon < 3/4$, and pulled for $\epsilon > 3/4$.

The rescaling necessary to bring (4.5) to our standard form (2.2) is discussed in (2.3) and (2.4), and yields

$$\partial_t \phi = \partial_x^2 \phi + \phi + \frac{1}{\bar\epsilon}\,\phi^3 - \left(1 + \frac{1}{\bar\epsilon}\right)\,\phi^5 \ , \tag{4.6}$$

$$\text{where} \quad \bar\epsilon = \frac{\sqrt{1+4\epsilon}-1}{2} \ , \ \varphi_s^2 = 1 + \bar\epsilon \ . \tag{4.7}$$

The critical $\bar\epsilon$, where the pushed/pulled transition occurs, is $\bar\epsilon_c = 0.5$.

We present data for the pushed front with $\bar\epsilon = 0.4$ ($\epsilon = 0.56$) and the pulled front with $\bar\epsilon = 0.6$ ($\epsilon = 0.96$). The initial condition is as before. The system size is $L = 250$, and the front is located at $x_0 = 50$. The data therefore should be reliable up to time of order 100, so the data presented extend over $0 \le t \le 100$.

In Fig. 7, we plot $v_\phi(t)$ as a function of t for both values of $\bar\epsilon$, in the same way as the plot of Fig. 6 for the other nonlinearity (solid lines). The dashed lines denote the asymptotic pulled velocity $v^* = 2$ predicted for $\bar\epsilon = 0.6$, and the asymptotic pushed velocity (cf. Appendix C)

$$v^\dagger = \frac{1+4\bar\epsilon}{\sqrt{3\bar\epsilon(1+\bar\epsilon)}} = 2.00594 \quad \text{for } \bar\epsilon = 0.4 \ . \tag{4.8}$$

We observe, (i) that the simulated fronts in fact do approach the predicted asymptotic velocities, (ii) that up to time $t \le 10$, both fronts show quite similar initial transients, (iii) that for time $t \gg 10$, however, the relaxation towards the asymptotic velocity $v^\dagger$ for $\bar\epsilon = 0.4$ is much more rapid than that towards v^* for $\bar\epsilon = 0.6$. This very clearly illustrates the difference between pushed exponential and pulled algebraic relaxation.

We do not plot the figures of shape relaxation equivalent to Fig. 5, since they look essentially the same: Fig. 5(a) anyhow essentially shows the initial transients in the interior up to time $t = 20$. Also Fig. 5(b) looks rather the same with the only difference, that for $\bar\epsilon = 0.4$ the conserved steepness $\lambda = \lambda_{init}$ at $\xi_X \gg 1$ is invaded by the pushed steepness $\lambda^\dagger$ determined by the front interior rather than by the pulled steepness λ^* determined by the Gaussian region of the leading edge.

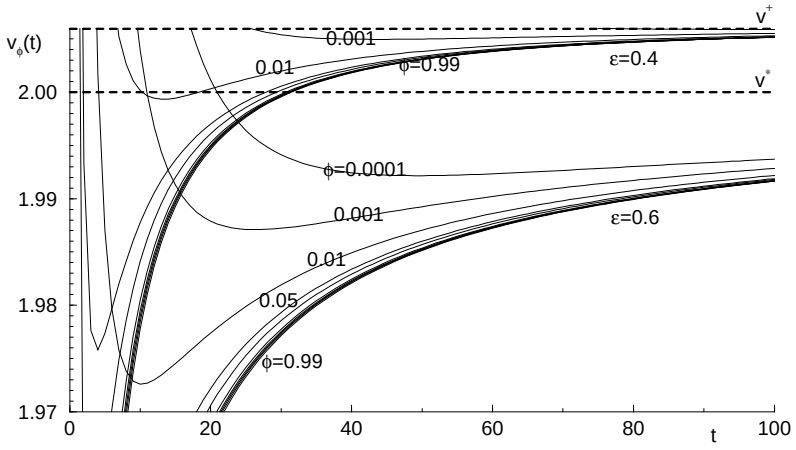

FIG. 7. Plot of $v_\phi(t)$ as a function of t as in Fig. 6(b), but now for nonlinearity (4.3). Simulations for $\bar\epsilon = 0.4$ ($\epsilon = 0.56$) and $\bar\epsilon = 0.6$ ($\epsilon = 0.96$) are shown. The dashed lines denote the asymptotic pulled velocity $v^* = 2$ of the front with $\bar\epsilon = 0.6$, and the asymptotic pushed velocity $v^\dagger = 2.00594$ of the front with $\bar\epsilon = 0.4$. Note the quick exponential relaxation towards $v^\dagger$ in contrast to the slow algebraic relaxation towards v^*. Further away from the transition $\bar\epsilon = 0.5$ ($\epsilon = 0.75$) from pulled to pushed front propagation, the relaxation in the pushed regime is even faster and the difference $v^\dagger - v^*$ is larger.

C. Comparison of simulations and analytical predictions

Let us return to our extensive simulation of the pulled front formed by the F-KPP equation $\partial_t\phi = \partial_x^2\phi + \phi - \phi^3$, and let us compare the simulation data to our analytical predictions from Table I ($v^* = 2$, $\lambda^* = 1 = D$).

1. Analysis of the velocity data

We first concentrate on the analysis of the velocity data $v_\phi(t)$ from Fig. 6. The prediction for the velocities $v_\phi(t)$ of the amplitudes ϕ is derived from the expressions in Table I as $v_\phi(t) = -\partial_t\phi/\partial_x\phi|_{\phi\text{ fixed}}$. The result is

$$v_\phi(t) = v^* + \dot{X} - \ddot{X}\ \left.\frac{\eta_{sh}}{\partial_\xi\Phi^*}\right|_{\phi\text{ fixed}} + O\left(\frac{1}{t^3}\right)\ . \qquad (4.9)$$

Remember, that $\dot{X}$ is universal only till order $1/t^{3/2}$ and will exhibit contributions in order $1/t^2$, that depend on initial conditions. The difference $v_{\phi_1}(t) - v_{\phi_2}(t)$, however, is universal up to order $1/t^{5/2}$. Let us now test this prediction on the simulations in a series of plots with growing precision in Figs. 8 – 10.

As the velocity correction $\dot{X}$ is $1/t$ in leading order, we plot $v_\phi(t)$ as a function of $1/t$ in Fig. 8, for the time range $5 < t < 400$ in Fig. 8(a), and for $100 < t < 400$ in Fig. 8(b). The dashed lines present the predicted asymptotes $v^* + \dot{X} = 2 - \dot{X}_1(t)$ (the lower dashed line), and $v^* + \dot{X} = 2 - \dot{X}_{3/2}(t)$ (the upper dashed line), where we define

$$\dot{X}_1(t) = -\frac{3}{2t}\ \ ,\ \ \dot{X}_{3/2}(t) = -\frac{3}{2t}\ \left(1 - \sqrt{\frac{\pi}{t}}\right)\ . \qquad (4.10)$$

First of all, in comparing Figs. 8(a) and 8(b), we recognize the asymptotic nature of the $1/\sqrt{t}$ expansion: whether the $\dot{X}_1$ or the $\dot{X}_{3/2}$ asymptote gives the better prediction, depends on the time scale: If we neglect the upper three solid lines with velocities $v_\phi(t)$ for the very small amplitudes $\phi = 0.01$, 0.001, and 0.0001, the asymptote $2 - \dot{X}_1$ clearly fits mutch better in Fig. 8(a) for times $5 < t < 400$ — while the asymptote $2 - \dot{X}_{3/2}$ essentially coincides with $v_{0.001}(t)$, an observation, we have no analytical explanation for. For times $100 < t < 400$ in Fig. 8(b), however, the coincidence with $2 - \dot{X}_{3/2}$ is excellent for all ϕ, and $2 - \dot{X}_1$ very clearly is "far off" on this very detailed scale. Therefore, we below will work with the asymptote $2 - \dot{X}_{3/2}(t)$, and we present data for the time regime $20 < t < 400$ in Figs. 9 and 10.

Let us now further zoom in on the ϕ dependent velocity corrections (4.9) to $\dot{X}$. Fig. 9(a) shows $v_\phi(t) - 2 - \dot{X}_{3/2}$ as a function of $\ddot{X}_{3/2} = 3/(2t^2)\ \left(1 - (3/2)\sqrt{\pi/t}\right)$. According to the prediction (4.9), the plot for small values of $\ddot{X}_{3/2} \to 0$ should show essentially straight ϕ-dependent lines, all approaching $v_\phi(t) - 2 - \dot{X}_{3/2} \to 0$ as $\ddot{X}_{3/2} \to 0$, and in fact, that is what they do.

Fig. 9(b) shows one further step of precision aiming now at the precise value of v^*: (4.9) predicts

$$\frac{v_\phi(t) - v^* - \dot{X}}{\ddot{X}} = -\left.\frac{\eta_{sh}}{\partial_\xi\Phi^*}\right|_{\phi\ fixed} + O\left(\frac{g(\phi)}{t}\right)\ . \qquad (4.11)$$

However, the evaluation of this expression with $\dot{X}_{3/2}$ (4.10) yields ϕ-independent corrections of order $1/\sqrt{t}$:

$$\frac{v_\phi(t) - v^* - \dot{X}}{\ddot{X}} = \qquad (4.12)$$

$$= \frac{v_\phi(t) - v^* - \dot{X}_{3/2} - \frac{c_2}{t^2} - \frac{c_{5/2}}{t^{5/2}} + O\left(\frac{1}{t^3}\right)}{\frac{3}{2t^2}\ \left(1 - \frac{3}{2}\sqrt{\frac{\pi}{t}}\right) + O\left(\frac{1}{t^3}\right)} =$$

$$= -\left(\left.\frac{\eta_{sh}}{\partial_\xi\Phi^*}\right|_\phi + \frac{2c_2}{3}\right)\left(1 + \frac{3}{2}\sqrt{\frac{\pi}{t}}\right) - \frac{2c_{5/2}}{3\sqrt{t}} + O\left(\frac{1}{t}\right)\ .$$

Remember, that the constants c_2, $c_{5/2}$ etc. depend on the initial conditions. If we plot $\left(v_\phi(t) - v^* - \dot{X}_{3/2}\right)/\ddot{X}_{3/2}$ as a function of $1/\sqrt{t}$, we expect these functions to approach a ϕ-dependent constant as $1/\sqrt{t} \to 0$.

Fig. 9(b) shows, that they in fact do so — but only if we choose the correct value of v^*! The dotted lines show the function for $v^* = 2$, the fat solid lines for $v^* = 2.000075$. The latter value is the analytical prediction of v^* taking the finite gridsize corrections of the numerical code into account, as explained in Sections IV A 1 and V F 6. The two values of v^* differ in the 6th significant figure. Fig. 9(b) is an extremely precise demonstration of the correctness of our analytical arguments from both Sections III and V, since it clearly confirms our predictions to more than 6 significant figures!

Our test in Fig. 9(b) is so sensitive, because we divide in Fig. 9(b) by the small quantities $\ddot{X}_{3/2}$, which are of order 10^{-5}. Without this division, the difference of the v^*'s in Fig. 9(a) is not yet visible. The plot therefore shows, that we fully understand the numerical features of pulled front solutions, both the effect of the finite difference code and of the finite system size, as discussed above in Sect. IV A.

We can eliminate v^* and the nonuniversal corrections $-c_2/t^2$ etc. by plotting $(v_\phi(t) - v_{0.5}(t))/\ddot{X}_{3/2}(t)$ as a function of $1/t$. Now (4.9) predicts

$$\frac{v_\phi(t) - v_{0.5}(t)}{\ddot{X}_{3/2}} = -\left.\frac{\eta_{sh}}{\partial_\xi\Phi^*}\right|_\phi + O\left(\frac{1}{t}\right)\ . \qquad (4.13)$$

Fig. 10 shows this plot with the solid lines for $\phi = 0.99$, 0.5, 0.01, and 0.0001. The crosses on the axis are not(!) extrapolated from the curves, but they mark the predicted asymptotes $-\eta_{sh}/\partial_\xi\Phi^*|_\phi$ for $\phi = 0.99$, 0.5, 0.01, and 0.0001. The necessary data on $\eta_{sh}(\xi)$ and $\Phi^*(\xi)$ are derived from the numerical solution of the appropriate *o.d.e.*'s, and completely independent from the numerical integration of the *p.d.e.* for the initial value problem. The coincidence of the extrapolated *p.d.e.* data with the analytically predicted, but also numerically evaluated *o.d.e.* asymptote is most convincing.

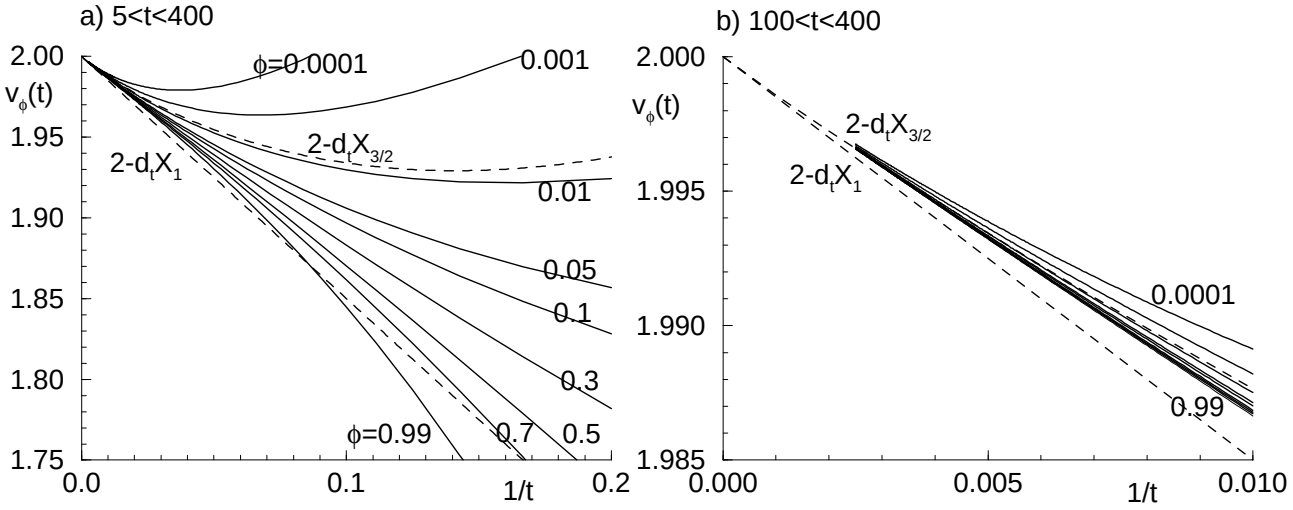

FIG. 8. The data $v_\phi(t)$ from Fig. 6, but now plotted over $1/t$. The lower straight dashed line is the asymptote $v(t) = 2 - \dot{X}_1(t)$ (4.10), the upper curved dashed line is the asymptote $v(t) = 2 - \dot{X}_{3/2}(t)$. *a*) time regime $5 < t < 400$, *b*) time regime $100 < t < 400$. Note that due to the $t^{-3/2}$ correction term, the effective slope in this plot is less than 3/2, even at these long times.

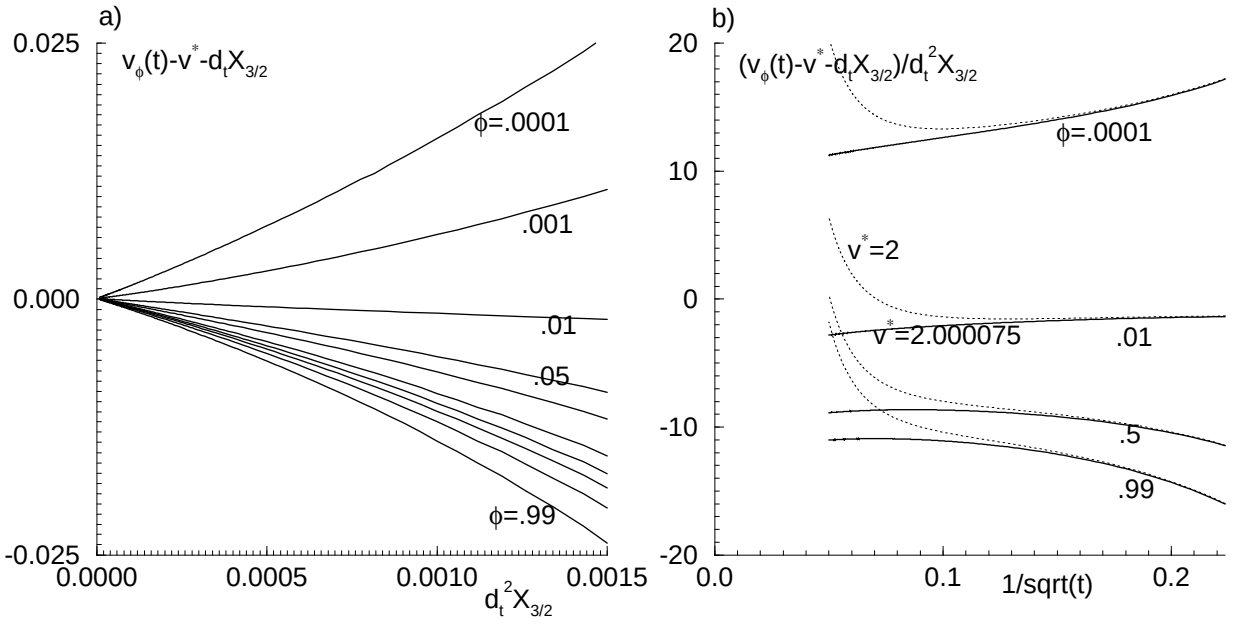

FIG. 9. The data $v_\phi(t)$ from Figs. 6 and 8 for times $20 \le t \le 400$ in different representations. *a*) $v_\phi(t) - 2 - \dot{X}_{3/2}$ as a function of $\ddot{X}_{3/2}$. See Eq. (4.10) for the definition of $\dot{X}_{3/2}$. *b*) $\left(v_\phi(t) - v^* - \dot{X}_{3/2}\right)/\ddot{X}_{3/2}$ as a function of $1/\sqrt{t}$ for $\phi = 0.99$, 0.5, 0.01, and 0.0001. Dotted lines: $v^* = 2$, solid lines: with the corrected value $v^* = 2.000075$ for our numerical scheme and gridsize according to Section V F 6.

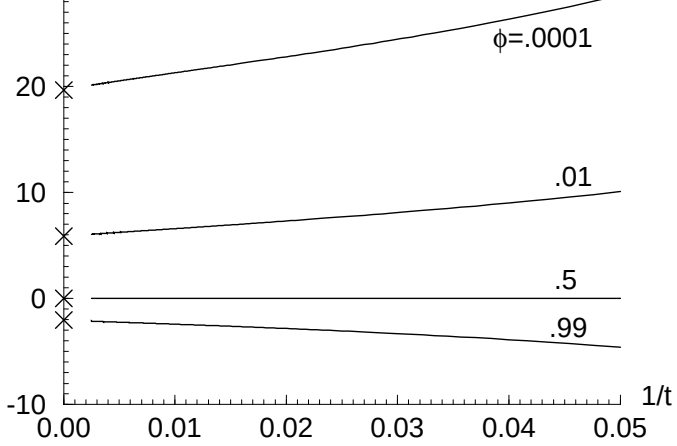

FIG. 10. The solid lines are again the data from Figs. 6, 8, 9 for times $20 \leq t \leq 400$, now plotted as $(v_\phi(t) - v_{0.5}(t))/\ddot{X}_{3/2}$ over $1/t$ for $\phi = 0.99$, 0.5, 0.01, and 0.0001. As explained in the text, this eliminates a nonuniversal $1/\sqrt{t}$ term, that depends on the initial conditions. The crosses result from solving the *o.d.e.*'s for Φ^* and η_{sh} numerically and plotting $-\eta_{sh}/\partial_\xi \Phi^*\big|_\phi$ for $\phi = 0.99$, 0.5, 0.01, and 0.0001. Eq. (4.13) predicts, that the lines should extrapolate to the crosses. Since they do, and since $\ddot{X}(t)$ is of order 10^{-5} at the latest times, these data confirm our predictions with extreme precision.

2. Analysis of the shape data

We now leave the analysis of the velocity data, and come back to the shape data from Fig. 5. Table I immediately yields

$$\frac{\phi(\xi_X,t)-\Phi^*(\xi_X)}{\dot{X}\ \eta_{sh}(\xi_X)} = 1 + O\left(\frac{1}{t}\right). \qquad (4.14)$$

This gives the clue on how to rewrite the shape data $\phi(\xi_X,t)$ at different times as a function of ξ_X. The solutions of the *o.d.e.*'s for η_{sh} and Φ^*, that are needed for evaluating (4.14), are derived numerically. They have been used for generating the crosses in Fig. 10, and are now also used in Fig. 11.

Plotting the l.h.s. of Eq. (4.14) allows us to combine the information about the interior from Fig. 5(a) and the information about the leading edge from Fig. 5(b) into one plot. In Fig. 11(a), we do not divide by $\dot{X}$, but present the data at the small times t = 1, 2, 3, 5, 7, 10, and 20 as $-(\phi-\Phi^*)/\eta_{sh}$ over ξ_X. In Fig. 11(b), the data at the large times t = 20, 40, 70, 100, 140, 200, 300, and 400 are shown as $(\phi-\Phi^*)/(\dot{X}\eta_{sh})$ over ξ_X, where we use again the approximation $\dot{X} = \dot{X}_{3/2}$ (4.10). For comparison, both plots also show $\Phi^*(\xi_X)$ and $\xi_X = 0$ as dashed lines. Also Fig. 11(b) has the large time prediction $(\phi-\Phi^*)/\dot{X}\eta_{sh} \to 1$ as $t \to \infty$ as a dotted line.

Fig. 11(a) shows how the interior of the front rapidly relaxes. Fig. 11(b) demonstrates, (i) that with $\dot{X} = \dot{X}_{3/2}$ (4.10), we indeed have chosen the correct asymptote, (ii) how the predicted asymptotic value $(\phi-\Phi^*)/(\dot{X}\eta_{sh}) \to 1$ as $t \to \infty$ is approached from above in the interior of the front, and from below in the leading edge.

Note, that in Fig. 11(b) all lines approximately cross one point of height unity far in the leading edge. We have no intuitive or analytical understanding of this observation.

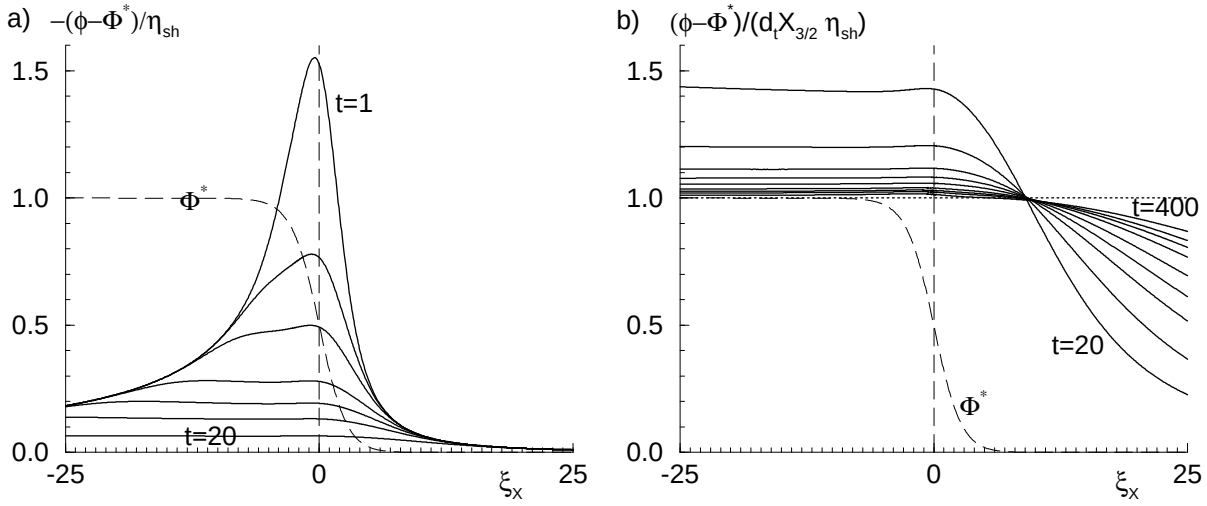

FIG. 11. In this figure, the shape data from Fig. 5 are represented differently, using data from the numerical solution of the *o.d.e.*'s for Φ^* and η_{sh}. *a*) $-(\phi-\Phi^*)/\eta_{sh}$ (solid) as a function of ξ_X for times t = 1, 2, 3, 5, 7, 10, and 20. *b*) $(\phi-\Phi^*)/(\dot{X}_{3/2}\eta_{sh})$ (solid) as a function of ξ_X for times t = 20, 40, 70, 100, 140, 200, 250, 300, 400. Dotted line: predicted asymptote $(\phi-\Phi^*)/(\dot{X}\eta_{sh}) \to 1$ as $t \to \infty$. Dashed lines in (a) and (b) give $\Phi^*(\xi_X)$ and $\xi_X = 0$ for orientation.

V. GENERALIZATION OF PULLING TO HIGHER ORDER (SETS OF) EQUATIONS

A. Introduction

In the last fifteen years, it has become clear that many of the observations and intuitive notions concerning the behavior of front solutions of the nonlinear diffusion equation (1.1) generalize to higher order equations or systems of coupled *p.d.e.*'s. First of all, taking the spreading velocity v^* of a linear perturbation of the unstable state [Eqs. (1.13) and (1.14)] as the generalization of $v^* = 2\sqrt{f'(0)}$ for (1.1), we observe that there are numerous examples [9,12,17,22,61,64–66] of fronts whose asymptotic velocity approaches the pulled value v^* given by (1.14). So there is no doubt that the mechanism of fronts "being pulled along" by the leading edge generalizes to a large class of equations. Second, there is also quite a bit of evidence for the existence of a pushed regime in more complicated equations. In a number of cases, the pushed regime was again found to be related to the existence of a strongly heteroclinic solution with velocity $v^\dagger > v^*$. An example of a non-monotonic but still uniformly translating pushed front solution in the EFK equation is shown in Fig. 8 of [65]. In the quintic complex Ginzburg Landau equation, it has turned out to be possible to solve for a strongly heteroclinic front profile exactly, and in numerical simulations it was empirically found that this solution does play the same role in the front selection process as the pushed front $\Phi^\dagger$ in the nonlinear diffusion equation [66]. Pushed fronts also emerge in coupled amplitude equations for chaotic domain boundary motion [21]. For extensions of the Swift-Hohenberg equation there are numerical and perturbative indications that both pulled and pushed regimes occur, and that one can tune the front velocity from one regime to the other with one of the nonlinear terms in the equation [65].

Much of our understanding of the above general findings has been intuitive and empirical, or based on conjectures. We shall now show that many of our results for the second order nonlinear diffusion equation generalize to other equations, not only to (sets of) partial differential equations of higher order, but also to other types of equations like difference-differential equations [22,71], or differential equations with memory kernels [107]. We will concentrate here on equations whose relevant front solutions are uniformly translating. For *p.d.e.*'s in this class, essentially the whole classification of nonlinearities and initial conditions $\phi(x,0)$ in Table III applies, provided the uniformly translating fronts Φ_v, and in particular the fronts Φ^* and $\Phi^\dagger$ exist. Again Cases I – IV need to be distinguished, and again Case IV with its slow algebraic relaxation is not tractable by linear stability analysis methods. Instead, the calculation of Section III has to be generalized. This generalization, that we will develop below, leads to *new* and *explicit* predictions for the front convergence in the pulled regime, as summarized in Table I. The fact that these predictions for various examples are fully corroborated numerically in Section V F makes us conclude that the velocity selection and relaxation of uniformly translating fronts is now essentially understood.

While this paper was nearing completion, it was becoming increasingly clear that even though pattern forming fronts — both fronts leading to regular periodic patterns, as in the Swift-Hohenberg equation [73,60,65], and fronts leading to chaotic patterns as in some parameter ranges of the complex Ginzburg-Landau equation — present additional complications, our most central result for the universal algebraic velocity relaxation carries over even to these. We will leave a discussion of this to the future, and focus here on *p.d.e.*'s whose asymptotic pulled fronts are uniformly translating front solutions of the type $\Phi^*(x - v^*t)$, just as in the nonlinear diffusion equation.

In writing this section, we face the following dilemmas:

(i) The extension of both the stability considerations of uniformly translating front solutions of section II and of the relaxation analysis of pulled fronts of section III depends quite crucially on two ingredients: First, that the front propagation into unstable states is in the pulled regime, and, second, that there is a family of uniformly translating front around $\Phi^*(x-v^*t)$: Only then can the relaxation in the front interior be along the manifold of front solutions according to $\phi(x,t) = \Phi_{v(t)}(\xi_X) + O(1/t^2)$. However, to our knowledge there is no general theory concerning the conditions under which fronts are pulled and concerning the multiplicity of front solutions: For particular equations under study or for some restricted classes of equations, one can often convince oneself that the front should be pulled and that Φ^* should be a member of a family of front solutions, but a general theory is lacking.

(ii) An immediate jump to the most general (but abstract) case is pedagogically not justified and moreover would assume knowledge of the derivation of the pulled velocity v^* that most readers probably do not have.

We have chosen to deal with this dilemma by simply summarizing our main assumptions and our results concerning the extensions of section II to more general equations below, relegating the details of the analysis to Appendices. Then, we proceed with the relaxation analysis of pulled fronts in two steps. We first consider in Section V C the analysis of a single *p.d.e.* which is of first order in time but of arbitrary order in space. After that, the extension to *p.d.e.*'s that are of higher order in time is discussed in Section V D. The extension to even more general classes of equations, including difference equations or integro-differential equations, e.g., with memory kernels, is then immediate, as we discuss in Section V E.

We there also discuss coupled equations. Section V F contains the explicit analytical and numerical results for the EFK equation (1.3), for the streamer equations (1.4) as an example for coupled equations, and for an example of a difference-differential equation, Eq. (1.5). We also briefly discuss an extension of the F-KPP equation with a second order temporal derivative (1.6) and with a memory kernel (1.7), and we present our analytical results on finite difference schemes for the numerical solution of nonlinear diffusion equations (1.8), that we already verified in the simulations of the previous section.

B. Basic assumptions underlying the relaxation analysis of pulled fronts; generalization of Table III

We investigate nonlinear partial differential equations, as well as difference or integro-differential equations and the generalization to coupled equations under the assumption that

A The front solutions are pulled, i.e., starting from a steep initial condition the asymptotic front speed v_{sel} equals the linear spreading speed v^* given by Eqs. (5.16) and (5.17) below.

B The asymptotic front is uniformly translating , i.e., of the form $\Phi^*(x - v^*t)$, and it is a member of a continuous family of uniformly translating solutions $\Phi_v(x - vt)$, parametrized by v.

If the above assumptions hold, most of the results of section II can be generalized:
• The family of solutions can be parametrized as well by the steepness λ which gives the rate of exponential decay of $\Phi_v(\xi)$ as $\xi \to \infty$.
• If there is one or more strongly heteroclinic solution then at each velocity where such a solution exists, there is a strongly heteroclinic mode of the linear stability operator which changes stability, i.e., which is such that the mode is stabilizing for velocities larger than this value and destabilizing for velocities less than this value. This implies in particular that the pushed velocity $v^\dagger$ is the largest velocity at which there is a strongly heteroclinic front solution $\Phi_v^\dagger$, and that front solutions with $v < v^\dagger$ are unstable (see Appendix G).
• The linear spreading velocity v^*, given by Eqs. (5.16) and (5.17) below, is the pulled front speed and coincides with the minimum of the velocities of uniformly translating fronts $v(\lambda)$ (see Section V C 2).
• If there are no strongly heteroclinic solutions with $v > v^*$, all front solutions with $v > v^*$ are stable to perturbations which are steeper than λ^*, while front solutions with $v < v^*$ are unstable: the pulled front solution is then the slowest and steepest solution which is stable.
• The fronts that dynamically emerge from steep initial conditions (falling off faster than $e^{-\lambda^* x}$) converge to pulled fronts propagating with speed v^*.

To put our general assumptions A and B into perspective, we finally note that for a given equation, the existence of a family of front solutions can often be demonstrated by counting arguments. This is shown in Appendix F for *p.d.e.*'s of first order in time that are invariant under space reflection. Such counting arguments also lead one to expect that generically either $\Phi^*(x-v^*t)$ is a member of a continuous family of front solutions, or there is no uniformly translating front solution Φ^* at all. For, if there is a discrete set of front solutions (solutions Φ_v exist at isolated values of the velocity), there is no particular symmetry reason to have one at $v = v^*$, since the existence of an isolated solution depends on the full nonlinear behavior of the ordinary differential equation, not just on the properties near one of the asymptotic fixed points. We comment in Section VI on what might happen when there is no uniformly translating front solution, even though the front dynamics is pulled.

C. Pulled front relaxation in single *p.d.e.*'s of first order in time

In the present Section C, we discuss an arbitrary *p.d.e.*

$$F\Big(\phi,\ \partial_x\phi,\ \ldots,\ \partial_x^N\phi,\ \partial_t\phi\Big) = 0\ . \tag{5.1}$$

for a single field $\phi(x,t)$. We assume that F is analytic in all its arguments, and that the equation admits homogeneous steady state solutions $\phi = 0$ and $\phi = 1$. Moreover, we assume $\phi = 0$ to be linearly unstable and $\phi = 1$ to be linearly stable, and we consider fronts connecting these two asymptotic states as in (2.12). Also, according to our assumption B, Eq. (5.1) admits a continuous family of uniformly translating fronts $\phi(x,t) = \Phi_v(x - vt)$, which remain bounded so that Φ_v does not diverge. The linearization of some front $\phi(x,t)$ about some Φ_v generalizes from (2.23) – (2.25) to

$$\phi(x,t) = \Phi_v(\xi) + \eta(\xi,t)\quad ,\quad \partial_t\eta = \mathcal{L}_v(\xi)\eta + O(\eta^2)\ , \tag{5.2}$$

where the linear operator is now

$$\mathcal{L}_v(\xi) = \sum_{n=0}^{N} f_n(\xi)\ \partial_\xi^n + v\ \partial_\xi\quad ,\quad f_n(\xi) = \frac{-F_n(\xi)}{F_{N+1}(\xi)}\ . \tag{5.3}$$

Here $F_n(\xi)$ denote the derivatives of F:

$$F_n(\xi) = \left.\frac{\delta F(\phi^{(0)},\ldots,\phi^{(N+1)})}{\delta\phi^{(n)}}\right|_{\substack{\phi^{(m)}=\partial_\xi^m\Phi_v(\xi),\ m<N+1\\ \phi^{(N+1)}=-v\partial_\xi\Phi_v(\xi)}}\quad , \tag{5.4}$$

In order that the F_n have no singularities, F_{N+1} should be of one sign; for convenience, we take $F_{N+1}(\xi) < 0$

for all ξ. and rescale time t such, that $F_{N+1}(\infty) = -1$ because it simplifies the notation in the Appendices. We also assume, that $F_N(\xi)$ neither vanishes nor changes sign for any ξ.

1. The pulled velocity v^*

In the pulled regime and with steep initial conditions, the asymptotic front velocity equals the linear spreading velocity v^*, i.e., the velocity with which a localized perturbation spreads according to the linearized equations. Since the calculation of v^* forms the basis of our subsequent analysis, we summarize its derivation in the context of our first order *p.d.e.* (5.1). The general formulation in Section V E, which is necessary to treat difference equations or integro-differential equations, is closest to the original "pinch point" analysis [56,58], from which many of these ideas originally emerged.

In the rest frame (x,t), the equation linearized about $\phi = 0$ is

$$\partial_t \phi = \mathcal{L}_0(\infty)\phi = \sum_{n=0}^{N} a_n \partial_x^n \phi \ , \tag{5.5}$$

which is the generalization of (2.52), and where we introduced the short hand notation $a_n = f_n(\infty)$. The dispersion relation $\omega(k)$ of a Fourier mode $e^{\,ikx - i\omega(k)t}$ is given by

$$-i\omega(k) = \sum_{n=0}^{N} a_n \ (ik)^n \ . \tag{5.6}$$

Since we later will again characterize fronts by their exponential spatial decay rate $\lambda = -ik$, we already define the growth rate $s(\lambda)$ of the steepness λ as

$$s(\lambda) = \mathrm{Re}\ \ (-i\omega(i\lambda)) = \mathrm{Re}\ \sum_{n=0}^{N} a_n \ (-\lambda)^n \tag{5.7}$$

for later use. We restrict the analysis to equations, where the temporal growth rate Re $(-i\omega(k))$ in (5.6) will be negative for short wave length Fourier modes k, i.e., where

$$\mathrm{Re}\ a_N \ (\pm i)^N \leq 0 \ , \tag{5.8}$$

since otherwise all smooth solutions will be unstable against perturbations of arbitrarily short wave lengths.

An arbitrary initial condition $\phi(y,0)$ will develop under (5.5) as

$$\phi(x,t) = \int_{-\infty}^{\infty} dy \ G(x-y,t) \ \phi(y,0) \ , \tag{5.9}$$

$$G(x,t) = \int_{-\infty}^{\infty} \frac{dk}{2\pi} \ e^{ikx - i\omega(k)t} \ . \tag{5.10}$$

in generalization of (2.56).

For steep initial conditions, i.e., when $\phi(y,0)$ in (5.9) is sufficiently localized in y, the asymptotic behavior of $\phi(x,t)$ can be obtained from the large-time asymptotics of the Green's function G. For large t, one can use a saddle point integration [105] (also known as "steepest decent approximation") to evaluate the integral (5.10). The result will depend on the frame of reference. In an arbitrary coordinate system $\xi = x - vt$ with v fixed, a saddle point k_n is a saddle of $-i\omega(k) + ivk$,

$$\frac{d}{dk}(-i\omega(k) + ivk)\Big|_{k_n} = 0 \quad \Longrightarrow \quad \frac{d\omega(k)}{dk}\Big|_{k_n} = v \ . \tag{5.11}$$

A polynomial of degree N (5.6) generically has $N-1$ saddle points k_n, $n = 1, \ldots, N-1$, (5.11) in the complex k plane. Because of (5.8), we can be sure, that the integral (5.10) actually will be dominated by a saddle point integral expanded about the saddle point $k^*(v)$ with the maximal growth rate:

$$\mathrm{Re}\ (-i\omega(k^*) + ivk^*) = \max_n \ \mathrm{Re}\ (-i\omega(k_n) + ivk_n) \ . \tag{5.12}$$

It will have

$$D(v) = \frac{1}{2} \ \frac{d^2 i\omega(k)}{dk^2}\Big|_{k^*(v)} \quad , \quad \mathrm{Re}\ D > 0 \ . \tag{5.13}$$

The expansion of the integral (5.10) about the saddle point $k^*(v)$ can be performed in a frame with arbitrary velocity v and yields

$$G(x,t) = e^{ik^*\xi + \left(-i\omega(k^*) + ivk^*\right) t} \ \mathcal{I}_v(\xi,t) \quad , \quad \xi = x - vt \ . \tag{5.14}$$

The integral $\mathcal{I}_v(\xi,t)$ is expressed after substitution of $(k - k^*) = \kappa/\sqrt{t}$ as

$$\begin{aligned} \mathcal{I}_v &= \int_{-\infty}^{\infty} \frac{d\kappa}{2\pi\sqrt{t}} \ e^{i\kappa\xi/\sqrt{t} - D\kappa^2 + O(D_3\kappa^3/\sqrt{t})} \\ &= \frac{e^{-\xi^2/(4Dt)}}{\sqrt{4\pi D t}} \ \left(1 + O\left(\frac{D_3\xi}{D^2 t}\right)\right) \end{aligned} \tag{5.15}$$

for large t and arbitrary ξ. Obviously, D plays the role of a diffusion coefficient. D_3 is defined below in (5.28).

Generically, the growth (or decay) rate of the saddle point mode Re $(-i\omega(k^*(v)) + ivk^*(v))$ will be nonvanishing. We now define the particular linear spreading or pulled velocity v^* through Re $(-i\omega(k^*) + iv^*k^*) = 0$, or

$$v^* = \frac{\mathrm{Im}\ \omega(k^*)}{\mathrm{Im}\ k^*} = \frac{s(-ik^*)}{\mathrm{Im}\ k^*} \quad , \quad k^* = k^*(v^*) \ . \tag{5.16}$$

This means, that in the frame moving with velocity v^*, the absolute value of the Green's function (5.14) neither grows nor decays in leading order. v^*, k^* and $\omega(k^*)$ are

determined by (5.12), (5.16), and by Eq. (5.11) evaluated at v^*:

$$\left.\frac{d\omega(k)}{dk}\right|_{k^*} = v^* \ . \tag{5.17}$$

In addition, the solution determines $D = D(v^*)$ (5.14).

Note that the leading order large t result (5.14), (5.15) for the Green's function G in (5.9) is diffusive just like in (2.57), despite the fact, that we are dealing here with an equation with higher spatial derivatives. We shall see in Sects. V D and V E that this even remains true for much more general types of equations.

Note also that in our discussion of *p.d.e.*'s in this and the next Section, we only take the spatial Fourier transform of $G(x,t)$, as in (5.10) above. However, the most general formulation, which also applies to difference equations or integro-differential equations, is most conveniently done by taking a Fourier transform in space and a Laplace transform in time. In the present context, the Green's function $G(k,\omega)$ is then defined as

$$G(k,\omega) = \int_0^\infty dt \int_{-\infty}^\infty dx\ e^{-ikx+i\omega t}\ G(x,t) = \frac{1}{S(k,\omega)} \ , \quad \text{where } S(k,\omega) = i\omega(k) - i\omega \ , \tag{5.18}$$

and the long time asymptotics is determined by the double roots of the characteristic equation $S(k,\omega(k)) = 0$ (5.6). We defer this type of formulation, which closer follows the "pinch point" analysis of [56,58], to Section V E.

In practice, one first will drop condition (5.12) and generically derive N solutions (k^*, v^*) from (5.16), (5.17) for a given dispersion relation. This raises the question of their physical nature, and of their relevance for the long time dynamics. First of all, typically there are solutions with $\lambda^* \equiv \mathrm{Im} k^* > 0$ and $v^* > 0$, which describe a profile spreading to the right and solutions with $\lambda^* < 0$ and $v^* < 0$ describing the spreading to the left. These solutions are related by symmetry, if the original *p.d.e.* is symmetric under space reflection: if (5.6) only contains even powers of k and if the a_n are real, then for every solution (k^*, v^*) there is a solution $(-k^*, -v^*)$. Moreover, there can be various nontrivial saddle point solutions which are not related by symmetry, if the degree N of spatial derivatives is sufficiently large. The saddle point analysis as well as the arguments of Section II E 1 for the competition between different solutions of the linearized equations clearly show that then the dynamically relevant solution is the one with the largest velocity v^*.

However, choosing the saddle point with the largest v^* might according to counting arguments (as in Appendix F) be inconsistent with assumption B from Sect. V B of the existence of a family of uniformly translating fronts, since one expects the multiplicity of front solutions to be different for every saddle point (v^*, k^*). The discussion of this issue we defer to Section VI D, as for the applications discussed in Sect. V F, this problem does not rise.

2. Uniformly translating solutions Φ_v

In the analysis of the nonlinear diffusion equation in Sect. II, we saw that the uniformly translating solution Φ_v decayed as $e^{-\lambda\xi}$ with λ real for $v \geq v^*$. Here, $\lambda = \lambda_-(v)$ (2.16) is the smallest root of $v = s(\lambda)/\lambda$, where $s(\lambda)$ (5.7) here equals $s(\lambda) = \lambda^2 + 1$. $v \geq v^*$ implied Re $k = 0$, $\lambda = \mathrm{Im}\, k > 0$. These front solutions were found to be stable to perturbations which are steeper than the front solution Φ_v itself, provided there is no pushed front solution $v_c = v^\dagger$. The solutions with $v < v^*$ had Re $k \neq 0$, Re $\omega \neq 0$, and were unstable.

We will focus here on the immediate generalization of these results, i.e., assume that fronts with $v \geq v^*$ have Re $k = 0$, so that their asymptotic spatial decay is as $e^{-\lambda\xi}$. In particular, this gives for the pulled fronts

$$\begin{aligned} &\mathrm{Re}\ k^* = 0 \ , \qquad \mathrm{Re}\ \omega(k^*) = 0 \ , \\ &\lambda^* \equiv \mathrm{Im}\ k^* > 0 \ , \quad s(\lambda^*) \equiv \mathrm{Im}\ \omega(k^*) > 0 \ , \\ &D = \frac{1}{2}\frac{d^2 s}{d\lambda^2}\bigg|_{\lambda^*} > 0, \quad \mathrm{Im}\ D = 0 \ . \end{aligned} \tag{5.19}$$

With this assumption, we consider only the generic case, that dynamically accessible, uniformly translating solutions of *real* equations will be characterized by a real spatial decay rate λ, and a real growth rate s, and that they will leave a homogeneous state $\phi = 1$ behind. This might exclude some pathological cases of uniformly translating front solutions, that are not characterized by a real λ[9].

If the saddle point obeys (5.19), the expression for $t \gg 1$ (5.14) and $v = v^*$ for the Green's function G reduces to

$$G(\xi,t) = e^{-\lambda^*\xi}\ \frac{e^{-\xi^2/(4Dt)}}{\sqrt{4\pi D t}}\ \left(1 + O\left(\frac{D_3\xi}{D^2 t}\right)\right) \ , \quad \xi = x - v^* t \ . \tag{5.20}$$

Except for a rescaling of time and length scales with the real constants λ^* and D, this is precisely the functional form of (2.57).

If we consider the velocity $v(\lambda)$ of the family of front solutions whose asymptotic spatial decay is as $e^{-\lambda\xi}$ with real λ, then it is straight forward to see, *that Φ^* is the*

[9] Elsewhere [75], we will discuss an extension of the notion of uniformly translating fronts, that allows to write pattern forming fronts in the Swift-Hohenberg equation as uniformly translating solutions of a suitable set of *complex* amplitude-like modes, and for these Re $k \neq 0$. Similar considerations hold for fronts in the complex Ginzburg-Landau equation itself [66].

slowest of all these uniformly translating fronts: According to the linearized equation (5.5) the solution in the leading edge is as $e^{-\lambda x - i\omega(i\lambda)t}$. The resulting velocity v is

$$v(\lambda) = \frac{-i\omega(i\lambda)}{\lambda} = \frac{s(\lambda)}{\lambda} \quad \text{for all } \lambda \ . \tag{5.21}$$

The minimum of this curve is given by

$$0 = \left.\frac{\partial v(\lambda)}{\partial \lambda}\right|_{\lambda^*} = \left.\frac{1}{\lambda}\left(\frac{\partial s(\lambda)}{\partial \lambda} - \frac{s(\lambda)}{\lambda}\right)\right|_{\lambda^*} . \tag{5.22}$$

$$\left.\frac{d^2 v(\lambda)}{d\lambda^2}\right|_{\lambda^*} = \frac{2D}{\lambda^*} > 0 \ . \tag{5.23}$$

Taking into account that $\omega(k)$ is analytic, Eqs. (5.21) and (5.22) are equivalent to Eqs. (5.16) and (5.17), because at a saddle of an analytic function, the maximum as a function of real k coincides with a minimum as a function of imaginary k.

The analysis of the stability of the uniformly translating solutions proceeds largely as in Section II C: the existence of a family of front solutions implies, according to counting arguments as given in Appendix F, that there is at least a continuous spectrum of eigenmodes of the stability operator. Indeed, if we again write the temporal behavior of the stability eigenmodes as $e^{-\sigma t}$ and the steepness of the modes as Λ, and if we first focus on the spectrum of perturbations, that is also continuous in Λ, then we have for the front solutions with $v(\lambda) \geq v^*$: $\sigma = -(s(\Lambda) - v(\lambda)\Lambda)$. Expanding the Λ of the perturbation about the λ of the front, we then get

$$\begin{aligned} \sigma(\Lambda) &\approx -\left(\frac{\partial s(\lambda)}{\partial \lambda} - v(\lambda)\right)(\Lambda - \lambda) \ , \\ &= -\lambda \frac{\partial v(\lambda)}{\partial \lambda}\,(\Lambda - \lambda) \ , \end{aligned} \tag{5.24}$$

using (5.21) in the second line. Since we showed above that $\partial v/\partial\lambda < 0$ for $\lambda < \lambda^*$ ($v > v^*$), $\sigma(\Lambda) > 0$ for $\Lambda > \lambda$. This generalizes the result (2.43) for the nonlinear diffusion equation that the front solutions Φ_v are stable to modes from the continuous spectrum which are steeper than the front itself. In addition to the continuous Λ spectrum, there again may be discrete perturbation modes associated with the existence of pushed front solutions.

We show in Appendix F that the existence of a strongly heteroclinic front solution $\Phi^\dagger$ implies the existence of unstable strongly heteroclinic stability modes for $v < v^\dagger$, again in parallel to the results for the nonlinear diffusion equation. The central assumption of our further analysis is, of course, that we are in the pulled regime, and hence that such solutions are absent.

We finally note that the fact that $v(\lambda)$ has a minimum for $\lambda = \lambda^*, v = v^*$, implies that for $v < v^*$ front solutions decay to zero in an oscillatory manner for $\xi \to \infty$ as they have $\mathrm{Re}k \neq 0$. By expanding the function $v(\lambda)$ about the bifurcation point at v^*, λ^*, it is easy to show that for small $|v - v^*|$, this branch of solutions has $\mathrm{Im}(k - k^*) = \lambda - \lambda^* \approx (\lambda^*)^2 v'''/(12D)|v - v^*|$, $\mathrm{Re}k \approx \sqrt{\lambda^*|v - v^*|/D}$, where $v''' = \frac{\partial^3 v(\lambda)}{\partial \lambda^3}|_{\lambda^*}$. One usually has $v''' < 0$ and then such solutions are unstable according to a slight generalization of (5.24).

3. The leading edge representation

As in our analysis of the pulled dynamics of the nonlinear diffusion equation, we will find it expedient to study the large time asymptotics in the leading edge by using the leading edge representation ψ. For uniformly translating fronts, the immediate generalization of the transformation (2.62) from Section II is

$$\psi(\xi, t) = \phi(x, t)\ e^{\lambda^* \xi} \quad , \quad \xi = x - v^* t \ . \tag{5.25}$$

The linearized dynamical evolution equation for the leading edge representation now generalizes (2.61) to

$$\partial_t \psi = \mathcal{D}\psi + o\left(\psi^2\ e^{-\lambda^* \xi}\right) \ , \tag{5.26}$$

where

$$\mathcal{D} = e^{\lambda^* \xi}\ \mathcal{L}_{v^*}(\infty)\ e^{-\lambda^* \xi} = \sum_{n=2}^{N} D_n\ \partial_\xi^n \ . \tag{5.27}$$

A short calculation (Appendix H) reveals that the constants D_n can be expressed in terms of the dispersion relation $\omega(k)$ (5.6) as as

$$\begin{aligned} D_n &= \frac{1}{n!}\,\frac{\partial^n}{\partial(-\lambda)^n}\left(-i\omega(i\lambda) - v^*\lambda\right)\Big|_{\lambda=\lambda^*} \ , \\ &= \frac{1}{n!}\,\frac{\partial^n}{\partial(-\lambda)^n}\left(s(\lambda) - v^*\lambda\right)\Big|_{\lambda=\lambda^*} \ . \end{aligned} \tag{5.28}$$

Note, that in this generalized leading edge representation (5.26) the coefficients of ψ and $\partial_\xi \psi$ again are vanishing. This is an immediate consequence of the proper choice of v^* and λ^*. In fact, for uniformly translating fronts (5.19), $D_0 = 0$ is equivalent to the proper choice of the velocity v^* (5.16), and $D_1 = 0$ is equivalent to the saddle point equation (5.17) fixing λ^* for given v^*. D_2 is obviously identical to D from (5.13). We will see below, that in the leading edge, the contribution proportional to $D_2 = D$ gives the dominant contribution, while D_3 appears only in the subdominant term, similar to what we already observed in (5.15). We therefore will essentially recover the results of the nonlinear diffusion equation (1.1), which had the particular property of $D_n = 0$ for $n > 2$.

4. The relaxation analysis

We have now laid the ground work for the extension of the analysis of the relaxation of pulled fronts for our more general equation (5.1) in the case of steep initial conditions

$$\lim_{x\to\infty} \phi(x,0)\, e^{\lambda^* x} = 0 \ . \tag{5.29}$$

The analysis in Section III for the nonlinear diffusion equation (1.1) was based on the following steps:

Step 1.
The proper choice of the comoving coordinate system

$$\xi_X = x - v^* t - X(t) \quad , \quad \dot{X} = \frac{c_1}{t} + \frac{c_{3/2}}{t^{3/2}} + \dots \ , \tag{5.30}$$

allowing for a logarithmic shift $X(t) \propto \ln t$ in comparison with to the asymptotic coordinate system $\xi = x - v^* t$,

Step 2.
An expansion of ϕ in the nonlinear interior part of the front about the asymptotic front profile $\Phi^*(\xi_X)$, taken, however, not in the frame moving with velocity v^*, but in the one with velocity $v(t) = v^* + \dot{X}(t)$

Step 3.
A resummation of this expansion of ϕ in the crossover region towards the leading edge, where the new variable $z = \xi_X^2/(4t)$ is introduced for the region with $\xi_X \geq O(\sqrt{t})$.

Step 4.
An analysis of the leading edge in variables z and t, where ϕ now is linearized about the unstable state $\phi = 0$, and not about Φ^*. The boundary condition that ϕ crosses over to the functional form of Step 3 for $z \ll 1$, and that ϕ is steeper than Φ^* for $z \gg 1$, now determine both the functional form of ϕ and the constants $c_{n/2}$ in $\dot{X}$. (We can think of this as a matching procedure.) In this analysis, the fact that the parameter $\alpha \neq 0$ in the asymptotics $\Phi^*(\xi_X) = (\alpha\xi_X + \beta)e^{-\lambda^*\xi_X}$ is nonzero (see Section II E 2) plays a central role.

The generalization of these steps to our equation (5.1) which is of higher order in space, is actually quite straight forward. We again use the general coordinate ξ_X (5.30) with $\dot{X}(t)$ to be determined. The interior expansion $\eta(\xi_X, t) = \phi - \Phi^*(\xi_X)$ from Section III B applies literally, except that we now need to use the linear operator $\mathcal{L}^* = \mathcal{L}_{v^*}(\xi_X)$ from (5.3). Accordingly, also the resummation (3.31) again is valid, and we again have

$$\phi = \Phi_{v(t)}(\xi_X) + O\left(\frac{1}{t^2}\right) \ , \tag{5.31}$$

with Φ_v a uniformly translating solution of (5.1) with velocity v. The correction $O(1/t^2)$ is again non-vanishing and non-universal, in that it will depend on the precise initial conditions.

The expansion of the interior shape towards the leading edge (3.36) depends on both the differential operator $\mathcal{L}^*$ for $\xi \to \infty$, and on the shape of the asymptotic front Φ^* (3.32). Here, in particular, $\alpha \neq 0$ plays a central role. Again, both the fact that the pulled velocity is precisely defined through the condition that two roots of the dispersion relation coincide (see the discussion in Section V C 2), and considerations similar to those in Section II E 2 show that again

$$\Phi^*(\xi) = (\alpha\xi + \beta)\, e^{-\lambda^*\xi} \ , \quad \xi \gg 1 \ , \tag{5.32}$$

with, generally,

$$\alpha \neq 0 \ , \tag{5.33}$$

since a calculation resulting in a generalization of (2.66) can be set up along similar lines: If there is a bounded uniformly translating solution $\Phi_v(\xi)$, then upon going to the leading edge representation and upon integrating the equation for $\psi_v(\xi)$ once over ξ, we find that α can be expressed in terms of the spatial integral over all nonlinear terms.

How does the dominating leading edge now develop under inclusion of the higher spatial derivatives? First of all, we observe, that the large-t-solutions (5.20) and (2.57) of the linearized equation (5.5) are in leading order identical up to rescaling, i.e., the saddle point approximation again renders the spreading around the asymptotic exponential solution diffusive. This suggests that the leading edge can be analyzed by the same type of similarity variables (z, t) as in (3.40). In fact, in our shifted coordinate frame ξ_X (5.30), the leading edge representation is

$$\phi(x,t) = e^{-\lambda^*\xi_X}\psi(\xi_X, t) \ , \tag{5.34}$$

$$\partial_t\psi = \mathcal{D}\psi + \dot{X}\,(\partial_\xi - \lambda^*)\,\psi + o(e^{-\lambda^*\xi_X}) \ , \tag{5.35}$$

with the differential operator $\mathcal{D}$ from Eq. (5.27). After a rescaling with

$$\zeta_Y = \lambda^*\xi_X \quad , \quad \tau = D_2{\lambda^*}^2 t \quad , \quad d_n = \frac{D_n{\lambda^*}^n}{D_2{\lambda^*}^2} \ ,$$
$$\dot{Y} = \frac{\dot{X}\lambda^*}{D_2{\lambda^*}^2} = \frac{C_1}{\tau} + \frac{C_{\frac{3}{2}}}{\tau^{3/2}} + \dots \ ,$$
$$C_n = c_n\lambda^* \left(D_2{\lambda^*}^2\right)^{n-1} \ , \tag{5.36}$$

this equation takes the form

$$\partial_\tau\psi = \left(\partial_\zeta^2 + \sum_{n=3}^{N} d_n\partial_\zeta^n\right)\psi + \dot{Y}\,(\partial_\zeta - 1)\,\psi \ , \tag{5.37}$$

which is very analogous to Eq. (3.38) except that there are now the higher derivatives ∂_ζ^n. As we show explicitly in Appendix I, the leading edge can be analyzed with the same ansatz as in (3.40) and (3.42),

$$\psi(\zeta_Y,\tau) = e^{-z}\, G(z,\tau) \quad , \quad z = \frac{\zeta_Y^2}{4\tau} \; , \tag{5.38}$$
$$G(z,\tau) = \sqrt{t}\, g_{\frac{-1}{2}}(z) + g_0(z) + \frac{g_{\frac{1}{2}}(z)}{\sqrt{t}} + \dots \; ,$$

and in rescaled variables, one gets

$$C_1 = \frac{-3}{2} \quad , \quad C_{\frac{3}{2}} = \frac{3\sqrt{\pi}}{2} \quad , \quad g_{\frac{-1}{2}}(z) = 2\alpha\sqrt{z} \; , \tag{5.39}$$
$$g_0(z) = \beta\,(1-2z) + 3\alpha(1+d_3)z - 2\alpha d_3 z^2 - \frac{3\alpha}{2}\, F_2(z)$$
$$+ 6\alpha\,\sqrt{\pi\, z}\,\left(1 - M\left(\frac{-1}{2},\frac{3}{2},z\right)\right) \; .$$

In these variables, the result is identical with that for the nonlinear diffusion equation in Section III, except for the additional terms proportional to d_3 in $g_0(z)$. In particular, the velocity parameters C_1 and $C_{3/2}$, and the leading order contribution $g_{\frac{-1}{2}}(z)$ are independent of the value of d_3, just like the subdominant term β from (5.32) only enters $g_0(z)$, but not the other quantities. That for the problem written in variables z and t, d_3 can only contribute in subleading order, is in fact immediately obvious after the transformation. It is surprising, however, that the subleading velocity coefficient $C_{3/2}$ is independent of the value of d_3. We will find it to be unchanged even for much more general equations.

In terms of the unscaled variables, the universal algebraic convergence of the velocity is given by

$$v(t) = v^* - \frac{3}{2\lambda^* t}\left(1 - \sqrt{\frac{\pi}{(\lambda^*)^2 D t}}\,\right) + \cdots \tag{5.40}$$

where v^* and λ^* are determined by the saddle point equations (5.16) and (5.17) together with (5.12), and where the diffusion coefficient D (5.13) equals D_2 from (5.28). The central results of this analysis are summarized in Table I.

D. Generalization to single *p.d.e.*'s of higher order in time

We now proceed in two further steps of generalization. In the present Section we first discuss partial differential equations for a single field $\phi(x,t)$, which include higher order temporal derivatives as well as mixed temporal and spatial derivatives. These are of the form

$$F\Big(\phi,\ \partial_x\phi,\ \dots,\ \partial_x^N\phi,\ \partial_t\phi,\ \dots,\ \partial_t^M\phi,$$
$$\partial_t\partial_x\phi,\ \dots,\ \partial_t^M\partial_x^N\phi\Big) = 0 \; , \tag{5.41}$$

generalizing (5.1) to $M \geq 1$. In Section V E, we then also deal with difference or integro-differential equations and coupled equations.

The extension to equations of type (5.41) presents no conceptual difficulty — we will follow here a route that is the immediate generalization of the discussion in the previous Section. The new elements in the discussion will be the fact that higher order temporal derivatives and mixed spatial and temporal derivatives are generated in the dynamical equation for the leading edge representation ψ, but as we shall see, these turn out not to affect the expression for the velocity relaxation and for the relaxation of the shape in the interior front region. The notation in (5.48) – (5.54), which may strike the reader at first sight as unnecessarily heavy, prepares for the discussion of even more general equations and sets of equations in V E, where finding a proper scalar leading edge representation is less straight forward than here.

If we linearize (5.41) about $\phi = 0$, we get an equation of the form

$$\sum_{m=0}^{M}\sum_{n=0}^{N} a_{mn}\, \partial_t^m\, \partial_x^n\, \phi(x,t) + o(\phi^2) = 0 \; . \tag{5.42}$$

For solving the initial value problem in time, it is convenient to Fourier-transform in space

$$\phi(x,t) = \int_{-\infty}^{\infty} \frac{dk}{2\pi}\, e^{ikx}\, \tilde{\phi}(k,t) \; . \tag{5.43}$$

Below we will use the superscript $\tilde{}$ to denote a quantity Fourier transformed in space.

The Fourier transformation of (5.42) results in an *o.d.e.* of order M for every Fourier mode $\tilde{\phi}(k,t)$:

$$\sum_{m=0}^{M} A_m(k)\, \partial_t^m\, \tilde{\phi}(k,t) = 0 \quad , \quad A_m(k) = \sum_{n=0}^{N} a_{mn}(ik)^n \; . \tag{5.44}$$

Obviously, we need M functions to specify the initial conditions. We write these as an M-dimensional vector:

$$\underline{\tilde{\phi}} = (\tilde{\phi}, \partial_t\tilde{\phi}, \dots, \partial_t^{M-1}\tilde{\phi}) \; . \tag{5.45}$$

The equation of motion (5.44) can now be written in Fourier space as

$$\partial_t\, \underline{\tilde{\phi}}(k,t) = -\underline{\underline{\tilde{T}}}(k) \cdot \underline{\tilde{\phi}}(k,t) \; , \tag{5.46}$$

with the $M \times M$ matrix

$$\underline{\underline{\tilde{T}}}(k) = \begin{pmatrix} 0 & -1 & 0 & \cdots & 0 \\ 0 & 0 & -1 & & 0 \\ & \vdots & & \ddots & \\ 0 & 0 & 0 & \cdots & -1 \\ \frac{A_0}{A_M} & \frac{A_1}{A_M} & \frac{A_2}{A_M} & \dots & \frac{A_{M-1}}{A_M} \end{pmatrix} \; . \tag{5.47}$$

For later use, we here already define the matrix

$$\underline{\underline{\hat{S}}}(k,\omega) = A_M(k)\ \left(\underline{\underline{\tilde{T}}}(k) - i\omega\ \underline{\underline{1}}\right)\ , \tag{5.48}$$

which later will result from a Fourier-Laplace transformation as in (5.18). Here and below, we use the superscript $\hat{}$ to denote a Fourier-Laplace transformed quantity, to distinguish it from spatially Fourier transformed quantities, which are indicated with a tilde.

The M eigenvalues $\omega_m(k)$ $(m = 1, \ldots, M)$ of the matrix $\underline{\underline{\tilde{T}}}(k)$ are determined by the characteristic equation $S\big(k, \omega_m(k)\big) = 0$, where $S(k,\omega)$ is the characteristic polynomial

$$\begin{aligned} S(k,\omega) = \det\, \underline{\underline{\hat{S}}}(k,\omega) &= \sum_{m=0}^{M} A_m(k)\ (-i\omega)^m \\ &= \sum_{m=0}^{M}\sum_{n=0}^{N} a_{mn}\ (-i\omega)^m\ (ik)^n\ . \end{aligned} \tag{5.49}$$

Defining the eigenvectors $\underline{\tilde{U}}_m(k)$ of the matrix $\underline{\underline{\tilde{T}}}(k)$ through

$$\underline{\underline{\tilde{T}}}(k) \cdot \underline{\tilde{U}}_m(k) = i\omega_m(k)\ \underline{\tilde{U}}_m(k)\ , \tag{5.50}$$

and their adjoints through

$$\underline{\tilde{U}}^{\dagger}_m(k) \cdot \underline{\tilde{U}}_n(k) = \delta_{mn}\ , \tag{5.51}$$

the matrix $\underline{\underline{\tilde{T}}}(k)$ can be written as

$$\underline{\underline{\tilde{T}}}(k) = \sum_{m=1}^{M} i\omega_m(k)\ \underline{\tilde{U}}_m(k) \times \underline{\tilde{U}}^{\dagger}_m(k)\ , \tag{5.52}$$

where $\times$ denotes the outer product.

Now (5.46) is easily integrated in time and the Fourier transformation inverted. We find in generalization of (5.9) and (5.10):

$$\underline{\phi}(x,t) = \int_y \underline{\underline{G}}(x-y,t) \cdot \underline{\phi}(y,0)\ , \tag{5.53}$$

$$\underline{\underline{G}}(x,t) = \sum_{m=1}^{M} \int \frac{dk}{2\pi}\ e^{ikx - i\omega_m(k)t}\ \underline{\tilde{U}}_m(k) \times \underline{\tilde{U}}^{\dagger}_m(k)\ . \tag{5.54}$$

Obviously, the quickest growing mode $\underline{\tilde{U}}_m(k)$ — characterized now by Fourier mode k and branch of solutions m — again will be determined by a saddle point (5.16), (5.17). We now have the choice from $M \times N$ saddle points. As in (5.12), we again pick the one with the largest velocity v^* in the comoving frame and determine its $k^* = i\lambda^*$, D etc. As before, we assume uniform translation as in (5.19), so that k^* and $\omega(k^*)$ are purely imaginary. Suppose, that v^* lies on the branch $\omega_1(k)$. We then find in the comoving frame $\xi = x - v^*t$ for long times t:

$$\underline{\underline{G}}(\xi,t) = e^{-\lambda^*\xi}\ \frac{e^{-\xi^2/(4Dt)}}{\sqrt{4\pi Dt}}\ \underline{\tilde{U}}_1(k^*) \times \underline{\tilde{U}}^{\dagger}_1(k^*) + \ldots\ , \tag{5.55}$$

in generalization of (5.20).

This result shows, that in the long time limit, the Green's function $\underline{\underline{G}}$ projects onto the eigendirection $\underline{\tilde{U}}_1(k^*)$. The result (5.55) is not restricted to the explicit form (5.47) of the matrix $\underline{\underline{T}}$, so it applies to sets of coupled *p.d.e.*'s just as well, as they also can be written in the form (5.46). Projection onto the eigendirection $\underline{\tilde{U}}_1(k^*)$ then defines the scalar leading edge equation resulting from coupled *p.d.e.*'s. We will further exploit this property in the following section.

In the present section, we just use (5.55) to calculate v^* and λ^*, and to demonstrate why the leading edge transformation catches the relevant dynamics. Proceeding as in earlier Sections, the scalar equation (5.42) now transforms under the leading edge transformation with v^* and λ^* to

$$\phi(x,t) = e^{-\lambda^*\xi}\ \psi(\xi,t)\ \ ,\ \ \xi = x - v^*t\ , \tag{5.56}$$

$$\begin{aligned} 0 &= \sum_{m=0}^{M}\sum_{n=0}^{N} a_{mn}\ (\partial_t - v^*\partial_\xi + v^*\lambda^*)^m\ (\partial_\xi - \lambda^*)^n\ \psi \\ &= \sum_{m=0}^{M}\sum_{n=0}^{M+N} b_{mn}\ \partial_t^m\ \partial_\xi^n\ \psi(\xi,t)\ . \end{aligned} \tag{5.57}$$

Just as the a_{mn} from Eq. (5.42) can be written in terms of derivatives of the characteristic polynomial $S(k,\omega)$ (5.49) as

$$a_{mn} = \frac{(i\partial_\omega)^m}{m!}\ \frac{(-i\partial_k)^n}{n!}\ S(k,\omega)\Big|_{(k=\omega=0)}\ , \tag{5.58}$$

so can the b_{mn} in (5.61) be written as derivatives as well, similar to (5.28). It simplifies the notation to use coordinates expanded about the saddle point by introducing the variables

$$\Omega = \omega - v^*k\ ,\quad q = k - k^* = k - i\lambda^*\ , \tag{5.59}$$

and by defining

$$\begin{aligned} S^*(q,\Omega) = S(k^*+q, \omega^* + v^*q + \Omega)\ , \\ k^* = i\lambda^*\ \ ,\ \ \omega^* = v^*k^*\ . \end{aligned} \tag{5.60}$$

When we will later consider the Fourier-Laplace transform of $\psi(\xi,t)$ in the frame ξ, the frequency in this frame will turn out to be Ω and the wavenumer will turn out to be q, since $e^{-i\omega t + ikx} = e^{-\lambda^*\xi}(e^{-i\Omega t + iq\xi})$. Accordingly, the long time–small gradient expansion of $\psi(\xi,t)$ will correspond to a small Ω–small q expansion. Indeed, in line with this interpretation, inspection of (5.57) shows that the b_{mn} are simply

$$b_{mn} = \frac{(i\partial_\omega)^m}{m!}\,\frac{(-i)^n(\partial_k + v^*\partial_\omega)^n}{n!}\,S(k,\omega)\Big|_{(k^*,v^*k^*)}$$
$$= \frac{(i\partial_\Omega)^m}{m!}\,\frac{(-i\partial_q)^n}{n!}\,S^*(q,\Omega)\Big|_{(q=\Omega=0)} \quad . \qquad (5.61)$$

We will discuss the precise correspondence between the formulation in terms of S and the dispersion relation $\omega_1(k)$ below, and just note here that the saddle point equations that determine λ^* and v^* are expressed by

$$b_{00} = S^*(0,0) = 0 \ , \quad b_{01} = -i\partial_q S^*(q,\Omega)|_{q=\Omega=0} = 0 \ . \qquad (5.62)$$

After dividing the whole equation (5.57) by b_{10} and introducing the notations

$$D_n = -\frac{b_{0n}}{b_{10}} \ , \quad w = \frac{b_{11}}{b_{10}} \ , \quad \tau_1 = \frac{b_{20}}{b_{10}} \ , \quad \text{etc.} \ , \qquad (5.63)$$

the terms with the lowest derivatives are

$$\Big(\partial_t + \tau_1\,\partial_t^2 + \ldots - D_2\,\partial_\xi^2 - D_3\,\partial_\xi^3 + \ldots \qquad (5.64)$$
$$+ w\,\partial_t\partial_\xi + \ldots\Big)\,\psi + o(\psi^2\,e^{-\lambda^*\xi}) = 0 \ .$$

This is the leading edge equation in its most general form. Note, that after the leading edge transformation, the coefficient w may be nonzero, even if the coefficient $a_{11} = 0$ of $\partial_t\partial_x\phi$ in the original equation of motion (5.44) vanishes.

To show the connection with our discussion of first order equations in earlier Sections, it is instructive to analyze the relation between S and the dispersion relation. The various branches $\omega_m(k)$ or $\Omega_m(q)$ of the dispersion relation are defined implicitly through the roots of

$$S(k,\omega_m(k)) = 0 \quad \Longleftrightarrow \quad S^*(q,\Omega_m(q)) = 0 \ , \qquad (5.65)$$

As before, let $\omega_1(k)$ ($\Omega_1(q)$) be the branch on which the saddle point determining v^* lies. Upon differentiating (5.65) once with respect to k or q and using Eqs. (5.61) and (5.62), we get our familiar result

$$\frac{d\omega_1(k)}{dk}\Big|_{k^*} = v^* \quad \Longleftrightarrow \quad \frac{d\Omega_1(q)}{dq}\Big|_{q=0} = 0 \ . \qquad (5.66)$$

Likewise, by differentiating (5.65) twice, we get

$$\frac{d^2\Omega_1(q)}{dq^2}\Big|_{q=0} = \frac{d^2\omega_1(k)}{dk^2}\Big|_{k^*} = -\,\frac{\partial_q^2 S(q,\Omega)}{\partial_\Omega S(q,\Omega)}\Big|_{q=\Omega_1(0)=0} \ . \qquad (5.67)$$

If we combine this with the expression $D = -b_{02}/b_{10}$, we recover our familiar expression

$$D = \frac{\partial_q^2 S(q,\Omega)}{2i\partial_\Omega S(q,\Omega)}\Big|_{q=\Omega_1(0)=0} = \frac{id^2\Omega_1(q)}{2dq^2}\Big|_{q=0} \ ,$$
$$= \frac{id^2\omega_1(k)}{2dk^2}\Big|_{k^*} \ . \qquad (5.68)$$

For the case of an equation which is of first order in time, one can easily check that our general expression for D_n reduces to the one given before in (5.28), $D_n = (-i/n!)d^n\omega/d(ik)^n|_{k^*}$.

Before we discuss the consequences of (5.64), we note in passing that formally, we could have proceeded directly from the linearized equation of motion (5.42) to the leading edge representation (5.57), and hence to (5.64), by choosing the two parameters v^* and λ^* such, that the two conditions $b_{00} = 0 = b_{01}$ are obeyed. The detour from this straightforward transformation via the saddle point analysis was taken to bring out the physical origin of the transformation in this context and to show why one has to use the saddle point (v^*, λ^*) with the largest v^*. In addition, it explicitly shows, how a particular "direction" $\underline{U}_1(k^*)$ of the vector field $\underline{\phi}$ corresponds to the slow leading edge dynamics. We will see in the next section, that for coupled equations, there is some freedom in choosing the most physical projection in defining the scalar leading edge variable.

Let us now analyze the implications of the leading edge representation (5.64). First of all, we observe, that a uniformly translating pulled front $\Phi^*(\xi) = e^{-\lambda^*\xi}\Psi^*(\xi)$ still will have the form (5.32) $\Psi^*(\xi) = (\alpha\xi + \beta)$, and that the argument for $\alpha \neq 0$ from Section II E 2 still does apply.

Can the extra terms $\tau_1\,\partial_t^2\psi$, $w\,\partial_t\partial_\xi\psi$ etc. change our relaxation prediction from Section V C? A short inspection shows, that after rewriting the equation in variables z and t, cf. (5.36) – (5.38) and (3.39), $w\,\partial_t\partial_\xi\psi$ will be of the same subleading order in $1/\sqrt{t}$ as $D_3\,\partial_\xi^3\psi$, while both the terms $\tau_1\partial_t^2\psi$ and $D_4\,\partial_\xi^4\psi$ will be one order lower. Also, when rewriting the equation in the variable $\xi_X = x - v^*t - X(t)$, higher temporal derivatives will create terms like $\ddot{X}$ and $\dot{X}^2$ from the exponential factor in the leading edge transformation $\phi(\xi_X,t) = e^{-\lambda^*\xi_X}\psi(\xi_X,t)$. Since these are of order $1/t^2$, they do not influence the leading and subleading terms.

We do not repeat the detailed calculation here, because it completely follows the lines of the earlier one. We find, that the result again is given by (5.39), except that the subleading $g_0(z)$ picks up another polynomial contribution from w besides the one from D_3, namely

$$g_0(z) = g_0(z)\Big((5.39)\Big) + 2\alpha\,w\lambda^*\,\left(z^2 - \frac{3}{4}\right) \ . \qquad (5.69)$$

The uniform velocity relaxation is invariably

$$v(t) = v^* - \frac{3}{2\lambda^* t}\left(1 - \sqrt{\frac{\pi}{(\lambda^*)^2 Dt}}\,\right) + \cdots \ , \qquad (5.70)$$

and the interior part of the front is again slaved to the tip like

$$\phi(x,t) = \Phi_{v(t)}(\xi_X) + O\left(\frac{1}{t^2}\right) \ . \qquad (5.71)$$

So the predictions from Table I also apply to *p.d.e.*'s with higher temporal derivatives like (5.40), if the front is pulled.

Thus we reach the important conclusion that *the universal power law convergence is not an artefact of the diffusion-type character of the nonlinear diffusion equation: it holds generally in the pulled regime of uniformly translating fronts, because the expansion about the saddle point, which governs the dynamics of the leading edge representation ψ, is essentially diffusive.*

E. Further generalizations

We now complete the last step in our discussion, and show that our results hold much more generally: even if the original dynamical equation is not a *p.d.e.*, the dynamical equation for the appropriate leading edge variable ψ is *still* the same diffusion type equation (5.64), and consequently, our results for the velocity and shape relaxation from Table I do apply.

When we have a set of coupled equations, we can view them as components of a vector field, using a notation as in (5.46) with a different matrix $\underline{\underline{\tilde{T}}}(k)$. The main complication we are facing in this case is that the leading edge dynamics then not only "selects" a velocity v^* in the pulled regime, but also an associated eigendirection $\underline{\tilde{U}}_m(k)$ in this vector space — this eigendirection determines the relative values of the various fields in the leading edge of the front. The long time dynamics in the frame moving with the pulled velocity v^* is then associated with a slow dynamics along this eigendirection, while the dynamics along the other eigendirections is exponentially damped. The appropriate *scalar* leading edge variable ψ will then turn out to be nothing but the projection of the dynamics along this slow direction.

The second complication is that we now consider equations, whose temporal dependence is not necessarily of differential type ∂_t^N: they may just as well be of difference type or contain memory kernels. To treat such equations, we also perform a Laplace transformation in time besides the Fourier transformation in space just as in (5.18) by defining

$$\hat{\phi}_m(k,\omega) = \int_0^\infty dt\ e^{i\omega t}\ \tilde{\phi}_m(k,t) \ . \qquad (5.72)$$

We thus consider dynamical systems that after the Fourier-Laplace-transformation are of the form

$$\sum_{m=1}^{M} \hat{S}_{nm}(k,\omega)\ \hat{\phi}_m(k,\omega) = \sum_{m=1}^{M} \tilde{H}_{nm}(k)\ \tilde{\phi}_m(k,t=0) \ , \quad n = 1,\ldots,M \qquad (5.73)$$

The terms on the right hand side generally arise upon partial integration of temporal derivative terms, when we take the Laplace transform. They contain the initial conditions. Before exploring the implications of (5.73), we first discuss in more detail the type of systems whose linear dynamical equations can be written in the above form.

Sets of p.d.e.'s: Single or coupled *p.d.e.*'s can generally be written in the matrix notation $\left(\partial_t + \underline{\underline{\tilde{T}}}(k)\right) \cdot \underline{\tilde{\phi}}(k,t) = 0$, Eq. (5.44), and after Laplace transformation immediately yield (5.73), with the matrices $\underline{\underline{\hat{S}}}(k,\omega) = A_M(k)\ \left(\underline{\underline{\tilde{T}}}(k) - i\omega\ \underline{\underline{\tilde{1}}}\right)$ as before in (5.48), and $\underline{\underline{\tilde{H}}}(k) = A_M(k)\ \underline{\underline{1}}$. The leading edge behavior of single *p.d.e.*'s, where the matrix $\underline{\underline{\tilde{T}}}(k)$ has the explicit form (5.47), was discussed in the previous section. For coupled *p.d.e.*'s, the derivation of a scalar leading edge equation is not as straight forward, and also leaves some freedom, as we discuss below and for an example in Appendix J. Nevertheless, we will see that the results summarized in Table I are robust, in that they do not depend on the particular choice made. We discuss examples of single *p.d.e.*'s in Sects. V F 1 and V F 4, and an example of sets of *p.d.e.*'s in V F 2. Of course, if one has a *p.d.e.* for a single scalar field ϕ, one can directly take the Fourier-Laplace transform without writing ϕ as a vector field. This yields a slight generalization of (5.73), the most important difference being that H then also depends on ω. Our results can obviously also be obtained via this route – see Section V E 2 for further details.

Difference-differential equations: When we have difference equations in space, the equations can also be reduced to the above form — the only difference is that upon Fourier transformation in space, the k-values can be restricted to lie in a finite interval (the "Brillouin zone", in physics terminology). An example will be discussed in Section V F 3. Likewise, when we analyze a dynamical equation with finite time difference, the Laplace integral can be replaced by a sum over integer times, but the "frequency" remains a continuous variable. The only difference is that upon Laplace inversion, the integral is over a finite interval of ω values. Examples of difference equations in both space and time, arising from numerical schemes, can be found in V F 6.

Equations with memory or spatial kernels: If the equation has memory and/or spatial kernels of the type $\int dx' \int_0^t dt' K(x-x', t-t')\phi(x',t')$ [107,108], then upon Fourier-Laplace transformation these just give rise to terms of the form $\hat{K}(k,\omega)\hat{\phi}(k,\omega)$ in (5.73), as will be illustrated with a simple example in Section V F 5. The only difference with the case of *p.d.e.*'s from this point of view then is that the elements $\hat{S}_{mn}$ then are not polynomials in ω and k, but more general functions of these arguments.

1. Long time asymptotics of the Green's function via a Fourier-Laplace transformation

We now return to the problem of extracting the long time behavior of the dynamical equation (5.73) in Laplace-Fourier representation. In analogy with our earlier analysis of *p.d.e.*'s, and following [56,58], we introduce the Green's function[10] $\underline{\underline{G}}(k,\omega)$ of the linear equations, defined by

$$\underline{\underline{\hat{G}}}(k,\omega) = \underline{\underline{\hat{S}}}(k,\omega)^{-1} \; . \tag{5.74}$$

$\underline{\underline{\hat{S}}}^{-1}$ is the inverse of the matrix $\underline{\underline{\hat{S}}}$. Eq. (5.73) now immediately can be solved as

$$\underline{\hat{\phi}}(k,\omega) = \underline{\underline{\hat{G}}}(k,\omega) \cdot \underline{\underline{\tilde{H}}}(k) \cdot \underline{\tilde{\phi}}(k, t=0) \; . \tag{5.75}$$

Now write the eigenvectors and eigenvalues of $\underline{\underline{\hat{S}}}$ in analogy to (5.50) – (5.52) as

$$\underline{\underline{\hat{S}}}(k,\omega) \cdot \underline{\hat{U}}_m(k,\omega) = u_m(k,\omega)\, \underline{\hat{U}}_m(k,\omega) \; . \tag{5.76}$$

The determinant of $\hat{S}$ can now be written as

$$S(k,\omega) = \det \underline{\underline{\hat{S}}}(k,\omega) = \prod_{m=1}^{M} u_m(k,\omega) \; . \tag{5.77}$$

and the characteristic equation

$$u_m(k, \omega_m(k)) = 0 \tag{5.78}$$

determines the dispersion relation $\omega_m(k)$ of the mode with eigendirection $\underline{\hat{U}}_m(k,\omega)$. Note that each eigenvalue $u_m(k,\omega)$ may be a nonlinear function of k and ω. Therefore it can happen that the equation $u_m(k,\omega) = 0$ specifies more than one branch $\omega(k)$ of the dispersion relation. For simplicity, we will not distinguish this possibility with our notation, but we stress, that our results are generally valid. For equations of the form (5.46), we can identify $u_m(k,\omega) = A_M(k)\,(i\omega_m(k) - i\omega)$ and $\underline{\hat{U}}_m(k,\omega) = \underline{\tilde{U}}_m(k)$.

Upon inverting the Fourier and the Laplace transformation, where the Laplace inversion requires a sufficiently large real γ, we now find for the Green's function in the comoving frame $\xi = x - vt$:

$$\begin{aligned}
\underline{\phi}(\xi,t) &= \int dy\, \underline{\underline{G}}(\xi - y, t) \cdot \int dy'\, \underline{\underline{H}}(y - y') \cdot \underline{\phi}(y', 0) \; , \\
\underline{\underline{G}}(\xi,t) &= \int_{-i\gamma-\infty}^{-i\gamma+\infty} \frac{d\omega}{2\pi} \int_{-\infty}^{\infty} \frac{dk}{2\pi}\, e^{ik\xi - i(\omega - vk)t}\, \underline{\underline{\hat{G}}}(k,\omega) \; , \\
\underline{\underline{\hat{G}}}(k,\omega) &= \sum_{m=1}^{M} \frac{\underline{\hat{U}}_m(k,\omega) \times \underline{\hat{U}}_m^{\dagger}(k,\omega)}{u_m(k,\omega)} \; .
\end{aligned} \tag{5.79}$$

The expression for $\underline{\underline{G}}(\xi,t)$ is the immediate generalization of (5.54). When we evaluate the Fourier-Laplace inversion of $\underline{\underline{G}}(\xi,t)$ in the long time limit, each term in the sum (5.79) can be evaluated by a so-called "pinch point" analysis [56,58] making use of expansions about zeroes of $u_m(k,\omega)$. We then need to deform not only the contour of k-integration, as in the saddle point analysis in the previous sections, but also the contour of ω integration. The pinch point analysis is based on first evaluating the k-integral, and then the resulting ω-integral. Alternatively, we can extract the long time dynamics by first closing the ω-contour, and then performing the k-integral. This last route is closer to the one of Sect. V D. For a further discussion of both approaches, we refer to Appendix K.

As always, there can in principle be several saddle point or pinch point solutions, and if this happens, the relevant one is the one corresponding to the largest velocity v^*. If we again write $u_1(k,\omega)$ for the eigenvalue on which this solution lies and as before use a superscript * for functions which are written in terms of the transformed variable Ω and q as in (5.59) and (5.60), the saddle or pinch point equations assume their familiar form

$$\begin{aligned}
u_1(k^*,\omega^*) = 0 \Longleftrightarrow u_1^*(0,0) = 0 \; , \\
(\partial_k + v^* \partial_\omega) u_1(k,\omega)|_{k^*,\omega^*} = 0 \Longleftrightarrow \partial_q u_1^*(q,\Omega)|_{0,0} = 0 \; .
\end{aligned} \tag{5.80}$$

Note that since S is the product of all eigenvalues, cf. Eq. (5.77), these equations are equivalent to those given before in terms of S, Eqs. (5.62). Likewise, we get for the long time asymptotics of the Green's function the immediate generalization of (5.55),

$$\underline{\underline{G}}(\xi,t) = e^{-\lambda^*\xi}\, \frac{e^{-\xi^2/(4Dt)}}{\sqrt{4\pi D t}}\, \frac{\underline{\tilde{U}}_1(k^*,\omega^*) \times \underline{\tilde{U}}_1^{\dagger}(k^*,\omega^*)}{i\partial_\omega u_1(k,\omega)|_{(k^*,\Omega^*)}} + \dots \; , \tag{5.81}$$

which is our usual Gaussian expression again, with D given by its familiar expression (5.68).

Our strategy in deriving the long–time front dynamics is always to use the long–time evaluation of the Green's function just to show how the pulled velocity v^* and the dominant exponential behavior $e^{-\lambda^*\xi}$ emerge, and to motivate why the leading edge variables $\psi(\xi,t)$ have

[10] A different choice for the definition of the Green's function is $\underline{\underline{\hat{G}}}(k,\omega) = \underline{\underline{\hat{S}}}(k,\omega)^{-1} \cdot \underline{\underline{\hat{H}}}(k)$, which avoids the convolution of the initial condition with $\underline{\underline{H}}(z)$ in (5.79), and also for equations of the form (5.44) leads to the easier expression $\underline{\underline{\hat{G}}}(k,\omega) = \left(\underline{\underline{\tilde{T}}}(k) - i\omega\, \underline{\underline{\mathbb{1}}}\right)^{-1}$. The advantage of the choice (5.74) is that we consistently work with derivatives of $S = \det \underline{\underline{\hat{S}}}$. We will discuss in Sect. V E 4, that the choice of $\underline{\underline{\hat{G}}}$ and of possible projections actually does not change the universal results from Table I.

essentially slow, diffusive dynamics. The analysis of the slow ψ dynamics and the matching to the front interior is most properly done by going back to the *p.d.e.*(s) for the spatio-temporal evolution of ψ. Switching back to the space–time formulation for ψ comes out most directly from Fourier-Laplace inversion of the small-q and small-Ω expansion of the ψ-equation. Indeed, for $\underline{\psi}(\xi,t)$, the appropriate Green's function is $e^{\lambda^*\xi}\underline{\underline{G}}(\xi,t)$, and according to (5.79) we have

$$e^{\lambda^*\xi}\,\underline{\underline{G}}(\xi,t) = \int \frac{d\Omega}{2\pi}\int \frac{dq}{2\pi}\, e^{iq\xi - i\Omega t}\,\hat{\underline{\underline{G}}}^*(q,\Omega)\ , \quad (5.82)$$

which confirms that Ω and q are the proper Fourier-Laplace variables of the leading edge variables $\underline{\psi}$.

2. The case of a single field

In contrast to our earlier matrix notation, a single equation for a single field $\phi(x,t)$ after Fourier-Laplace transformation can also be written in a scalar form:

$$S(k,\omega)\,\hat{\phi}(k,\omega) = \quad (5.83)$$
$$\text{initial conditions}\left\{\tilde{\phi}(k,0), \partial_t\tilde{\phi}(k,t)|_{t=0}, \cdots\right\}\ .$$

The most common and direct way to arrive at the above equation is by performing a Fourier-Laplace transformation on the original dynamical equation. In this case, one immediately gets the characteristic function $S(k,\omega)$ on the left hand side, while the partial integrations (or partial summations in the case of difference equations, where also the derivatives in the initial condition terms are replaced by finite difference versions) of higher order temporal derivatives yield ω-dependent initial condition terms on the right in (5.83). Of course, we can also arrive at this equation via the route of Section V D, where we introduced a vector notation for a scalar *p.d.e.* of higher order in time, so that the dynamical equation is of matrix form (5.73). Indeed, when we then calculate $\det \underline{\underline{S}}(k,\omega)$ with $\underline{\underline{S}}(k,\omega) = A_M(k)\left(\hat{\underline{\underline{T}}}(k) - i\omega\hat{\underline{\underline{1}}}\right)$ by developing the determinant along the last row of the matrix, one easily sees that one just retrieves the above result.

Of course, the asymptotic analysis of $\phi(\xi,t)$ parallels the earlier discussion of Section V D, irrespective of whether or not the equation is written in vector form. Again, the asymptotic spreading speed is given by a saddle point of $S(k,\omega)$. However, as we have seen, for analyzing the proper front dynamics, we want to return to the dynamical equation for the leading edge variable ψ. For the case of a *p.d.e.*, this can be done simply by transforming the original equation for ϕ to the leading edge representation $\psi(\xi,t) = e^{\lambda^*\xi}\phi(\xi,t)$, but for difference equations or equations with memory terms, additional steps are clearly necessary. The general analysis is based on the observation that in the leading edge representation, the dynamical equation is of the form

$$S^*(q,\Omega)\,\hat{\psi}(q,\Omega) = \text{initial condition terms.} \quad (5.84)$$

If we expand S^* in q and Ω_m and perform an inverse Fourier-Laplace transform, we immediately arrive at the *p.d.e.* (5.57) for $\psi(\xi,t)$ with coefficients b_{mn} given in terms of the derivatives of S^* according to (5.61)! From there on, the analysis completely follows the one in the last part of Section V D, and we recover again all our familiar expressions for the relaxation of the front velocity and the profile.

We stress that for a *given* equation, the transformation to the leading edge variable can be done *exactly*. If this is done for a *p.d.e.*, we again get a *p.d.e.* of finite order. As no approximations are made, the resulting equation still allows one to study the fast or small scale dynamics in the linear region as well. For finite difference equations or for integro-differential equations, the transformation to the leading edge variable ψ still results in a finite difference equation of integro-differential equation: the usual *p.d.e.* for ψ then only emerges if *in addition* a gradient expansion is made for ψ. Such an expansion will obviously contain an infinite number of terms. (We will see explicit examples of this in Sections V F 3, V F 5, and V F 6). Normally, such an expansion is, of course, not of much use. However, when we turn to the long time relaxation towards pulled fronts, ψ becomes *arbitrarily smooth and slow* and hence the derivatives become nicely ordered. Moreover, the long-time large-scale relaxation of ψ corresponds precisely to the low-frequency small-wavenumber behavior of the Fourier-Laplace transform and this is why the expansion of S^* gives the proper evolution equation to analyze the front relaxation: As (5.61) shows, the coefficients b_{mn} in this equation are then nothing but the expansion coefficients of the characteristic equation $S^*(q,\Omega)$ for small q and Ω. In other words, *independently of whether we started from a differential, a difference or an integro-differential equation, we find at this point always the same p.d.e. for the leading edge variable ψ, and hence the same expression for the velocity relaxation!*

Let us finally remark, that instead of the leading edge transformation, we here also could have performed a leading edge projection onto the slow dynamics, as discussed in the following section. We will show, that the universal results of Table I do not depend on this choice.

3. The case of a set of fields and possible projections

For dynamical equations which inherently consist of sets of equations for more than one field, one obviously can only arrive at an equation for a scalar variable ψ by some kind of projection onto the slow direction. The way in which one projects out the slow dynamics clearly entails a certain freedom of choice. For a given equation, the "best" choice may be obvious, but in general there

is some ambiguity. We will illustrate this explicitly in Appendix J.

We note first, that a vector field $\underline{\hat{\psi}}(q,\Omega)$ can be decomposed into its dynamical components $\hat{\pi}_m(q,\Omega)$ as

$$\underline{\hat{\psi}}(q,\Omega) = \sum_{m=1}^{M} \hat{\pi}_m(q,\Omega)\, \underline{\hat{U}^*}_m(q,\Omega) \ , \tag{5.85}$$

$$\hat{\pi}_m(q,\Omega) = \underline{\hat{U}^*}_m{}^{\dagger}(q,\Omega) \cdot \underline{\hat{\psi}}(q,\Omega) \ , \tag{5.86}$$

where the superscript * on the eigenvectors $\underline{U}_m$ and eigenvalues u_m is to remind us that these are written in terms of the variables q and Ω.

Each $\hat{\pi}_m(q,\Omega)$ has its own dynamics, cf. (5.84),

$$u^*_m(q,\Omega)\, \hat{\pi}_m(q,\Omega) = \text{initial condition terms}_m \ . \tag{5.87}$$

The natural projection onto a scalar leading edge variable is thus onto the eigendirection with the largest v^*, which we denote with $\underline{\hat{U}^*}_1(q,\Omega)$. We then identify the scalar leading edge variable with $\hat{\pi}_1(q,\Omega)$. Inverting now the Fourier-Laplace transformation, we find a *p.d.e.* for $\pi_1(\xi,t)$ of the form (5.57) with the coefficients

$$b^{(1)}_{mn} = \frac{(i\partial_\Omega)^m}{m!}\, \frac{(-i\partial_q)^n}{n!}\, u^*_1(q,\Omega)\Big|_{(q=\Omega=0)} \ . \tag{5.88}$$

Defining the saddle point parameters just as in (5.62) and (5.63) for Eq. (5.57), they in general will depend on whether we derived the coefficients from S or from u_1. However, we will argue below, that the saddle point parameters v^*, λ^* and D do not depend on this choice.

Though the projection onto $\underline{\hat{U}^*}_1(q,\Omega)$ is formally the simplest one, the direction of projection is actually not very practical, as it depends on q and Ω. In practice, one will want to project along a fixed direction. Our previous analysis, summarized by Eq. (5.81), indeed suggested to project the long time dynamics of the Green's function onto $\underline{U}_1(k^*,\omega^*) = \underline{\hat{U}^*}_1(0,0)$. Projection of $\underline{\hat{\psi}}(q,\Omega)$ onto this eigendirection yields

$$\begin{aligned}\hat{\psi}^p(q,\Omega) &= \underline{\hat{U}^*}_1{}^{\dagger}(0,0) \cdot \underline{\hat{\psi}}(q,\Omega) \\ &= \sum_{m=1}^{M} \hat{\pi}_m(q,\Omega)\, \underline{\hat{U}^*}_1{}^{\dagger}(0,0) \cdot \underline{\hat{U}^*}_m(q,\Omega) \ .\end{aligned} \tag{5.89}$$

Now only for $q \approx 0 \approx \Omega$, we have $\hat{\psi}^p(q,\Omega) \approx \hat{\pi}_1(q,\Omega)$, while for finite q and Ω, also $\hat{\pi}_m(q,\Omega)$ with $m > 1$ will contribute. Inverting the Fourier-Laplace transform and working in the frame $\xi = x - v^*t$, we find the contributions from $\hat{\pi}_{m>1}$ to decay exponentially in time. Such contributions we encountered already a number of times before, for the first time in Sect. II E. The more important contribution comes from the coefficient of $\hat{\pi}_1$, which is $\underline{\hat{U}^*}_1{}^{\dagger}(0,0) \cdot \underline{\hat{U}^*}_1(q,\Omega) = 1 - O(q,\Omega)$. These algebraic corrections in q and Ω actually modify the b_{mn} for the projection $\hat{\psi}^p(q,\Omega)$ in comparison to (5.88), except for the diffusion coefficient D, as we will see below.

Still other projections might be physically useful, and we discuss an explicit example in Appendix J. We now turn to the consequences of all these different choices.

4. The freedom of projection and the universality of Tables I and IV

At first sight, the leading edge transformation or the different leading edge projections each determine their own saddle or pinch point equations or expansion parameters b_{mn}, compare, e.g., (5.61) with (5.88).

Nevertheless, the definition of the saddle or pinch point parameters v^*, λ^* and D in Table IV does not depend on the choice of the leading edge transformation or projection, and hence, the universal relaxation results for the velocity $v(t)$ and the shape $\Phi_{v(t)}$ in Table I are independent of these as well.

For the saddle/pinch point equations of Table IV this conclusion is based on two observations: (*i*) $S(k,\omega)$ contains $u_1(k,\omega)$ as a factor (5.77). The saddle point is determined by a double root in k of $u_1(k,\omega)$, which can be written as

$$\begin{aligned}u^*_1(q,\Omega) &= b^{(1)}_{10}\ \left(-i\Omega + Dq^2 + \ldots\right) \\ = u_1(k,\omega) &= b^{(1)}_{10}\ \left(-i(\omega - v^*k) + D(k-k^*)^2 + \ldots\right) \ .\end{aligned} \tag{5.90}$$

D here obviously is defined as $D = -b^{(1)}_{02}/b^{(1)}_{10}$ with $b^{(1)}_{mn}$ from (5.88). The root (5.90) fully determines the lowest derivatives of $S = \prod_m u_m$ at the saddle point $q = 0 = \Omega$ — up to a constant prefactor, resulting from the other factors in S. (*ii*) The saddle point parameters are defined by homogeneous equations (5.62) or ratios of derivatives (5.63). So the prefactors depending on differentiation of either u_1 or S will cancel in the equations that determine v^*, λ^* and D. In particular, D defined by $D = -b_{02}/b_{10}$ in (5.63) is identical with $D = -b^{(1)}_{02}/b^{(1)}_{10}$ here and with other D's resulting from different projections.

The subleading terms D_3 and w for the scalar leading edge variable in (5.64), in contrast, do depend on the choice of projection. Hence, as there always will be a leading edge equation of form (5.64), and as the universal results summarized in Table I do not depend on the values of D_3 or w, Table I is a universal result, independent of the particular projection chosen. The subleading contribution $g_0(z)$ in the leading edge will always be solved as in (5.69), so it will not depend on initial conditions, but it will depend on the direction of projection through the parameters D_3 and w.

In conclusion, we reiterate that the relaxation results also apply to dynamical equations other than *p.d.e.*'s, because the dynamics of the leading edge representation ψ becomes arbitrarily slow and diffusive for long times. This allows one to do a gradient expansion in time and space for ψ, *even if the original equations are not p.d.e.'s!* In this case the path of analysis via the Fourier-Laplace transformation and pinch point analysis is necessary. For equations, that are of differential form in time, Fourier transformation in space and saddle point analysis is sufficient.

Definition of $\omega_m(k)$: $\quad S(k,\omega_m(k)) = 0$

Saddle point equations: (definition: $\lambda^* = ik^*$)

$$S(k^*,\omega^*) = 0 \iff \omega^* = \omega_m(k^*)$$

$$\left(\partial_k + v^*\partial_\omega\right) S|_{(k^*,\omega^*)} = 0 \iff v^* = \left.\frac{\partial\omega_m(k)}{\partial k}\right|_{(k^*,\omega^*)}$$

Comoving frame:

$$\text{Im }\left(\omega^* - v^*k^*\right) = 0 \iff v^* = \frac{\text{Im }\omega_m(k^*)}{\text{Im }k^*}$$

Diffusion constant:

$$D = \left.\frac{-i\left(\partial_k + v^*\partial_\omega\right)^2 S}{2\,\partial_\omega S}\right|_{(k^*,\omega^*)} \iff D = \left.\frac{i\partial^2\omega_m(k)}{2\,\partial k^2}\right|_{(k^*,\omega^*)}$$

In general, only saddle points with $\text{Re } D > 0$ *are relevant.*
In this paper only saddle points with D *real are considered.*

Table IV: The saddle or pinch point equations, determining v^*, $k^* = i\lambda^*$ and D for a given characteristic polynomial $S(k,\omega) = \det \underline{\underline{\hat{S}}}(k,\omega)$. If there are several saddle point solutions (v^*,λ^*), take the one with the largest v^*.

F. Applications

In this subsection, we support the above arguments by summarizing the results of numerical simulations of three equations — a spatially fourth order *p.d.e.*, a set of two coupled *p.d.e.*'s and a difference-differential equation — which are all in complete agreement with our predicted universal relaxation trajectory as in Table I, consisting of the velocity convergence (5.70), the slaved interior (5.71), and the cross-over to a diffusive type of dynamics in the leading ege for $\xi \gtrsim \sqrt{t}$. We also briefly consider a *p.d.e.* with second order temporal derivatives, an extension of the nonlinear diffusion equation with a memory kernel, and the discretization corrections in the Euler and in the semi-implicit numerical integration method for a nonlinear diffusion equation. The last is an example of a partial difference equation, both in time and in space, and we numerically verified its predictions already in Section IV.

1. The EFK equation

The EFK ("extended Fisher Kolmogoroff") equation is an extension of the nonlinear diffusion equation [65,64], which has been investigated quite intensely in the mathematical literature [70]. It reads

$$\partial_t\phi = \partial_x^2\phi - \gamma\partial_x^4\phi + \phi - \phi^3 \ . \tag{5.91}$$

A straightforward calculation [63] shows that the saddle point equations (5.16), (5.17) and (5.13) yield

$$\begin{aligned} v^* &= 2\lambda^*\left(1 - 2\gamma\lambda^{*2}\right) , \\ \lambda^* &= \left(\frac{1-\sqrt{1-12\gamma}}{6\gamma}\right)^{1/2} , \\ D &= \sqrt{1-12\gamma} \qquad \text{for } \gamma < \frac{1}{12} \ . \end{aligned} \tag{5.92}$$

For $\gamma > 1/12$, the saddle point solution has $\text{Re } k^* \neq 0$, and in agreement with this, the pulled fronts in this equation are then found to be non-uniformly translating and to generate periodic patterns [64]. We will therefore focus here on the regime $\gamma < 1/12$. The arguments of the Appendix of [65] for the multiplicity of front solutions (summarized in Appendix F) give evidence that this equation indeed admits a family of uniformly translating fronts in this regime. One also can prove, that the front cannot propagate with a larger velocity than v^*, if the initial conditions are sufficiently steep [74,75]. The convergence towards the pulled front solution should therefore be given by Eq. (5.40) for $v(t)$ and Eq. (5.31) or Eqs. (5.38)–(5.39) for the interior of the leading edge of the front profile. Fig. 12 shows some of the results of our numerical simulations for $v(t)$ at $\gamma = 0.08$. This value of γ is closely below the bifurcation value $\gamma_c = 1/12 = 0.083$.

The plot is of the same type as in Fig. 9(a) for the nonlinear diffusion equation.

The numerical grid sizes of the simulation are $\Delta x = 0.01 = \Delta t$. The system size is $L = 200$, the initial condition is characterized by $\lambda_{init} = 20$ and $x_0 = 25$. The analytical prediction for $\gamma = 0.08$ is according to (5.92): $D = 0.2$, $\lambda^* = \sqrt{5/3} = 1.29$, and $v^* = 4.4 \cdot \lambda^*/3 = 1.89$. The ratio between the $1/t$- and the $1/t^{3/2}$-contribution in $v(t)$ according to (5.40) is measured on the time scale

$$T = 1/({\lambda^*}^2 D) \ , \tag{5.93}$$

as in the dimensional analysis (5.36). For $\gamma = 0.08$, we have $T = 3$. The plot of Fig. 9(a) gave good results from time $t = 20$ on, where $T = 1$. It is therefore consistent, that the plot of Fig. 12 with $T = 3$ is good from times $t = 60$ on. We thus plot here the time interval $60 \leq t \leq 200$. One already can anticipate from the plot, that again a correction of v^* for the numerical finite difference code will be required, if we proceed to even higher precision. In conclusion, we find the results to be in full accord with our analytical predictions.

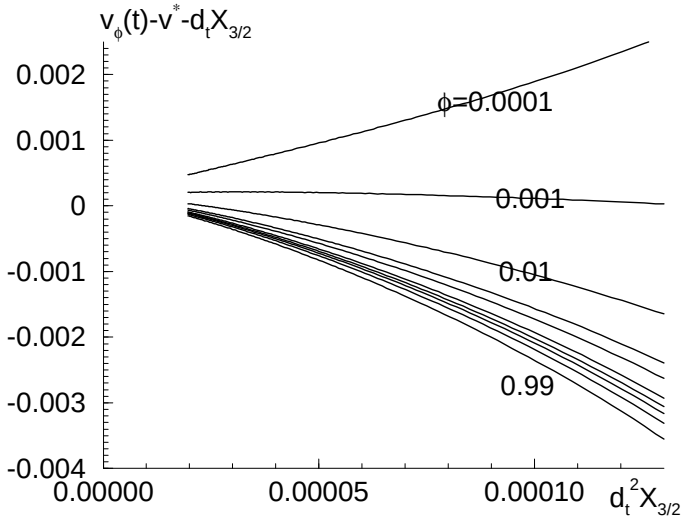

FIG. 12. Velocity relaxation in the EFK equation (5.91) for $\gamma = 0.08$: Plot of $v_\phi(t) - 2 - \dot{X}_{3/2}$ as a function of $\ddot{X}_{3/2}$ as in Fig. 9(a) for times $60 \leq t \leq 200$. System size $L = 200$, front position $x_0 = 25$, initial steepness $\lambda_{init} = 20$ in (4.4). Grid sizes $\Delta x = 0.01 = \Delta t$.

2. The streamer equations

Streamers are discharge patterns which result from the competition between an electron avalanche formation due to impact ionization, and the screening of the electric field by charges. For planar streamer fronts, the equation for the electron density σ and electric field E are [15]

$$\begin{aligned} \partial_t \sigma &= D_\sigma \partial_x^2 \sigma + \partial_x(\sigma E) + \sigma f_{str}(E) \ , \\ \partial_t E &= -D_\sigma \partial_x \sigma - \sigma E \ , \end{aligned} \tag{5.94}$$

where we have assumed, that in the region $x \gg 1$, where the electron density vanishes $\sigma^+ = \sigma(x \to \infty, t) = 0$, the electric field $E^+ = E(x \to \infty, t)$ does not change in time: $\partial_t E^+ = 0$. The field dependent ionization rate has a functional form like, e.g., $f_{str}(E) = |E| \ e^{-1/|E|}$. This is the functional form we use in our simulations. The state $(\sigma, E) = (0, E^+)$ is unstable, and also for these equations it is known [15], that they admit a one parameter family of uniformly translating front solutions. The dispersion relation for linear perturbations about the unstable state $\sigma = 0$, $E = E^+ < 0$ reads $-i\omega(k) = ikE^+ + f_{str}(E^+) - D_\sigma k^2$, where we choose to analyze the leading edge in a projection onto the σ-axis. The saddle point equations (5.16), (5.17) and (5.13) then yield

$$\begin{aligned} v^* &= -E^+ + 2\sqrt{D_\sigma f_{str}(E^+)} \ , \\ \lambda^* &= \sqrt{f_{str}(E^+)/D_\sigma} \ , \qquad (5.95) \\ D &= D_\sigma \ . \qquad (5.96) \end{aligned}$$

Again, the simulations of these equations show that the velocity convergence follows our analytical prediction (5.40). An example of our results is shown in Fig. 13 in a plot as in Figs. 9(a) and 12, where we track various heights of the electron density σ. The dimensionless time is $T = 1/f_{str}(E^+) = e^1 = 2.718$ for $E^+ = -1$. We plot our data for times $40 \leq t \leq 200$, and again find our predictions to hold.

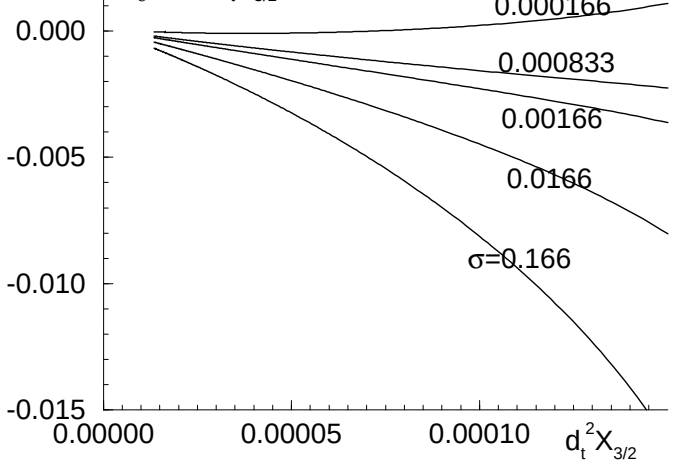

FIG. 13. Velocity relaxation in the streamer equations (5.94) for $E^+ = -1$ and $D = 0.1$, plotted as in Figs. 9(a) and 12 for times $40 \leq t \leq 200$. Initial condition: Gaussian electron density $\sigma(x,0) = 0.9\ e^{-x^2}$ (thus $\lambda_{init} = \infty$), $E(x,0) = -1$. System size $L = 400$, front position shifted back to $x_0 = 100$, after it is reached. Grid sizes: $\Delta x = 0.01$, $\Delta t = 0.0025$.

3. A difference-differential equation

We now summarize some key elements of our analysis [71] of the difference-differential equation

$$\partial_t C_j(t) = -C_j + C_{j-1}^2 \ \ , \ C_0(t) = 0 \ , \ C_{j\gg 1}(t) = 1 \ , \tag{5.97}$$

with j integer. This equation originates from kinetic theory [17]. If we transform with $\phi_j(t) = 1 - C_j(t)$ to

$$\begin{aligned} \partial_t \phi_j(t) &= -\phi_j + 2\phi_{j-1} - \phi_{j-1}^2 \ , \\ \phi_0(t) &= 1 \ \ , \ \phi_{j\gg 1}(t) = 0 \ , \end{aligned} \tag{5.98}$$

we have our usual notation with the state $\phi_j = 0$ being unstable and the state $\phi_j = 1$ stable. As usual, we consider fronts between these states, starting from sufficiently steep initial conditions. It is easy to see, that such initial conditions will create a pulled front [71].

Equation (5.98) provides the first illustration of our argument from Sect. V E, that our analysis applies to difference equations as well — with the only difference, that the spatial Fourier modes k now extend over a finite interval or "Brillouin zone" $0 \leq k < 2\pi$ only. Substitution of the Fourier ansatz $\phi_j \sim e^{-i\omega t + ikj}$ into the equation of motion linearized about the unstable state $\phi_j = 0$

$$\partial_t \phi_j = -\phi_j + 2\phi_{j-1} \tag{5.99}$$

yields the dispersion relation

$$-i\omega(k) = 2e^{-ik} - 1 \iff s(\lambda) = 2e^{\lambda} - 1 \ . \tag{5.100}$$

As discussed before, the long time asymptote of the leading edge is again determined by the saddle point which obeys (5.13), (5.16) and (5.17). This results in

$$v^* = 2e^{\lambda^*} = \frac{2e^{\lambda^*} - 1}{\lambda^*} \tag{5.101}$$

When we choose the solution with $v^* > 0$, the saddle point equations are solved by

$$\begin{aligned} -ik^* &= \lambda^* > 0 \ \text{ real} \\ v^* &= 2e^{\lambda^*} = 4.31107 \ , \\ \lambda^* &= (2e^{\lambda^*} - 1)/(2e^{\lambda^*}) = 0.768039 \ , \\ D &= D_2 = v^*/2 \ \ , \ \ D_n = (-)^n v^*/n! \ . \end{aligned} \tag{5.102}$$

The D_n are determined from (5.28). We now perform the leading edge transformation

$$\phi_j(t) = e^{-\lambda^* \xi}\ \psi(\xi, t) \ , \quad \xi = j - v^* t \ . \tag{5.103}$$

The large-time, small-gradient expansion in the leading edge now results in the *p.d.e.*

$$\partial_t \psi = D\partial_\xi^2 \psi + D_3 \partial_\xi^3 \psi + \dots \ . \tag{5.104}$$

The velocity convergence should again be given by (5.40), with v^*, λ^* and D given by (5.102). We do find indeed that the fronts in this equation are pulled, and that the velocity convergence follows (5.40). This is illustrated in Fig. 14, where we plot $(v(t) - v^* + 3/(2\lambda^* t))/t^{-3/2}$ as a function of $1/\sqrt{t}$. $v(t) = \dot{x}(t)$ is the velocity of the front defined as $x(t) = \sum_{j=0}^{\infty} \phi_j(t)$. The curve in Fig. 14 should extrapolate to $3/(2\lambda^*) \cdot \sqrt{\pi/({\lambda^*}^2 D)} = 3.0699$ as $1/\sqrt{t} \to 0$. This predicted asymptote is marked by the cross on the axis. Indeed, the data of $(v(t) - v^* + 3/(2\lambda^* t))/t^{-3/2}$ for $40 \leq t \leq 4000$ extrapolate very well to the predicted asymptote — also in view of the fact, that $t^{3/2} = O(2 \cdot 10^5)$ at the latest times. The slight offset at the end might be due either to finite system size L or to finite numerical discretization Δt.

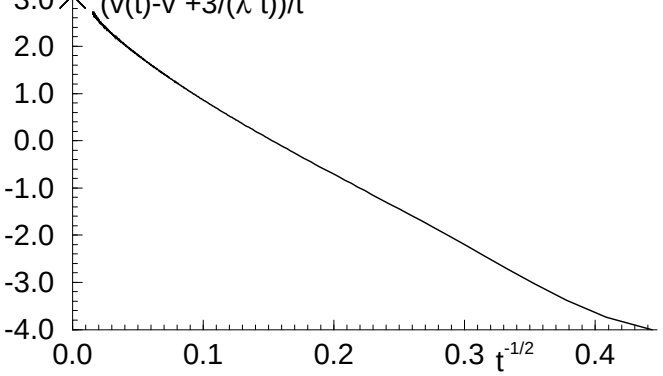

FIG. 14. Velocity relaxation for the difference-differential equation (5.97), where $v(t) = \dot{x}(t)$, and $x(t) = \sum_{j=0}^{\infty} \phi_j(t)$, see Eq. (5.98). Plotted is here $\big(v(t) - v^* + 3/(2\lambda^* t)\big)/t^{-3/2}$ as a function of $1/\sqrt{t}$ for times $40 \le t \le 4000$. The curve is predicted to extrapolate to $c_{3/2}$ as $1/\sqrt{t} \to 0$. The predicted value of $c_{3/2}$ is marked by the cross on the axis. Initial condition $\phi_j(0) = e^{-j^2}$. System size $N = 4000$ grid points. Front shifted back to $n_0 = 75$, after it has been reached. Temporal grid size $\Delta t = 0.0005$.

4. Diffusion equation with second order time derivative

Quite recently, it was shown [80] that, not surprisingly, fronts in a second order extension of the F-KPP equation,

$$\tau_2 \frac{\partial^2 \phi}{\partial t^2} + \frac{\partial \phi}{\partial t} = \frac{\partial^2 \phi}{\partial x^2} + \phi - \phi^3 \ , \tag{5.105}$$

are also pulled. One interesting aspect of this equation is that while the diffusive spreading in a first order diffusion equation is, in a sense, infinitely fast, the second order term gives a finite speed of propagation of the disturbances.

As discussed in Section V D, our results immediately apply to this equation, so the velocity and front relaxation is then given by Eqs. (5.70) and (5.71), with

$$\begin{aligned} v^* &= \frac{2}{\sqrt{1+4\tau_2}} \ , \\ \lambda^* &= \sqrt{1+4\tau_2} \ , \\ D &= \frac{1}{(1+4\tau_2)^2} \ . \end{aligned} \tag{5.106}$$

The expression for D nicely illustrates the effictive renormalization of the diffusion coefficient due to the second order time derivative.

5. An extension of the F-KPP equation with a memory kernel

As an example of an equation with a memory kernel, consider the extension of the F-KPP equation

$$\partial_t \phi(x,t) = \partial_x^2 \phi(x,t) + \int_0^t dt' K(t-t') \phi(x,t') - \phi^k(x,t) \ , \quad (k > 1) \ . \tag{5.107}$$

Upon Fourier–Laplace transformation as in (5.18), this equation is a scalar version of (5.73) with $S(k,\omega) = i\omega - k^2 + \tilde{K}(\omega)$, and so according to our discussion of Section V E, our analysis directly applies. If we take for instance

$$K(t-t') = \frac{1}{\sqrt{\pi}\tau_3} e^{-(t-t')^2/4\tau_3^2} \ , \tag{5.108}$$

the equation reduces to the F-KPP equation in the limit $\tau_3 \to 0$, and the characteristic equation becomes

$$\lambda^2 - s + e^{\tau_3^2 s^2} \mathrm{erfc}(\tau_3 s) = 0 \ , \tag{5.109}$$

where we follow the notation of Section V C 2 in writing $s = \mathrm{Im}\ \omega$, $\lambda = \mathrm{Im}\ k$, and where erfc is the complementary error function. The results for v^*, λ^* and D, obtained by solving (5.109) together with the saddle point condition $\partial s/\partial \lambda = s/\lambda|_{\lambda^*}$ numerically, are shown in Fig. 15.

Other examples of equations with memory kernels can, e.g., be found in [107,108].

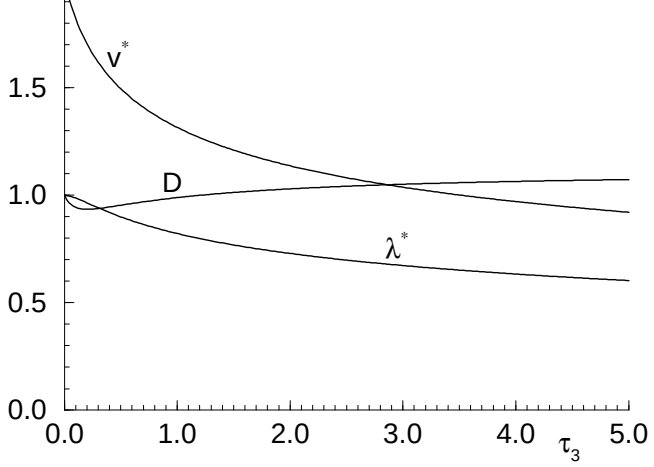

FIG. 15. Plot of v^*, λ^*, and D as a function of τ_3 for the extension (5.107) of the F-KPP equation with a memory kernel (5.108).

6. Exact results for numerical finite difference schemes

The fact that our results also apply to finite difference equations has the important implication that if we study a *p.d.e.* with pulled fronts numerically using a finite difference approximation with gridsize Δx and timestep Δt, we can calculate $v^*(\Delta x, \Delta t)$ as well as $v(t; \Delta x, \Delta t)$ *exactly*. This allows us to estimate analytically the intrinsic discretization error in these quantities, and hence to decide beforehand which grid and step size are needed to obtain a given accuracy.

As a first illustration, suppose, that one integrates the F-KPP equation (1.1) numerically with an explicit Euler scheme. This amounts to approximating the *p.d.e.* by

$$\frac{u_j(t+\Delta t) - u_j(t)}{\Delta t} = \frac{u_{j+1}(t) - 2u_j(t) + u_{j-1}(t)}{(\Delta x)^2} + u_j(t) - u_j^k(t) \ . \quad (5.110)$$

Upon substitution of $u_j(t) \sim e^{st-\lambda x}$, $x = j\ \Delta x$ into the linearized equation (we again follow the notation of Section V C 2 by writing $s = \mathrm{Im}\,\omega$, $\lambda = \mathrm{Im}\,k$), we obtain

$$\frac{e^{\,s\Delta t} - 1}{\Delta t} = 1 + \left(\frac{\sinh \lambda \Delta x/2}{\Delta x/2}\right)^2 \ , \quad (5.111)$$

which is straight forward to solve for $s(\lambda; \Delta x, \Delta t)$. As we emphasized above, by solving the saddle point condition $\partial s/\partial \lambda = s/\lambda|_{\lambda^*} = v^*$, we can obtain the exact values of v^*, λ^* and D for any step and grid size, and in this way determine the accuracy of the numerical scheme. In general, these equations have to be solved by a simple numerical iteration routine, but for small Δx and Δt, the result can easily be calculated analytically: Expanding in Δx and Δt, we find the dispersion relation

$$s(\lambda; \Delta x, \Delta t) = 1 + \lambda^2 + \frac{\lambda^4 (\Delta x)^2}{12} - \frac{(1+\lambda^2)^2 \Delta t}{2} + \dots \ . \quad (5.112)$$

For $\Delta t \to 0$, $\Delta x \to 0$, this reduces to the continuum result $s(\lambda) = 1 + \lambda^2$, as it should. For the saddle point parameters, we find

$$\begin{aligned} v^* &= 2 - 2\Delta t + \frac{1}{12}(\Delta x)^2 + \cdots \\ \text{Euler: } \lambda^* &= 1 + \Delta t - \frac{1}{8}(\Delta x)^2 + \cdots \\ D &= 1 - 4\Delta t + \frac{1}{2}(\Delta x)^2 + \cdots \ , \end{aligned} \quad (5.113)$$

In practice, the Euler scheme is not used very often, because it is numerically very unstable and not very accurate. We have done all our simulations in Section IV and in the present section with a more stable and accurate semi-implicit method [109], which for the F-KPP equation amounts to the discretization

$$\begin{aligned} \frac{u_j(t+\Delta t) - u_j(t)}{\Delta t} = & \\ \frac{1}{2}\left[\frac{u_{j+1}(t) - 2u_j(t) + u_{j-1}(t)}{(\Delta x)^2}\right] + & \\ + \frac{1}{2}\left[\frac{u_{j+1}(t+\Delta t) - 2u_j(t+\Delta t) + u_{j-1}(t+\Delta t)}{(\Delta x)^2}\right] + & \\ + \frac{1}{2}\left[u_j(t) + u_j(t+\Delta t)\right] - & \\ - \frac{1}{2}\left[2u_j^k(t) + k u_j^{k-1}(t)(u_j(t+\Delta t) - u_j(t))\right] \ . & \end{aligned} \quad (5.114)$$

The term on the last line is obtained by expanding $u_j^k(t+\Delta t)$ about $u_j^k(t)$ to first order in $u_j(t+\Delta t) - u_j(t)$, so that one obtains a linear equation for the $u_j(t+\Delta t)$. This expansion makes what would otherwise have been an implicit method, into a semi-implicit method.

The dispersion relation is now given by

$$\frac{\tanh s\Delta t/2}{\Delta t/2} = 1 + \left(\frac{\sinh \lambda \Delta x/2}{\Delta x/2}\right)^2 \ , \quad (5.115)$$

which immediately yields $s(\lambda; \Delta x, \Delta t)$. For small Δx and Δt the result is

$$s(\lambda; \Delta x, \Delta t) = 1 + \lambda^2 + \frac{\lambda^4 (\Delta x)^2}{12} + \frac{(1+\lambda^2)^3 (\Delta t)^2}{12} + \dots \,. \tag{5.116}$$

For this integration scheme, it is now straight forward to find

$$\begin{aligned} v^* &= 2 + \frac{2}{3}(\Delta t)^2 + \frac{1}{12}(\Delta x)^2 + \cdots \\ \text{Semi-implicit: } \lambda^* &= 1 - \frac{2}{3}(\Delta t)^2 - \frac{1}{8}(\Delta x)^2 + \cdots \\ D &= 1 + 3(\Delta t)^2 + \frac{1}{2}(\Delta x)^2 + \cdots \end{aligned} \tag{5.117}$$

We stress that these are the exact expressions for the application of this numerical scheme to a nonlinear diffusion equation, scaled to the normal form (2.1), (2.2). They are therefore the "ideal" finite difference correction terms in the absence of numerical instabilities, round-off errors et cetera. The correctness and accuracy of the prediction (5.117) for v^* is demonstrated in Section IV in Fig. 9(b).

We finally note that an early example of pulled front relaxation observed in a finite difference equation in space *and* time was seen in a mean-field model of ballistic growth [22]. In this paper, the prefactor of the $1/t$ term, obtained by plotting v versus $1/t$, was found to be about 9 percent too *small*. Presumably, this discrepancy is due to the corrections from the $1/t^{3/2}$ term: According to (5.70), the term $(1 - \sqrt{\pi/({\lambda^*}^2 D t)})$ generally gives rise to a *lowering* of the effective slope in a v versus $1/t$ plot, as Fig. 8(b) clearly demonstrates.

VI. SUMMARY AND OUTLOOK

A. Summary of the main results

The essential result of this paper is that for front propagation into unstable states, starting from steep initial conditions, the convergence of front velocity and shape is given in the pulled regime by the *universal* expressions

$$v(t) = v^* + \dot{X}(t) \ , \tag{6.1}$$

$$\dot{X}(t) = -\frac{3}{2\lambda^* t}\left(1 - \sqrt{\frac{\pi}{(\lambda^*)^2 D t}}\right) + O(t^{-2}) \ , \tag{6.2}$$

$$\phi = \Phi_{v(t)}(\xi_X) + O\left(\frac{1}{t^2}\right) \ , \quad \xi_X \lesssim \sqrt{t} \ , \tag{6.3}$$

$$\xi_X = x - v^* t - X(t) \ , \tag{6.4}$$

provided the asymptotic front profile is uniformly translating. All terms in the expression for $v(t)$, λ^*, v^* and D, are given explicitly in terms of the dispersion relation of dynamical equation, linearized about the unstable state [see Eqs. (5.16), (5.17) and (5.19) or Table IV]. These results are also summarized in Table I. The dependence on pushing or pulling and on the initial conditions is sketched in Table III.

With *universal* we mean that not only the asymptotic profile is unique, but also the relaxation towards it, provided we start with sufficiently steep initial conditions. Moreover, the relaxation is universal in that it is independent of the precise nonlinearities in the equation, and of the precise form of the equation: It holds for *p.d.e.*'s, sets of *p.d.e.*'s, difference–differential equations, equations with memory kernels, etc., provided fronts are pulled and that the asymptotic front solution is uniformly translating, and provided that we are not at the bifurcation point from the pulled to the pushed regime, or at the bifurcation point $D = 0$ towards pattern forming fronts (e.g., at $\gamma = 1/12$ in the EFK-equation). The fact that the results also apply to finite difference equations has a nice practical consequence: If a *p.d.e.* is studied numerically using a finite difference approximation scheme, both v^* and the prefactors of the algebraic relaxation terms can also be calculated *exactly* for the numerical scheme. This allows one to estimate in advance how big step and grid sizes need to be, in order to achieve a particular numerical accuracy (see Section V F 6).

The remarkable relaxation properties are reminiscent of the universal corrections to scaling in critical phenomena, if we think of the relaxation as the approach to a unique fixed point in function space along a unique trajectory. An alternatively way to express this in more mathematical terms is to say that we have constructed the *center manifold* for front relaxation in the pulled regime.

The above expressions contain *all* universal terms: those of order t^{-2} depend on the precise initial conditions and on the nonlinearities in the equations. The order of the limits is important here: Our results are the exact expressions in a $1/t$ expansion, i.e., when we take the large time limit while tracking the velocity of a point where the dynamical field reaches a fixed value. To order $1/t^2$, this is equivalent to keeping ξ_X fixed. When we interchange the limits by taking ξ_X large at fixed time, there is a cross-over to a different intermediate asymptotic regime for $\xi_X \gtrsim \sqrt{t}$. The different dynamical regions of a pulled front are sketched in Fig. 2.

The slow algebraic convergence to the asymptotic velocity has important consequences, as it prohibits the derivation of a standard moving boundary approximation for patterns in more than one dimension that consist of propagating pulled fronts whose width is much smaller than their radius of curvature [37].

While we have limited the analysis in this paper to equations that admit uniformly translating front solutions, it turns out that most elements of our analysis can be extended to pattern forming fronts for which Re $k^* \neq 0$ and Re $\omega^* \neq 0$. In this case, the expression (6.2) with $1/\sqrt{D}$ replaced by Re $(1/\sqrt{D})$ applies [75,76].

In addition to our derivation of the above expressions for the convergence of pulled fronts, we have reformulated and extended the connection between front selection and the stability properties of fronts. This leads to an essentially complete picture also of front relaxation in the pushed regime (Cases I and II in Table III) and in the case of leading edge dominated dynamics resulting from flat initial conditions (Case III). For an interpretation of these results, again a consideration of the different dynamical regions of a front as in Fig. 2 is helpful. The relaxation behavior in the pulled regime (Case IV) can not be obtained simply from the properties of the stability operator of the pulled front solution, and therefore had to be obtained along a different route, which is summarized below.

B. Summary of the main conceptual steps of the analysis

The derivation of our central result on pulled front relaxation is based on the following steps:

1. From the dispersion relation $\omega(k)$ or from the characteristic function $S(k,\omega)$, we obtain v^*, λ^* and D (see Table IV).

2. The double root condition which determines v^* and λ^* implies that the asymptotic large ξ behavior of uniformly translating front solutions is as $\Phi^*(\xi) = (\alpha\xi + \beta)e^{-\lambda^*\xi}$, where generically $\alpha \neq 0$.

3. The double root condition which determines v^* and λ^* also implies that the lowest order spatial derivative term in the dynamical equation for the leading edge representation $\psi = e^{\lambda^*\xi}\phi(\xi,t)$ is of the diffusion type, $D\partial^2\psi/\partial\xi^2$ (see Sections V C 3, V D, and V E).

4. The diffusion type dynamics implied by *3.* shows that in the co-moving frame $\xi = x - v^*t$, the front profile shifts back with the collective coordinate $X(t)$ which

grows logarithmically in time. Linearization about the asymptotic front solution $\Phi^*(\xi)$ in the ξ frame is therefore impossible (see Sections III A 3 and III A 4). Instead, we introduce the frame $\xi_X = x - v^*t - X(t)$ with the expansion $\dot{X}(t) = c_1/t + c_{3/2}/t^{3/2} + \cdots$ and the corresponding leading edge transformation $\psi(\xi_X, t) = e^{\lambda^* \xi_X} \phi(x, t)$.

5. In the *front interior*, the long time expansion for $\dot{X}$ generates an expansion for the corrections to the front profile in inverse powers of t. To order t^{-2} temporal derivatives of the front corrections do not come in, so that to this order the equations for the profile shape reduce to those for $\Phi_{v(t)}$. This immediately leads to (6.3) for the time dependence of the front profile.

6. In the *leading edge*, where nonlinearities can be neglected, we use an asymptotic expansion for $\psi(\xi_X, t)$, linearized about $\psi \neq 0$, in terms of functions of the similarity variable $z = \xi_X^2/(4Dt)$ of the diffusion equation. Now for small values of z the expansion has to match the boundary condition $\psi \approx e^{-\lambda^* \xi_X} \Phi^*(\xi_X) \approx \alpha \xi_X + \beta$ (implied by observation *2.*), and for large ξ_X the terms in the (intermediate) asymptotic expansion have to decay as a Gaussian $e^{-z} = e^{-\xi_X^2/(4Dt)}$ times a polynomial in the similarity variable z. These two requirements fix the constants $c_1, c_{3/2}, \ldots$ in the expansion of $\dot{X}$, and hence (6.2).

C. Open problems

What one considers as remaining open problems concerning pulled front propagation, will depend largely on one's background and standards regarding the desired mathematical rigour. While our results are exact and yield an almost complete understanding of the general mechanism of pulled front propagation, they have, of course, not been derived rigorously. In physics, such a situation is often not just quite acceptable but even quite gratifying, but more mathematically inclined readers may wish to take up the challenge to provide a more rigorous justification. More work could also be done on enlarging the classes of equations for which the assumptions underlying our approach can be shown to hold, i.e., for which one can show that fronts are pulled and that there exists a family of uniformly translating front solutions.

Within the realm of our approach, one can consider two extensions to special cases. First, our results apply to steep initial conditions such that the steepness $\lambda = -\lim_{x\to\infty} \ln \phi(x, 0)$ is larger than λ^*. Bramson [77] has also obtained some results for the marginal case that for large x $\phi(x, 0) \sim x^{-\nu} e^{-\lambda^* x}$ with $\nu > 0$. We have not investigated whether we can recover his results with our approach. Second, at the bifurcation point from uniformly translating solutions to pattern forming fronts, which in the EFK equation (5.91) happens at $\gamma = 1/12$, the diffusion coefficient D vanishes [see Eq. (5.92)]. At this bifurcation point, the equation for the leading edge representation ψ is not of the diffusion type, so our asymptotic expansion breaks down right at this point. We have not investigated what happens then.

As mentioned before, we will elsewhere address what we consider the most interesting remaining challenges, the extension of (part of) these results to pattern forming and chaotic fronts [75,76] and the question whether weakly curved fronts can be analyzed with a moving boundary approximation [37], an issue which is of central importance for understanding fronts in two and three dimensions like steamers [15].

D. The multiplicity of front solutions and of solutions of the saddle point equations

As we discussed in Section V B, our general discussion of the convergence of pulled fronts to their asymptotic velocity and shape is based on the assumption that a uniformly translating front solution $\Phi^*(\xi)$ exists (see (5.19) for a definition), and that it is a member of a one-parameter family of front solutions. What happens if this family of front solutions does not exist has, to our knowledge, not been investigated systematically for real equations. However, experience with various pattern generating fronts — especially with a similar case in which no generalized uniformly translating solutions exist in the quintic complex Ginzburg-Landau equation [66], even though the dynamics is pulled — yields the scenario that the leading edge just spreads according to the linearized equations, and that the front interior "just follows", in the sense that if there are uniformly translating fronts solutions, the leading edge relaxes smoothly, while if there are none, it is forced to follow the spreading in some other way. This leads one to conjecture that if there is no family of uniformly translating front solutions, the velocity relaxation will still be described by Eqs. (6.1) and (6.2) in the leading edge, but that in the interior front region the dynamics will inherently time-dependent, e.g., incoherent.

This can occur in particular in the following situation: As mentioned in Section V C 1, it can happen that the dispersion relation is such that there is more than one nontrivial solution for the equations for v^* and λ^*. According to the linearized equation, arbitrary sufficiently steep initial conditions will spread out asymptotically with the largest of the speeds v^*. Hence the asymptotic spreading speed of pulled fronts emerging from steep initial conditions is simply the largest velocity v^*. Now, according to a counting argument for the multiplicity of uniformly translating front solutions, the multiplicity of front solutions associated with different solutions of the saddle point equations for v^* will differ: If there are two solutions v_1^* and v_2^* with $\lambda_1^* < \lambda_2^*$, the multiplicity of front solutions with velocity near v_2^* and an asymptotic spatial decay rate near λ_2^* will be smaller than that of those with velocity near v_1^* and a spatial decay rate near λ_1^*. Investigations of the issue of the competition between

various solutions v^* will therefore also bear on the issue raised in the beginning of this section, the question what happens when there is no uniformly translating solution Φ^*. In particular, the dynamics in an equation that has a family of uniformly translating fronts associated with the solution v_1^*, should show a transition from smoothly relaxing interior dynamics for $v_1^* > v_2^*$ to incoherent interior dynamics for $v_1^* < v_2^*$.

E. A step by step guideline for applying these results

If one just wants to apply our results to a given dynamical equation with a given initial condition without worrying about the derivation and justification, one can simply follow the following guidelines:

(i) Linearize the dynamical equation about the unstable state, and determine the characteristic equation $S(k,\omega) = 0$ for modes $e^{-i\omega t+ikx}$ in the linearized equation.

(ii) Solve the double root or saddle point conditions from table IV to determine v^*, k^* and D.

(iii) Check whether the leading edge of the initial conditions is steeper than Re e^{ik^*x}. Only then the front is a candidate for pulling (Case IV in Table III), otherwise Cases II or III apply.

(iv) Check whether the conditions (5.19) under which fronts are expected to be uniformly translating, Re $k^* =$ Re $\omega^* = 0$, Im $D = 0$ are satisfied. If not, the fronts will be pattern generating rather than uniformly translating (see Section VI D above).

(v) Assuming the conditions under *(iv)* are obeyed, so that the asymptotic front is expected to be uniformly translating, investigate by a counting argument or otherwise whether there is a one-parameter family of uniformly translating front profiles $\Phi_v(\xi)$ that includes $\Phi^*(\xi)$.

(vi) Determine, by using bounds, comparison theorems or physical arguments, whether the fronts will be pushed or pulled. This determines, whether either Case I or Case IV from Table III applies.

(vii) If according to points *(iv)*–*(vi)* there is a family of front solutions that includes Φ^*, and if the dynamics is pulled, then our predictions (6.1)–(6.3) or Table I apply. If the conditions under *(iv)* are satisfied but there is no family of uniformly translating solutions according to *(v)*, then our formula (6.2) should apply but one then expects intrinsic nontrivial dynamics in the front interior to remain, so that (6.3) does not apply. If *(iv)* is not satisfied (as for the EFK equation (5.91) for $\gamma > 1/12$), one expects pattern generating fronts with a similar algebraic convergence [75,76].

F. The subtle role of the nonlinearities: an alternative intuitive explanation

As we have seen in (2.58) and (5.20), the convergence of the *linear* spreading velocity to the asymptotic value v^* is as $v(t) = v^* - 1/(2\lambda^* t) + \cdots$, while the convergence of nonlinear fronts is as $v(t) = v^* - 3/(2\lambda^* t) + \cdots$. The prefactor of the $1/t$ in the latter case is just three times larger than for the linear spreading velocity. What is this subtle difference due to?

In this paper, we have attributed the difference to the presence of the term $\alpha\xi$ in the large-ξ asymptotics $(\alpha\xi + \beta)e^{-\lambda^*\xi}$ of $\Phi^*(\xi)$. We used an argument closely related to the one presented below, to prove in Section II E 2, that $\alpha \neq 0$. The functional form of Φ^* leads to the requirement that the leading term in the expansion in similarity solutions in the leading edge is $(\xi/t^{3/2})e^{-\xi^2/(4Dt)}$, *not* $(1/t^{1/2})e^{-\xi^2/(4Dt)}$ (see Section III A 1). Nevertheless, one may want to have a better intuitive understanding of why the asymptotics of the linear spreading velocity is not correct for the nonlinear front relaxation — after all, one might at first sight think that the linear spreading results should be correct sufficiently far into the leading edge where the nonlinearities can be neglected. The following picture allows us to understand why this is wrong, and why the same type of algebraic convergence also applies to pattern forming and chaotic fronts [75,76].

Consider for simplicity the F-KPP equation (1.1). As discussed in the introduction and Section II E 2, the dynamical equation for the leading edge representation $\psi(\xi,t)$ of ϕ is

$$\partial_t\psi(\xi,t) = \partial_\xi^2\psi(\xi,t) - \psi^3(\xi,t)e^{-2\lambda^*\xi} \ . \qquad (6.5)$$

We can think of the nonlinear $\psi^3 e^{-2\lambda^*\xi}$ term as a localized sink term in the diffusion equation for ψ: the term vanishes for positive ξ due to the exponential term, and for large negative ξ since ψ vanishes exponentially in the region to the left where ϕ saturates. Thus, if we think of ψ as representing the density of diffusing particles, then in the region where this term is nonvanishing, it describes the death or annihilation of particles. For the half space to the right of it, where the particles freely diffuse, this term therefore acts like an absorbing boundary on the left. This is actually all that remains of the nonlinearities in the equation! Whenever the integrated sink strength α [the spatial integral of the nonlinear term, in agreement with (2.66)] is nonzero, the problem in the leading edge reduces to that of the buildup of a diffusion field in the presence of an absorbing boundary (and at the same time, as (2.66) shows, $\alpha \neq 0$). In this language, the pulled to pushed transition occurs precisely when the absorption strength α vanishes, and indeed precisely at this point the velocity convergence is as $v(t) = v^* - 1/(2\lambda^* t) + \cdots$ [see Eq. (3.66)].

There is one complication: unlike the usual problems of diffusion in the presence of a given absorbing bound-

ary, the "sink" in (6.5) depends on the relaxing field ψ itself. In fact, as we discussed extensively in the paper, the diffusive dynamics of ψ leads to a logarithmic shift of the sink in time, in the frame ξ. That is why in this interpretation we have to go, for selfconsistency, to the frame $\xi_X = \xi - X(t)$. In this frame, the "sink" or "absorbing wall" remains essentially fixed in time, and so the dynamics of ψ is, in leading order, that of a diffusion field in the presence of a fixed absorbing wall. As is well known, in such a case a linear gradient $\psi \propto \xi_X$ will build up in front of the wall, to balance the constant annihilation of particles in the wall region.

Clearly, even if the "sink" strength is not stationary in time, the buildup of the linear diffusion gradient far ahead of it will not be affected. The present interpretation therefore yields a natural starting point for analyzing the velocity relaxation of non-uniformly translating fronts. This will be explored elsewhere [71,75,76].

We end this paper by stressing that while we have shown that nonlinear fronts relax according to the "3/2 law" $v(t) = v^* - 3/(2\lambda^* t) + \cdots$, one can not apply this result completely with closed eyes. An amusing illustration of this warning is the following. It has been noted, that the spreading velocity in the equation

$$\frac{\partial \phi}{\partial t} = \frac{\partial^2 \phi}{\partial x^2} + \phi + e\left(\frac{\partial \phi}{\partial x}\right)^2 \tag{6.6}$$

is follows the "1/2 law" $v(t) = v^* - 1/(2\lambda^* t)\cdots = 2 - 1/(2t) + \cdots$ [110]. At first sight, this equation therefore might appear to yield a counterexample to our assertions. In fact, it does not. Our results only hold for equations where the growth of the dynamical field saturates behind the front, *not* in the case in which the growth is unbounded. If the growth is unbounded, our arguments for why $\alpha \neq 0$, and hence for the "3/2 law", break down. The above equation is precisely an example in which the growth does not saturate: For $e > 0$ and positive ϕ, the nonlinear term only increases the growth. Hence there is no saturation and the spreading velocity $v_{nl}(t)$ in the presence of the nonlinearities is larger than the one of the linear equation: $v_{nl}(t) \geq v^* - 1/(2t) + \cdots$. Apparently, in practice the equality is obeyed asymptotically.

Acknowledgement: The work described in this paper started from discussions with C. Caroli. The work of U.E. was supported by the Dutch Science Foundation (NWO) and the EU-TMR-network "Patterns, Noise, and Chaos".

APPENDIX A: AN UPPER BOUND FOR V_C IN THE NONLINEAR DIFFUSION EQUATION

With a generalization of the leading edge transformation introduced in Sect. II F, it is straight forward to prove the well-known upper bound $v_c \leq v_{sup}$, where

$$v_{sup} = 2 \sup_{0 \leq \phi \leq 1} \sqrt{\frac{f(\phi)}{\phi}} \ , \tag{A1}$$

for the selected front velocity in the nonlinear diffusion equation, if the initial conditions have steepness $\lambda > v_{sup}/2$. The steepness λ of a front is defined in (2.6). To prove this bound, transform (2.1) to a frame $\xi = x - vt$, and write

$$\psi(\xi, t) = e^{v\xi/2} \phi(x, t) \ . \tag{A2}$$

The equation of motion is now

$$\partial_t \psi = \partial_\xi^2 \psi - \frac{v^2}{4} \ \psi + e^{v\xi/2} \ f\left(\psi \ e^{-v\xi/2}\right) \ . \tag{A3}$$

If the initial steepness is $\lambda > v/2$, then

$$\lim_{\xi \to \pm\infty} \psi(\xi, t) = 0 \ \text{ for all } 0 \leq t < \infty \ , \tag{A4}$$

since the steepness of the leading edge ($\xi \to \infty$) is conserved for all finite times, cf. the discussion in Sect. II E; and since convergence at $\xi \to -\infty$ is garantueed by $\phi \to 1$ behind the front together with the transformation (A2). Thus the decay of ψ at $\xi \to \pm\infty$ is exponential in ξ for $t < \infty$. Hence, the whole equation can be multiplied by ψ and integrated over ξ. This yields

$$\partial_t \int_\xi \frac{\psi^2}{2} = - \int_\xi \left\{ (\partial_\xi \psi)^2 + \psi^2 \ \left[\frac{v^2}{4} - \frac{f\left(\psi \ e^{-v\xi/2}\right)}{\psi \ e^{-v\xi/2}} \right] \right\} \ , \tag{A5}$$

where all integrals are finite. The r.h.s. of this equation is strictly negative, if $v > v_{sup}$ (A1). Therefore, in a frame moving with velocity $v > v_{sup}$, the integral $\int_\xi \psi^2$ decays in time. This means, that the frame is propagating too rapidly, so that the front shrinks away in the leading edge representation ψ (A2). Only a frame moving with velocity $v \leq v_{sup}$ can propagate along with the speed of the front. v_{sup} is therefore an upper bound for the asymptotic velocity of any initial condition with $\lambda > v_{sup}/2$.

For nonlinearity $f_{KPP} = \phi - \phi^k$, we have $v_{sup} = 2$. But on the other hand, we know (see Sect. II), that $v_{sup} \geq v_c \geq v^* = 2$. Hence, these fronts are pulled with $v_c = v^* = 2$. For nonlinearity $f_\epsilon = \epsilon\phi + \phi^{n+1} - \phi^{2n+1}$, we have $v_{sup} = \sqrt{1 + 4\epsilon} > 2\sqrt{\epsilon} = v^*$.

This version of the argument for $v < v_{sup}$ [74] can be generalized to equations with higher spatial derivatives, forming both uniformly translating fronts or pattern forming fronts [75].

APPENDIX B: THE GENERALIZED NONLINEAR DIFFUSION EQUATION

Analyse an equation with first temporal and second spatial derivative:

$$F\left(\phi, \ \partial_x \phi, \ \partial_x^2 \phi, \ \partial_t \phi\right) = 0 \ . \tag{B1}$$

A front translating uniformly with velocity v solves

$$F\left(\Phi_v, \ d_\xi \Phi_v \ , d_\xi^2 \Phi_v, \ -v d_\xi \Phi_v\right) = 0 \ \ , \ \ \xi = x - vt \ . \tag{B2}$$

The stability analysis of such a solution and the further treatment of convergence is identical with what we did for the nonlinear diffusion equation (1.1) in Sections II and III. We only first have to transform the linear operators appropriately. We here show, how to do this transformation. Our analysis is directly relevant for the equation studied in [111].

We use the definition of functional derivatives as in (5.32) – (5.36). A linear perturbation $\eta(\xi, t)$ (2.23) about a uniformly translating state Φ_v then solves the linear equation $\partial_t \eta = \mathcal{L}_v \eta$ (2.24) resp. (5.30) with the linear operator being now

$$\mathcal{L}_v = f_2(\xi) \ \partial_\xi^2 + f_{1,v}(\xi) \ \partial_\xi + f_0(\xi) \ \ , \ \ f_{1,v} = v + f_1 \ . \tag{B3}$$

For transforming to a Schrödinger problem $\partial_t \psi = \mathcal{H}_v \psi + o(\psi^2 e^{-\alpha})$, $\mathcal{H}_v = -\partial_y^2 + V_v(y)$, we now have to make the coefficient of the first order derivative ∂_ξ vanish, and the coefficient of the second order derivative ∂_ξ^2 constant. This can be achieved through a transformation similar to (2.26) and (2.27), combined with a nonlinear transformation $y(\xi)$ of the length scale ξ:

$$\psi = e^\alpha \ \eta \quad , \quad d\alpha(\xi) = \frac{2 f_{1,v} - \partial_\xi f_2}{4 f_2} \ d\xi \ , \tag{B4}$$

$$\mathcal{H}_v(y) = - \ e^{\alpha(\xi)} \ \mathcal{L}_v \ e^{-\alpha(\xi)} = - \ \partial_y^2 + V_v(y) \ , \tag{B5}$$

$$dy(\xi) = \frac{d\xi}{\sqrt{f_2(\xi)}} \quad \left(\ \Leftrightarrow \ \partial_y = \sqrt{f_2(\xi)} \ \partial_\xi \ \right) \ , \tag{B6}$$

$$V_v(y(\xi)) = \frac{f_{1,v}^2 - 4 f_0 f_2}{4 f_2} + \frac{f_2 \ d_\xi f_{1,v} - f_{1,v} \ d_\xi f_2}{2 f_2} + \frac{3 \ (d_\xi f_2)^2 - 4 f_2 \ d_\xi^2 f_2}{16 f_2} \ . \tag{B7}$$

We use again the convention $\lim_{\xi \to \infty} \Phi_v(\xi) = 0$. By construction the pulled velocity v^* is the velocity, where $V_{v^*}(\infty) = 0$. Accordingly now

$$v^* = 2\sqrt{f_0(\infty) \ f_2(\infty)} - f_1(\infty) \ . \tag{B8}$$

The steepness of the leading edge is

$$\lambda^* = \partial_\xi \alpha \Big|_{\xi \to \infty, \ v = v^*} = \sqrt{\frac{f_0(\infty)}{f_2(\infty)}} \ . \tag{B9}$$

(In the convention of Section V B: $f_n(\infty) = c_n$.) In the leading edge region, the relation between y and ξ is linear: $y = \xi/\sqrt{f_2(\infty)}$.

If $V_{v^*}(y) \geq 0$ for all y, there are no destablizing linear modes within the Hilbert space of (B5). Then the front propagating with v^* is stable. The remaining analysis translates from Sections II and III step by step with only the explicit notation of the linear operators $\mathcal{L}_v$ and $\mathcal{H}_v$ and the transformation operator e^α having a more involved notation.

If there is a range of y such that $V_{v^*}(y)$ becomes negative, there might be a destabilizing mode in the spectrum of linear perturbations. In this case, there must be a pushed front solution with some velocity $v^\dagger > v^*$ with steepness $\lambda = \lambda_+(v^\dagger) > \lambda_0(v^\dagger) = v^\dagger/2$. Such a pushed front might even be integrated analytically, if one can find an analytic solution $\psi(\phi)$ of

$$F\left(\phi,\ \psi,\ \psi\ \frac{d\psi}{d\phi},\ -v\psi\right) = 0\ , \tag{B10}$$

equivalent to (C3). $\xi(\phi)$ can then be integrated as in (C5). (Again, a closed form for $\psi(\phi)$ cannot be found for pulled fronts, except possibly for equations at the pushed/pulled transition.)

APPENDIX C: ANALYTICAL SOLUTIONS FOR PUSHED NONLINEAR DIFFUSION FRONTS AND TRANSITION TO PULLING

We here discuss, how to find analytical solutions for uniformly translating fronts $\phi(\xi)$ in the equation

$$\partial_\xi^2\phi + v\partial_\xi\phi + f(\phi) = 0\ . \tag{C1}$$

• We rephrase and straighten the method from [65] (see also [112,113]) how to find analytical front solutions.
• We recall, that analytical solutions can be found only for pushed fronts (propagating either into a meta- or into an unstable state, Cases I and II from Table III), but not for pulled fronts (Case IV).
• We recall, that only a strongly heteroclinic orbit, i.e., a front approaching $\phi = 0$ with $\lambda > \lambda_0(v)$, is a candidate for a pushed front. This allows us to calculate the critical ϵ for the pushed/pulled transition in the case of the nonlinearity (1.11).

Write the equation as a flow in phase space as in (2.22)

$$\partial_\xi \begin{pmatrix}\psi\\ \phi\end{pmatrix} = \begin{pmatrix}-v\psi - f(\phi)\\ \psi\end{pmatrix}\ , \tag{C2}$$

where ξ parametrizes the flow. If ϕ is monotonic in ξ, ψ can be parametrized by ϕ instead of by ξ. This substitution yields for $\psi(\phi)$

$$\psi\ \frac{\partial\psi}{\partial\phi} + v\psi + f(\phi) = 0\ . \tag{C3}$$

This is the differential equation for the trajectory in phase space, where now the translational degree of freedom is removed together with the parametrization ξ of the flow. The resulting differential equation is one order lower than the original differential equation (C1). According to (2.14), the initial condition for the integration at $\phi \approx 1$ is

$$\begin{aligned}\psi(\phi = 1-\delta) &= -\tilde\lambda_- + o(\delta)\ ,\\ \tilde\lambda_- &= v/2 - \sqrt{v^2/4 - f'(1)}\ ,\end{aligned} \tag{C4}$$

so the front trajectory is unique and can be integrated. In some cases, the integration can be done analytically, if one is lucky enough to find an analytical solution $\psi(\phi)$ of Eq. (C3) for a given $f(\phi)$. If we have a solution $\psi(\phi)$, then the function $\xi(\phi)$ can be integrated as

$$\xi = \int_{\phi(0)}^{\phi(\xi)} \frac{d\phi}{\psi(\phi)}\ . \tag{C5}$$

The final step consists in finding the inverse function $\phi = \phi(\xi)$, if this is possible.

Note now, that solutions $\psi(\phi)$ can be found analytically only, if ϕ approaches $\phi = 0$ with a single exponential $\phi \propto e^{-\lambda\xi}$, since only then $\psi(\phi)$ has the simple analytic form $\psi(\phi) = -\lambda + o(\phi)$. Any other form of the approach to $\phi = 0$, cf. (2.15), would not be expressible in a simple analytic expression for $\psi(\phi)$. In particular, a generic Φ^* front with $\Phi^* \propto (\alpha\xi + \beta)e^{-\lambda^*\xi}$ in the leading edge does not have a simple analytical expression for $\psi(\phi)$, so a pulled front generically cannot be integrated analytically.

Given an analytical front solution with velocity v and decay rate λ, one has to check the nature of the front. A pushed front is a strongly heteroclinic front, i.e., it has leading edge steepness $\lambda = \lambda_+(v) > \lambda_0(v)$. (For the notation of λ's, compare Eq. (2.18).) If $\lambda = \lambda_0(v) = \lambda_\pm(v)$, we have found a front at the transition point from pushed to pulled with leading edge behavior $\phi \propto e^{-\lambda^*\xi}$. This is the only pulled front, we can integrate. If $\lambda = \lambda_-(v) < \lambda_0(v)$, we have a particular flat front, that has evolved from an initial condition with the same flatness in the leading edge.

Finding analytical solutions for pushed fronts can even be turned into a machinery, if we don't fix f and look for a ψ, but if we define $\psi(\phi)$ and then calculate $f(\phi)$. For

$$\psi = -\lambda\phi(1-\phi^n) \tag{C6}$$

we calculate, e.g.,

$$\begin{aligned}f(\phi) &= \lambda(v-\lambda)\phi + \lambda(\lambda(n+2) - v)\phi^{n+1} - \lambda^2(n+1)\phi^{2n+1}\\ &= \bar\epsilon\phi + \phi^{n+1} - (1+\bar\epsilon)\phi^{2n+1}\ ,\end{aligned} \tag{C7}$$

where we have to identify $v = (n+2)\lambda - 1/\lambda$, and $\bar\epsilon = \lambda(v-\lambda)$. The analytic front solution for (C6) can be calculated from (C5) and inverted to yield

$$\phi(\xi) = \left[1 + \left(\phi(0)^{-n} - 1\right) e^{\lambda n \xi}\right]^{-1/n} \ . \qquad \text{(C8)}$$

This solution is a pushed front, if $\lambda \geq \lambda_0(v) = v/2$, which implies $\bar{\epsilon} \leq 1/n$. For such $\bar{\epsilon}$, we find pushed fronts with decay rate $\lambda = \sqrt{(\bar{\epsilon}+1)/(n+1)}$, velocity $v = (1+\bar{\epsilon}(n+2))/\sqrt{(n+1)(1+\bar{\epsilon})}$, and analytical form (C8). For $\bar{\epsilon} = 1/n$, the solution is a front on the transition point from pushed to pulled fronts with asymptotic decay $\phi \propto e^{-\lambda^* \xi} + o(\phi^2)$. For $\bar{\epsilon} > 1/n$, the solution (C8) is a flat front evolving from flat initial conditions. Fronts evolving from sufficiently steep initial conditions are then pulled, propagate with velocity $2\sqrt{\bar{\epsilon}}$, have decay rate $\lambda^* = \sqrt{\bar{\epsilon}}$ and no analytic form of the front solution can be found.

Eq. (1.1) with nonlinearity (C7) can also be rescaled to bring the equation to the more familiar form

$$\partial_\tau \varphi = \partial_y^2 \varphi + \epsilon\varphi + \varphi^{n+1} - \varphi^{2n+1} \qquad \text{(C9)}$$

$$\epsilon = \bar{\epsilon}(1+\bar{\epsilon}) \ \ , \ \ (1+\bar{\epsilon}) = \frac{t}{\tau} = \left(\frac{x}{y}\right)^2 = \left(\frac{\varphi}{\phi}\right)^n \ . \qquad \text{(C10)}$$

This reproduces precisely the form of the nonlinearity (1.11) with the stable state now at $\varphi_s = \left[\left(1+\sqrt{4\epsilon+1}\right)/2\right]^{1/n}$. Accordingly the critical ϵ is now $\epsilon_c = (n+1)/n^2$. Fronts propagate for $\epsilon < \epsilon_c$ with the pushed velocity $v^\dagger = \left[(n+2)\sqrt{1+4\epsilon} - n\right]/\left[2\sqrt{n+1}\right]$ and decay rate $\lambda_+(v^\dagger) = \left[1+\sqrt{1+4\epsilon}\right]/\left[2\sqrt{n+1}\right]$. For $\epsilon > \epsilon_c$, they propagate with the pulled velocity $v^* = 2\sqrt{\epsilon}$ and decay rate $\lambda^* = \sqrt{\epsilon}$.

APPENDIX D: GENERAL INTEGRATION OF $G^{SP}_{N/2}(Z)$

We here show, how to find special solutions $g^{sp}_{n/2}(z)$ of inhomogeneous equations like (3.44) or (3.45) in general. The general form of such an equation is

$$\hat{T}_n[z, d_z]\ g(z) = i_n(z) \ , \qquad \text{(D1)}$$

with $i_n(z)$ the inhomogeneity and $\hat{T}_n[z, d_z]$ the operator

$$\hat{T}_n[z, d_z] = z\ \frac{d^2}{dz^2} + \left(\frac{1}{2} - z\right)\frac{d}{dz} + \frac{n}{2} \ . \qquad \text{(D2)}$$

We search for a particular solution $g(z)$ of Eq. (D1). A particular solution of the homogeneous equation ($i_n(z) = 0$) can be expressed by Hermite polynomials:

$$\hat{T}_n[z, d_z]\ h_n(z) = 0 \qquad \text{(D3)}$$

$$h_0(z) = 1 \ \ , \ \ h_1(z) = \sqrt{2z} \ \ , \ \ h_2(z) = 1 - 2z \ \text{ etc.}$$

The ansatz $g(z) = h_n(z)\ u_n(z)$ reduces (D1) to an equation for $d_z u_n(z)$ of first order:

$$\hat{T}_n\ g = z\ h_n(z)\ \left(\frac{d}{dz} + \frac{d\ \ln h_n(z)}{dz} + \frac{1-2z}{2z}\right)\frac{du_n(z)}{dz}$$

$$= z\ h_n(z)\ \frac{d_z\left(M_n(z)\ d_z u_n(z)\right)}{M_n(z)} \ , \qquad \text{(D4)}$$

where in the last line we introduced the integrating factor

$$M_n(z) = h_n^2(z)\ \sqrt{z}\ e^{-z} \ . \qquad \text{(D5)}$$

Identify now $\hat{T}_n\ g_n = i_n$, integrate twice, and substitute M_n by the full expression. A special solution of (D1) then reads

$$g(z) = h_n(z) \int_a^z dx\ \frac{\int_b^x dy\ i_n(y)\ h_n(y)\ e^{-y}/\sqrt{y}}{h_n^2(x)\ \sqrt{x}\ e^{-x}} \ , \qquad \text{(D6)}$$

where the integration constants a and b are free. If we in particular choose $b = \infty$, the integrated exponential e^{x-y} cannot exceed unity, and $g^{sp}_n(z)$ can at most diverge algebraically, if the integrated inhomogeneity $i_n(z)$ is algebraic.

Integrating Eq. (3.55) for $g_0(z)$ as in (D6) with $b = \infty$, we find for the algebraic divergence of $g_0(z)$ for large z:

$$g_0(z) \sim 3\alpha\ z\ \ln z \ \ \text{as } z \to \infty \ , \qquad \text{(D7)}$$

while the solution of the homogeneous equation diverges only as $h_2(z) \sim z$. For determining the small z expansion of (D6), it must be noted that the factor $h_n(x)^{-2}$ is singular at the zeroes of $h_n(x)$. Hence, (D6) needs to be evaluated separately in each interval between the zeroes of $h_n(x)$. This can be done by a proper choice of a. It can be shown, that the results in each interval join smoothly.

APPENDIX E: ALGEBRAIC CONVERGENCE AT THE PUSHED/PULLED TRANSITION

In Section III we have analyzed equations, that are within the pulled regime. We here analyze equations, that are at the pushed/pulled transition. Leading edges of fronts within the pulled regime have the form $\Phi^* = (\alpha\xi + \beta)\ e^{-\xi} \propto \xi\ e^{-\xi}$ ($\xi \gg 1$), cf. (2.15). Leading edges of fronts within the pushed regime are given by $\Phi^\dagger \propto e^{-\lambda_+(v^\dagger)\,\xi}$, cf. (2.21). Leading edges of fronts at the pushed/pulled transition accordingly behave as

$$\Phi^* = \beta\ e^{-\xi} \text{ for } \xi \gg 1 \ \ , \ \ \lambda_+(v^*) = \lambda^* = 1 \ . \qquad \text{(E1)}$$

For our example nonlinearity (1.11), fronts are within the pulled regime for $\epsilon > (n+1)/n^2$ and at the pushed/pulled transition for $\epsilon = (n+1)/n^2$.

At the pushed/pulled transition, the spectrum of linear perturbations is still gapless, and convergence therefore is algebraic. On the other hand, the form of the leading edge played a crucial role in determining the velocity corrections $\dot{X}$. Compare our qualitative discussion in Section III A 1. The leading edge behavior (E1) immediately lets us expect, that now $v(t) = 2 - 1/(2t) + \ldots$, in contrast to (3.5) and (3.66) for fronts within the pulled regime, and in agreement with (2.58) for the spreading of

perturbations under the linearized equation. Intuitively, we can argue, that the slower convergence of fronts within the pulled regime is due to the leading edge having to pull the interior part of the front along. This also makes the leading edge flatter. The quicker convergence of fronts at the pushed/pulled transition and in the linearized equation then resembles the fact, that the leading edge and the interior part of the front "impose the same speed".

Let us now do the explicit convergence analysis for fronts developing from initial conditions steeper than e^{-x} for $x \gg 1$ and aproaching (E1) for large times. The analysis of the interior is identical with Section III B, where constants $c_{\frac{n}{2}}$ are yet undetermined. When expanding the interior shape towards the leading edge as in Section III C, the inhomogeneities created by Φ^* (E1) are different, because now $\alpha = 0$. The differential equations for the $\psi_{\frac{n}{2}}$ result from (3.34) with $\alpha = 0$, $\gamma = \beta$ and start with

$$\partial_\xi^2 \psi_1 = c_1 \beta \ , \qquad \partial_\xi^2 \psi_{\frac{3}{2}} = c_{\frac{3}{2}} \beta \ , \tag{E2}$$
$$\partial_\xi^2 \psi_2 = [-1 + c_1(1 - \partial_\xi)]\psi_1 + c_2 \beta + o(e^{-\xi_X}) \ \text{ etc.}$$

Integrating and resumming, we now find for $\xi \gg 1$

$$\begin{aligned} \psi \quad &= \quad \beta + \\ &+ \frac{c_1 \beta \, \xi_X^2}{2!\, t} + \frac{c_1 \delta \, \xi_X}{t} + O\left(\frac{1}{t}\right) \\ &+ \frac{c_{\frac{3}{2}} \beta \, \xi_X^2}{2!\, t^{3/2}} + O\left(\frac{\xi_X}{t^{3/2}}\right) \\ &+ \frac{c_1(c_1 - 1)\beta \, \xi_X^4}{4!\, t^2} + \frac{c_1(c_1\delta - \delta - c_1\beta) \, \xi_X^3}{3!\, t^2} + O\left(\frac{\xi_X^2}{t^2}\right) \\ &+ \frac{c_{\frac{3}{2}}(2c_1 - \frac{3}{2})\beta \, \xi_X^4}{4!\, t^{5/2}} + O\left(\frac{\xi_X^3}{t^{5/2}}\right) \\ &+ \ldots + \ldots \ . \end{aligned} \tag{E3}$$

Here δ is an unknown integration constant fixed by condition (3.9). We will see below, that it is not involved in fixing the velocity, just as also the subleading β for the leading edge (3.32) within the pulled regime is not involved in fixing the velocity, cf. calculation till (3.65).

Again, for $\xi_X \gg \sqrt{t}$ we have to reorder the expansion in powers of $\sqrt{z} = \sqrt{\xi_X^2/(4t)}$ and $1/\sqrt{t}$, and find

$$\begin{aligned} \psi = \beta \ &\left(1 + \frac{c_1(4z)}{2!} + \frac{c_1(c_1 - 1)(4z)^2}{4!} + O(z^3)\right) \\ &+ \frac{1}{\sqrt{t}} \ \left(c_1 \delta \ (4z)^{1/2} + \frac{c_{\frac{3}{2}} \beta \ (4z)}{2!} + \right. \\ &\left. + \ \frac{c_1(c_1\delta - \delta - c_1\beta) \ (4z)^{3/2}}{3!} + \frac{c_{\frac{3}{2}}(2c_1 - \frac{3}{2})\beta \ (4z)^2}{4!}\right) \\ &+ O\left(\frac{1}{t}\right) \ . \end{aligned} \tag{E4}$$

The structure of the expansion is the same as in (3.42), except that now the leading order term is of order t^0:

$$G(z,t) = e^z \psi = g_0(z) + \frac{g_{\frac{1}{2}}(z)}{\sqrt{t}} + \ldots \ . \tag{E5}$$

The equations of motion for the leading and subleading term are derived from (3.43) – (3.45) through putting $g_{\frac{-1}{2}} = 0$. For g_0 we find now the homogenous equation

$$\left[z\partial_z^2 + \left(\frac{1}{2} - z\right)\partial_z - \frac{1}{2} - c_1\right] \ g_0 = 0 \ . \tag{E6}$$

Just like (3.43) was solved by (3.52), we now solve (E6) with

$$c_1 = \frac{-1}{2} \quad , \quad g_0(z) = \beta \ . \tag{E7}$$

The equation for $g_{\frac{1}{2}}$ is now, cf. (3.45) and (E7),

$$\left[z\partial_z^2 + \left(\frac{1}{2} - z\right)\partial_z + \frac{1}{2}\right] \ g_{\frac{1}{2}} = \beta \left[c_{\frac{3}{2}} - \frac{\sqrt{z}}{2}\right] \ . \tag{E8}$$

Again a special solution of the inhomogeneous equation can be found, and the general solution contains the constants of integration $k_{\frac{1}{2}}$ and $l_{\frac{1}{2}}$:

$$\begin{aligned} g_{\frac{1}{2}} \quad &= \quad \beta \left[2c_{\frac{3}{2}} - \frac{\sqrt{z}}{2} \sum_{n=1}^{\infty} \frac{(1)_{n-1} \ z^n}{\left(\frac{3}{2}\right)_n \, n!}\right] \\ &\quad + k_{\frac{1}{2}} \ M\left(\frac{-1}{2}, \frac{1}{2}, z\right) + l_{\frac{1}{2}} \ \sqrt{z} \end{aligned} \tag{E9}$$

$$\stackrel{z \ll 1}{=} \ 2\beta c_{\frac{3}{2}} + k_{\frac{1}{2}} + l_{\frac{1}{2}}\sqrt{z} + O(z) \tag{E10}$$

$$\stackrel{z \to \infty}{\sim} \frac{-\beta\sqrt{\pi}}{4z} \ e^z - \frac{k_{\frac{1}{2}}}{2z} \ e^z \ . \tag{E11}$$

Comparing (E10) to the order $1/\sqrt{t}$ in (E4) and imposing proper convergence of (E11) for $z \to \infty$, we find

$$2\beta c_{\frac{3}{2}} + k_{\frac{1}{2}} = 0 \quad , \quad l_{\frac{1}{2}} = -\delta \quad , \quad \beta\sqrt{\pi} + 2k_{\frac{1}{2}} = 0 \ . \tag{E12}$$

With these constants, the velocity correction $c_{\frac{3}{2}}$ is

$$c_{\frac{3}{2}} = \frac{\sqrt{\pi}}{4} \ , \tag{E13}$$

and for $g_{\frac{1}{2}}$ we find

$$\begin{aligned} g_{\frac{1}{2}} = \frac{\beta\sqrt{\pi}}{2} \ &\left[1 - M\left(\frac{-1}{2}, \frac{1}{2}, z\right) - \sqrt{\frac{z}{\pi}} \sum_{n=1}^{\infty} \frac{(1)_{n-1} \ z^n}{\left(\frac{3}{2}\right)_n \, n!}\right] \\ &- \delta\sqrt{z} \ . \end{aligned} \tag{E14}$$

In summary, we find for the convergence to a front at the pushed/pulled transition, whose leading edge accordingly takes the form (E1), that the velocity correction is given by

$$\dot{X} = -\frac{1}{2t}\left(1 - \frac{1}{2}\sqrt{\frac{\pi}{t}}\right) + O\left(\frac{1}{t^2}\right) \ . \tag{E15}$$

In the interior, i.e., for $\xi_X \ll \sqrt{t}$, the front is given by (3.31) just like a front within the pulled regime. In the leading edge, where $\xi_X \gg \sqrt{t}$, the front is given by

$$\phi(\xi_X, t) = e^{-\xi_X - \xi_X^2/(4t)}\, G\left(\frac{\xi_X^2}{4t}, t\right) \ , \tag{E16}$$

where

$$G(z,t) = \beta + \frac{g_{\frac{1}{2}}(z)}{\sqrt{t}} + O\left(\frac{1}{t}\right) \ . \tag{E17}$$

APPENDIX F: MULTIPLICITY OF FRONTS AND LINEAR EIGENMODES FOR REFLECTION SYMMETRIC EQUATIONS OF FIRST ORDER IN TIME

The generical multiplicity of uniformly translating fronts Φ_v can be determined by counting arguments analogous to those performed in Section II B. Uniformly translating solutions $\Phi_v(\xi)$ of (5.1) can be understood as a heteroclinic orbit in N-dimensional phase space between fixed points characterized by $\Phi_v = 1$ at $\xi \to -\infty$ and $\Phi_v = 0$ at $\xi \to \infty$. For a linear perturbation $\delta = 1 - \Phi_v$ about the fixed point $\phi = 1$ from (5.2), we get the equation

$$\mathcal{L}_v(-\infty)\ \delta + O(\delta^2) = 0 \ , \tag{F1}$$

which is a linear ordinary differential equation with constant coefficients with the linear operator $\mathcal{L}$ being defined in (5.3). The same is true for a linear perturbation $\Phi_v = 0 + \delta$ of the fixed point $\phi = 0$, which solves

$$\mathcal{L}_v(\infty)\ \delta + O(\delta^2) = 0 \ . \tag{F2}$$

In linear order of δ, each of these equations has N solutions $e^{-\lambda_n(v)\,\xi}$, $n = 1, \ldots, N$.

Let us restrict the analysis to real equations which are isotropic in space, i.e., where (5.41) is invariant under $x \to -x$. Such equations are even in ∂_x, so N needs to be even. According to arguments presented in Appendix A of [65], Eqs. (F1) and (F2) for $v > 0$ will have $N/2+1$ eigenvalues λ_n with positive real part and $N/2-1$ ones with a negative real part, if the state, about which we linearize, is linearly unstable against a range of Fourier modes. If it is stable, we will have $N/2$ eigenvalues with positive real part and $N/2$ ones with a negative real part. We assume $\phi = 1$ to be stable, so at $\xi \to -\infty$ there are $N/2$ directions in phase space with negative real part of λ, that need to be excluded. If $\phi = 0$ is unstable, we have only $N/2-1$ bad eigendirections at $\xi \to \infty$. We then generically have a front connecting these fixed points for arbitrary values of v. If, however, the state $\phi = 0$ is metastable, there are $N/2$ bad eigendirections at $\xi \to \infty$. Then also v needs to be tuned to find a solution. So for fronts propagating into unstable states, we generically have a front solution Φ_v for a continuum of velocities, while for fronts into metastable states, there are solutions Φ_v only for discrete values of v, in generalization of the arguents from Section II B.

The multiplicity of linear perturbations is determined along the same lines. We again decompose the linear perturbations η (5.30) into $\eta(\xi, t) = \eta_\sigma(\xi)\ e^{-\sigma t}$ by separation of variables. The η_σ then solve the *o.d.e.*

$$[\mathcal{L}_v(\xi) + \sigma]\ \eta_\sigma(\xi) = 0 \ . \tag{F3}$$

For counting the generic multiplicity of solutions, we need to linearize the equations about $\xi \to \pm\infty$, which amounts to a problem equivalent to (F1) and (F2), except for a shift of the constant contribution of $\mathcal{L}_v(\xi)$ by σ. For fronts propagating into unstable states, we in general expect a continuous spectrum σ of linear perturbations at least in some finite interval of σ, in generalization of Section II C.

APPENDIX G: STRONGLY HETEROCLINIC ORBITS AND CHANGE OF STABILITY AT $V^\dagger$

According to the counting argument from Appendix F, the front $\Phi^*(\xi)$ propagating uniformly with velocity v^* does exist. The question is now, whether it is stable and whether it will be approached by steep initial conditions. In particular, we want to analyze initial conditions $\phi(x, 0)$, that are steeper than $e^{-\lambda^* x}$ in the leading edge.

This amounts to the question, whether in the spectral decomposition η_σ (F3) of a generic $\phi(x,0) - \Phi^*(x)$, there are destablizing modes with $\sigma < 0$. As in Section II C, the contributing modes in general will all decay at least as quick as Φ^* in the leading edge. The leading edge properties of the η_σ in general will depend smoothly on σ, just as in (2.43), so generically Φ^* will still be stable against all perturbations, that in the leading edge decay quicker than Φ^*.

An exemption is again the generalization of $A_\sigma = 0$ from (2.38). For an equation of order N with $\phi = 0$ unstable, there are $N/2+1$ exponents $\Lambda_n(\sigma, v) > 0$. The leading edge will be a superposition of all the exponentials

$$\eta_\sigma(\xi) = \sum_{n=1}^{N/2+1} A_\sigma^{(n)}\ e^{-\Lambda_n \xi} \quad \text{as} \quad \xi \gg 1 \ . \tag{G1}$$

The condition $A_\sigma^{(1)} = 0$, where Λ_1 is the smallest one of the positive Λ_n, fixes a discrete set of σ's, which might have negative σ, but a steepness in the leading edge larger than Φ^*. The stability of the pulled front Φ^* thus again depends on the "strongly heteroclinic" perturbations.

If there are strongly heteroclinic perturbations, that destabilize the pulled front propagating with velocity v^*, then there will be a steeper and quicker front $\Phi^\dagger$, which can be constructed as a strongly heteroclinic orbit of (5.41). The zero mode $\partial_\xi \Phi^\dagger$ then again is a strongly

heteroclinic perturbation, and as in Section II C 2 we can conclude, that the quickest of all strongly heteroclinic orbits cannot be destabilized, so it will attract all sufficiently steep initial conditions.

We conclude, that Table III generalizes to higher order equations, which form uniformly translating fronts, if we only appropriately adjust the explicit definitions of the velocities v and steepnesses λ.

APPENDIX H: RELATION BETWEEN THE GENERALIZED DIFFUSION CONSTANTS D_N AND THE DISPERSION RELATION

If we use the expansion (5.6) for the dispersion relation $\omega(k)$, we get

$$\begin{aligned}\mathcal{D} &= e^{\lambda^*\xi}\left(\sum_{m=0}^{N} a_m\partial_\xi^m - v^*\partial_\xi\right) e^{-\lambda^*\xi} ,\\ &= \sum_{m=0}^{N} a_m(\partial_\xi-\lambda^*)^m - v^*(\partial_\xi-\lambda^*) ,\\ &= \sum_{m=0}^{N}\sum_{n=0}^{m} a_m\frac{m!}{n!(m-n)!}(-\lambda^*)^{(m-n)}\partial_\xi^n - \\ &\qquad -v^*(\partial_\xi-\lambda^*) ,\\ &= \sum_{n=0}^{N}\left(\frac{\partial^n}{\partial(-\lambda^*)^n}\sum_{m=n}^{N} a_m(-\lambda^*)^m\right)\frac{1}{n!}\partial_\xi^n \\ &\qquad -v^*(\partial_\xi-\lambda^*) . \end{aligned} \tag{H1}$$

This immediately yields the expansion (5.27) with the identification (5.28).

APPENDIX I: EDGE ANALYSIS OF UNIFORMLY TRANSLATING PULLED FRONTS WITH $M = 1$

We analyze the leading edge representation (5.37) for a uniformly translating front whose equation of motion (5.41) is of arbitrary order N in space and of first order in time $M = 1$:

$$\partial_\tau\psi = \left(\partial_\zeta^2 + \sum_{n=3}^{N} d_n\partial_\zeta^n\right)\psi + \dot{Y}\,(\partial_\zeta - 1)\,\psi . \tag{I1}$$

We generalize the leading edge analysis from Sections III C and III D.

With the notions and ansatz

$$\mathcal{D} = \partial_\zeta^2 + \sum_{n=3}^{N} d_n\partial_\zeta^n \quad , \quad \dot{Y} = \sum_{n=2}^{\infty}\frac{C_{\frac{n}{2}}}{\tau^{n/2}} , \tag{I2}$$

$$\psi(\zeta_Y, t) = \alpha\,\zeta_Y + \beta + \frac{\psi_{\frac12}}{t^{1/2}} + \frac{\psi_1}{t} + \frac{\psi_{\frac32}}{t^{3/2}} + \dots , \tag{I3}$$

the expansion of the interior in the region of $\zeta_Y \gg 1$ at the crossover towards the leading edge reads

$$\begin{aligned}&\mathcal{D}\psi_{\frac12} = 0 ,\\ &\mathcal{D}\psi_1 = C_1(\alpha\,\zeta_Y + \gamma) \quad , \quad \gamma = \beta - \alpha ,\\ &\mathcal{D}\psi_{\frac32} = C_{\frac32}(\alpha\zeta_Y + \gamma) , \quad \dots \quad ,\end{aligned} \tag{I4}$$

in generalization of (3.34). These equations can be integrated explicitely. The result can be written in leading edge variables $z = \zeta_Y^2/(4\tau)$ as

$$\begin{aligned}\psi = \sqrt{\tau}\,\alpha&\left((4z)^{1/2} + \frac{C_1(4z)^{3/2}}{3!} + \dots\right)\\ &+ \tau^0\,\left(\beta + \frac{C_1(\beta - \alpha(1+d_3))(4z)}{2!} + \dots\right)\\ &+ O(1/\sqrt{\tau}) .\end{aligned} \tag{I5}$$

This generalizes the results of Section III C and supplies us with the small z expansion of the leading edge function

$$\psi(\zeta,\tau) = e^{-z}\,G(z,\tau) \quad . \quad z = \frac{\zeta^2}{4\tau} . \tag{I6}$$

G solves [compare Eq. (3.41)]

$$\begin{aligned}&\left[z\partial_z^2 + \left(\frac12 - z\right)\partial_z - \frac12 - t\partial_t - C_1\right]\,G\;=\\ &= \frac{1}{\sqrt{t}}\left[C_{\frac32} + C_1\sqrt{z}(1-\partial_z)\right]\,G\\ &\quad - \frac{d_3\sqrt{z}}{\sqrt{t}}\left[\frac32\,(\partial_z-1)^2 + z\,(\partial_z-1)^3\right]\,G\\ &\quad + O\left(\frac{1}{t}\right) ,\end{aligned} \tag{I7}$$

where we wrote all operators of order t^0 on the l.h.s. of the equation and the operators of order $t^{-1/2}$ on the r.h.s.

With the ansatz

$$G(z,\tau) = \sqrt{t}\,g_{\frac{-1}{2}}(z) + g_0(z) + \frac{g_{\frac12}(z)}{\sqrt{t}} + \dots \tag{I8}$$

as in (3.42), we find that $g_{\frac{-1}{2}}(z)$ solves again (3.43), so we copy from Section III D, that

$$C_1 = \frac{-3}{2} \quad , \quad g_{\frac{-1}{2}}(z) = 2\alpha\sqrt{z} . \tag{I9}$$

For $g_0(z)$ we then find instead of (3.55):

$$\begin{aligned}&\left[z\partial_z^2 + \left(\frac12 - z\right)\partial_z + 1\right]\,g_0 = \\ &= 2\alpha\,\left[\frac{3\,(1+d_3)}{4} + c_{\frac32}\sqrt{z} - \frac32\,z + d_3(z^2 - 3z)\right] .\end{aligned} \tag{I10}$$

A special solution of the inhomogeneous equation is now instead of (3.58):

$$g_0^{sp}(z) = 2\alpha \left(\frac{3\,(1+d_3)}{4} + 2c_{\frac{3}{2}}\sqrt{z} - \frac{3}{4}\,F_2(z) - d_3 z^2 \right) , \tag{I11}$$

with $F_2(z)$ from (3.56). The general solution is

$$\begin{aligned} g_0(z) &= g_0^{sp}(z) + k_0\,(1-2z) + l_0\,\sqrt{z}\,M\left(\frac{-1}{2},\frac{3}{2},z\right) \\ &\overset{z\ll 1}{=} \left(\frac{3\alpha}{2}\,(1+d_3)+k_0\right) + \left(4\alpha c_{\frac{3}{2}} + l_0\right)\sqrt{z} + O(z) \\ &\overset{z\to\infty}{\sim} -\left(\frac{3}{2}\,\alpha\,\sqrt{\pi} + \frac{l_0}{4}\right)\,z^{-3/2}\,e^z \ , \end{aligned} \tag{I12}$$

Note, that $d_3 \neq 0$ does not cause any divergences at $z \to \infty$. It only shifts the constant contribution at $z \to 0$.

Suppressing the divergence at $z \to \infty$ in (I12), and comparing its small z expansion to (I5) yields again

$$C_{\frac{3}{2}} = \frac{3\sqrt{\pi}}{2} \ , \tag{I13}$$

and

$$\begin{aligned} g_0(z) = \beta\,(1-2z) + 3\alpha(1+d_3)z - 2\alpha d_3 z^2 \\ - \ \frac{3\alpha}{2}\,F_2(z) + 6\alpha\,\sqrt{\pi\,z}\,\left(1 - M\left(\frac{-1}{2},\frac{3}{2},z\right)\right) \ . \end{aligned}$$

APPENDIX J: LEADING EDGE PROJECTIONS FOR COUPLED EQUATIONS: AN EXAMPLE

As a simple illustration of the various questions related to the projection discussed in Section V E 3, we consider two coupled F-KPP equations,

$$\begin{aligned} \partial_t \phi_1 &= \partial_x^2 \phi_1 + \phi_1 - \phi_1^3 \ , \\ \partial_t \phi_2 &= D\partial_x^2 \phi_2 + \phi_2 - \phi_2^3 + K\phi_1 \ . \end{aligned} \tag{J1}$$

The dynamics of this set of equations for fronts propagating into the state $\phi_1 = \phi_2 = 0$ with steep initial conditions, is of course immediately obvious: when $K = 0$, the two equations are uncoupled, and fronts in the first equation propagate with speed $v_1^* = 2$, while those in the second equation propagate with speed $v_2^* = 2\sqrt{D}$. The dynamics of ϕ_1 is always independent of that of ϕ_2, even for $K \neq 0$, so for $K > 0$ and $D < 1$, the dynamics of the coupled equations amounts to a normal F-KPP ϕ_1 front, with relaxation given by our usual expressions. This front entrains a front with speed $v = v_1^* = 2$ in ϕ_2. For $D > 1$, the ϕ_1 and ϕ_2 fronts keep on propagating with different speeds. We consider the case $D < 1$, and make a leading edge transformation $\phi_1 = e^{-\lambda^* \xi}\psi_1$, $\phi_2 = e^{-\lambda^*\xi}\psi_2$ to the frame moving with velocity $\xi = x - v_1^* t$. The equations then become

$$\begin{aligned} \partial_t \psi_1 &= \partial_\xi^2 \psi_1 + \psi_1 \ , \\ \partial_t \psi_2 &= D\partial_\xi^2 \phi_2 + 2(D-1)\partial_\xi \psi_2 + (D-1)\psi_2 + K\psi_1 \ . \end{aligned} \tag{J2}$$

The matrix $\underline{\underline{S}}^*(q,\Omega)$ of the linearized equations is in this case

$$\underline{\underline{S}}^*(q,\Omega) = \begin{pmatrix} i\Omega - q^2 & 0 \\ K & i\Omega - q^2 + J(q) \end{pmatrix} \ , \tag{J3}$$

where $J(q) = (D-1)(1+2iq-q^2)$. Since the element $S_{12}^*(q,\Omega) = 0$, the eigenvalues u_1^* and u_2^* are simply the diagonal element of $\underline{\underline{S}}^*(q,\Omega)$, $u_1^*(q,\Omega) = i\Omega - q^2$ and $u_2^*(q,\Omega) = i\Omega - q^2 + J(q)$. However, the eigenvectors are *not* both along the ψ_1 and ψ_2 axis. Indeed, we have in the notation of V E

$$\underline{U}_1^*(q) = \begin{pmatrix} 1 \\ -K/J(q) \end{pmatrix} \qquad \underline{U}_1^{*\dagger} = (1,0) \ , \tag{J4}$$

$$\underline{U}_2^* = \begin{pmatrix} 0 \\ 1 \end{pmatrix} \qquad \underline{U}_2^{*\dagger}(q) = (K/J(q),1) \ , \tag{J5}$$

The appropriate saddle point is $\Omega = q = 0$, and since $J(0) = (D-1)$, we have

$$\underline{U}_1^*(0) = \begin{pmatrix} 1 \\ -K/(D-1) \end{pmatrix} \ . \tag{J6}$$

The fact that the second component is nonzero just expresses the fact that the variable ψ_2 is entrained by the leading edge in ψ_1. We can now illustrate our assertion that different choices of projection lead to different dynamical equations for the projected leading edge variable ψ^p, but that the universal results from Table I are independent of the particular choice of projection. Clearly, one obvious intuitively appealing choice is to take $\psi^p = \psi_1$, since the ψ_1 dynamics is independent of that of ψ_2. In this case, the dynamical equation for ψ^p is nothing but the single F-KPP equation, and all the results for this equation carry over in detail. Likewise, the choice $\psi^p = \pi_1(q,\Omega)$ (5.86) leads to the linearized F-KPP equation for ψ^p since $u_1^*(q,\Omega(q)) = 0$ gives the dispersion relation of the F-KPP equation. However, this choice is more formal than practical, since the direction in the vector space (ψ_1,ψ_2) is not fixed, but depends on the variable q which influences the dynamics. A more practical choice for the coupled variables would be to take ψ^p as the component along $\underline{U}_1^*(0)$, as this corresponds to a fixed ratio of ψ_1 and ψ_2. Since $\underline{U}_2^{*\dagger} \cdot \underline{U}_1^* = K(J(q) - J(0) = -2Kiq/(D-1) + O(q^2)$, the projected equation for in this case picks up a third order derivative term $D_3\partial_\xi^3\psi^p$, amoungh other ones.

Thus, we observe in this particular example, that indeed the universal results from Table I on velocity and shape relaxation are independent of the choice of projection, while the subleading contribution $g_0(z)$ in the leading edge is universal in the sense, that it is independent of the precise initial conditions, but it does depend on the direction of projection.

APPENDIX K: PINCH POINT VERSUS SADDLE POINT ANALYSIS

In this appendix, we briefly discuss the major differences and similarities between the saddle point and the pinch point approach for evaluating the integral

$$\mathcal{I}_m = \int_{i\gamma-\infty}^{i\gamma+\infty} \frac{d\omega}{2\pi} \int_{-\infty}^{\infty} \frac{dk}{2\pi}\, e^{ik\xi - i(\omega - vk)t}\, \frac{\underline{\underline{\hat{M}}}_m(k,\omega)}{u_m(k,\omega)} \quad \text{(K1)}$$

from Eq. (5.79) on a given branch m. Here $\gamma > 0$ needs to be large enough, that the integrand is analytic along and above the path of ω integration in the complex ω plane. We introduced the abbreviation $\underline{\underline{\hat{M}}}_m(k,\omega) = \underline{\hat{U}}_m(k,\omega) \times \underline{\hat{U}}^\dagger_m(k,\omega)$. In the moving frame ξ, it obviously is convenient to transform to the variable $\Omega = \omega - vk$, and to introduce

$$u^v_m(k,\Omega) = u_m(k,\Omega + vk) = u_m(k,\omega) \quad , \quad \Omega = \omega - vk \; . \quad \text{(K2)}$$

The characteristic equation

$$u_m(k,\omega_m(k)) = 0 \iff u^v_m(k,\Omega_m(k)) = 0 \quad \text{(K3)}$$

defines the dispersion relation $\omega_m(k)$ or $\Omega_m(k)$. The integrals are now of the form

$$\mathcal{I}_m = \int_{i\gamma-\infty}^{i\gamma+\infty} \frac{d\Omega}{2\pi} \int_{-\infty}^{\infty} \frac{dk}{2\pi}\, e^{ik\xi - i\Omega t}\, \frac{\underline{\underline{\hat{M}}}_m(k,\Omega+vk)}{u^v_m(k,\Omega)} \; . \quad \text{(K4)}$$

The "saddle point" type approach, that we follow in Sects. V C – V E of this paper, is based on first evaluating the Ω integral by closing the Ω contour in the lower half plane for $t > 0$ around the simple pole $\propto (\Omega - \Omega_m(k))$. The integral then yields

$$\mathcal{I}_m = \int_{-\infty}^{\infty} \frac{dk}{2\pi}\, e^{ik\xi - i\Omega_m(k)t}\, \frac{\underline{\underline{\hat{M}}}_m(k,\Omega_m(k)+vk)}{i\partial_\Omega u^v_m(k,\Omega_m(k))} \; , \quad \text{(K5)}$$

where γ needs to be larger than $\max_{k \text{ real}} (\text{Im } \Omega_m(k))$. From here on, the saddle point analysis proceeds essentially as in Sect. V D: the k contour is deformed so as to go through the saddle corresponding to the maximum growth rate, a general saddle point being a double root in k of $u^v_m(k,\Omega)$, so that

$$\begin{aligned} u^v_m(k,\Omega)\big|_{sp} = 0 &\iff \omega_{sp} = \omega_m(k_{sp}) \quad \text{(K6)} \\ &\iff \Omega_{sp} = \omega_m(k_{sp}) - vk_{sp} \; , \end{aligned}$$

and

$$\begin{aligned} \partial_k u^v_m(k,\Omega)\big|_{sp} = 0 &\iff (\partial_k + v\partial_\omega)\, u_m(k,\omega)\big|_{sp} = 0 \\ &\iff v = -\frac{\partial_k u_m(k,\omega)\big|_{sp}}{\partial_\omega u_m(k,\omega)\big|_{sp}} \; . \quad \text{(K7)} \end{aligned}$$

By expanding about such a saddle point, we then get for large t to leading order

$$\mathcal{I}_m = \left.\frac{\underline{\underline{\hat{M}}}_m(k,\omega)}{i\partial_\omega u_m(k,\omega)}\right|_{sp} e^{ik_{sp}\xi - i\Omega_{sp}t} \int_q e^{iq\xi - D_{sp}q^2 t} + \dots \; , \quad \text{(K8)}$$

with the diffusion constant

$$D_{sp} = \frac{-i\;\left(\partial_k + v\partial_\omega\right)^2 u_m\big|_{sp}}{2\;\partial_\omega u_m|_{sp}} = \frac{-i\;\partial_k^2 u^v_m\big|_{sp}}{2\;\partial_\omega u^v_m|_{sp}} \; . \quad \text{(K9)}$$

The remaining integral over real $q = k - k_{sp}$ is a simple Gaussian integral of the form discussed previously in Sect. V C 1. As before, we are in the comoving frame, if

$$\text{Im } \Omega_{sp} = 0 \iff v = \frac{\text{Im } \omega_m(k_{sp})}{\text{Im } k_{sp}} \; . \quad \text{(K10)}$$

Differentiating the dispersion relation $u(k,\omega_m(k)) = 0$ with respect to k: $\partial_k u(k,\omega_m(k)) = 0$, and comparing to (K7), we can immediately identify

$$v = \left.\frac{\partial\omega_m(k)}{\partial k}\right|_{sp} \; . \quad \text{(K11)}$$

From $\partial_k^2 u(k,\omega_m(k)) = 0$ and (K9), we get

$$D = \left.\frac{i\partial^2\omega_m(k)}{2\partial k^2}\right|_{sp} \; . \quad \text{(K12)}$$

Choosing in (5.79) the saddle point with the largest velocity $v_{sp} = v^*$, Eq. (5.81) immediately results.

If the denominator of an integral like (K4) contains a product of characteristic functions $\prod_{m=1}^M u^v_m(k,\Omega)$, then each factor $u^v_m(k,\Omega)$ will contribute with its pole and yield an integral as in (K5), so that the total integral amounts to a sum of M integrals of the form (K5). Again the dominating contribution for ξ fixed and $t \gg 1$ will be the one with the largest velocity v_{sp}.

The pinch point analysis [56] is based on evaluating (K1) by a different order of the integrations, i.e., by first closing the k contour to get $k = k(\Omega)$ and then evaluating the remaining Ω integral. (For $\xi > 0$, the k contour must be closed in the upper half plane.) As discussed most clearly by Bers [56], this is done as follows. γ in (K4) has to be large enough to lie above the maxima of the dispersion relation $\Omega_m(k)$ for real k. When Ω varies along the integration path, the poles in the k plane move. Now when γ is lowered sufficiently, that it approaches the maximum of the line $\Omega_m(k)$ traced out by the real k values, a pole in the k plane will approach the real k axis. When that happens, the k contour can be continuously deformed to avoid this pole. This in turn allows one to lower the value of γ. This process can continue until two

poles in the k plane approach the k contour from opposite sides, and "pinch off" the k contour at a particular value of Ω^*. Clearly, that point corresponds to a double root, since for that given value of Ω the two k roots coincide. When the k contour is closed, this point generates a branch-cut in the Ω plane, since near Ω^* we have $k - k^* = \pm\sqrt{(\Omega - \Omega^*)/D}$. When the Ω contour is subsequently closed in the lower half Ω plane, these branch points then generate the usual leading asymptotic behavior (5.14), (5.15).

In both approaches, there are clearly mild assumptions concerning the analytic behavior of the dispersion relations, that arise in slightly different ways. In the saddle point approach, the assumption is that the contour in the k plane can be deformed continuously to go through the saddle point with the highest velocity and Re $D > 0$. This means that the downhill "valleys" at both sides of the saddle are not completely separated by "ridges" from the real k axis. In this formulation, the condition Re $D > 0$ naturally comes out. In the pinch point formulation, the condition usually mentioned is that the poles in the k plane "pinch off" the k contour, while the condition Re $D > 0$ is usually not mentioned, but it is actually hidden in the fromulation as well: it just expresses that the pinch point is associated with a point of the dispersion relation, where the growth rate is maximal. In fact, the examples discussed on pages 466, 467 in [56] for solutions of the saddle point equations which are no pinch points, are just cases where Re $D > 0$, i.e., solutions which are excluded by a saddle point formulation as well.

---

[1] C. Mathis, M. Provansal, and L. Boyer, J. Phys. Lett. **45**, L483 (1984); G.S. Triantafyllou, K. Kupfer, and A. Bers, Phys. Rev. Lett. **59**, 1914 (1987).

[2] G. Ahlers and D.S. Cannell, Phys. Rev. Lett. **50**, 1583 (1983).

[3] K. L. Babcock, G. Ahlers, and D. S. Cannell, Phys. Rev. Lett. **67**, 3388 (1992).

[4] J. Fineberg, V. Steinberg, Phys. Rev. Lett. **58**, 1332 (1987).

[5] A. Tsameret and V. Steinberg, Phys. Rev. E **49**, 1291 (1994).

[6] R.C. Ball and R.L H. Essery, J. Phys.: Condens. Matter **2**, 10303 (1990); R.A.L. Jones, L.J. Norton, E.J. Kramer, F.S. Bates, and P. Wiltzius, Phys. Rev. Lett. **66**, 1326 (1991).

[7] L. Limat, P. Jenffer, B. Dagens, E. Touron, M. Fermigier, and J. E. Wesfreid, Physica D bf 61, 166 (1992).

[8] J. S. Langer and H. Müller-Krumbhaar, Phys. Rev. A **27**, 499 (1983).

[9] T. R. Powers and R. E. Goldstein, Phys. Rev. Lett. **78**, 2555 (1997).

[10] R. J. Deissler, Phys. Lett. A **120**, 334 (1987).

[11] R. J. Deissler, J. Stat. Phys. **54**, 1459 (1989).

[12] K. Nozaki and N. Bekki, Phys. Rev. Lett. **51**, 2171 (1983).

[13] E. K. H. Salje, J. Phys.: Condens. Matter **5**, 4775 (1993).

[14] S. J. Di Bartolo A. T. Dorsey, Phys. Rev. Lett. **77**, 4442 (1996), and references therein.

[15] U. Ebert, W. van Saarloos, and C. Caroli, Phys. Rev. Lett. **77**, 4178 (1996), and Phys. Rev. E **55**, 1530 (1997).

[16] M. Niklas, M. Lücke, and H. Müller-Krumbhaar, Phys. Rev. A **40** 493 (1989).

[17] R. van Zon, H. van Beijeren, and Ch. Dellago, Phys. Rev. Lett. **80**, 2035 (1998).

[18] C. Uhlig and J. Eggers, Z. Phys. B **103**, 69 (1997).

[19] See the articles by J. E. Maclennan, N. A. Cark, and T. Carlsson and by P. E. Cladis and W. van Saarloos in: *Solitons in Liquid Crystals* (Springer, Berlin, 1991).

[20] W. van Saarloos, M. van Hecke, and R. Hołyst, Phys. Rev. E. **52**, 1773 (1995).

[21] Y. Tu and M. C. Cross, Phys. Rev. Lett. **69** 2515, (1992).

[22] J. Krug and P. Meakin, Phys. Rev. A **43**, 900 (1991).

[23] A. Torcini, P. Grassberger, and A. Politi, J. Phys. A **27**, 4533 (1995); A. Torcini and S. Lepri, Phys. Rev. E **55**, R3805 (1997).

[24] M. L. van Hecke, E. de Wit, and W. van Saarloos, Phys. Rev. Lett. **75**, 3830 (1995).

[25] A. Couairon and J. M. Chomaz, Physica D **108**, 236 (1997), and Phys. Rev. Lett. **79**, 2666 (1997).

[26] M. van Hecke, C. Storm, and W. van Saarloos, *Sources, sinks and wavenumber selection in coupled CGL equations and implications for counter-propagating wave systems*, to appear in Physica D (http://xxx.lanl.gov/archive/patt-sol/9902005).

[27] D. Carpentier and P. Le Doussal, Phys. Rev. Lett. **81**, 2558 (1998).

[28] M. C. Cross and P. C. Hohenberg, Rev. Mod. Phys. **65**, 851 (1992).

[29] Ya. B. Zeldovich, G. I. Barenblatt, V. B. Librovich, and G. M. Makhviladze, *The Mathematical Theory of Combustion and Explosions* (Consultants Bureau, New York, 1985).

[30] P. C. Fife, *Mathematical Aspects of Reacting and Diffusing Systems*, Lect. Notes in Biomathematics **28** (Springer, Berlin, 1979).

[31] R. J. Field and M. Burger, eds., *Oscillations and Traveling Waves in Chemical Systems* (John Wiley, New York, 1985). See especially the article by A. Shaul and K. Showalter in this book.

[32] N. F. Britton, *Reaction-diffusion equations and their applications to Biology*, (Acadamic, New York, 1986).

[33] D. Horváth, V. Petrov, S. K. Scott, and K. Showalter, J. Chem. Phys. **98**, 6332 (1993).

[34] A. Malevanets, A. Careta, and R. Kapral, Phys. Rev. E **52**, 4724 (1995).

[35] D. Horváth and A. Tóth, J. Chem. phys. **108**, 1447 (1998).

[36] J. A. Murray, *Mathematical Biology* (Springer, Berlin, 1989). J.D. Logan, *An Introduction to Nonlinear Partial Differential Equations* (Wiley, New York, 1994).

[37] U. Ebert and W. van Saarloos (unpublished).
[38] P. C. Fife, *Dynamics of Internal Layers and Diffusive Interfaces* (SIAM, Philadelphia, 1988).
[39] A. Karma, and W.-J. Rappel, Phys. Rev. E **53**, R3017 (1996).
[40] G. F. Mazenko, O. T. Valls, and P. Ruggiero, Phys. Rev. B **40**, 384 (1989).
[41] O. T. Valls and L. M. Lust, Phys. Rev. B **44**, 4326 (1991).
[42] A. Lemarchand, A. Lesne, A. Perera, M. Moreau, and M. Mareschal, Phys. Rev. E. **48**, 1568 (1993).
[43] H. Breuer, W. Huber, and F. Petruccione, Physica D **73**, 259 (1994).
[44] J. Riordan, C. R. Doering, and D. ben-Avraham, Phys. Rev. Lett. **75**, 565 (1995).
[45] J. Armero, J. M. Sancho, J. Casademunt, A. M. Lacasta, L. Ramirez-Piscina, and F. Sagues, Phys. Rev. Lett. **76**, 3045 (1996).
[46] J. Armero, J. Casademunt, L. Ramrez-Piscina, and J. M. Sancho, Phys. Rev. E 58, 5494 (1998).
[47] As mentioned by Murray, Ref. [36] on page 277, the equation was apparently already considered in 1906 by Luther, who obtained the same analytical form as Fisher for the wave front.
[48] A. Kolmogoroff, I. Petrovsky, and N. Piscounoff, Bulletin de l'université d'état à Moscou, Ser. int., Section A, Vol. 1 (1937); translated and reprinted in P. Pelcé, *Dynamics of Curved Fronts* (Academic Press, San Diego, 1988).
[49] R. A. Fisher, Ann. Eugenics **7**, 355 (1937).
[50] D.G. Aronson and H.F. Weinberger, Adv. Math. **30**, 33 (1978).
[51] P. Collet and J. P. Eckmann, *Instabilities and Fronts in Extended Systems* (Princeton University Press, Princeton, 1990).
[52] H. P. McKean, Commun. Pure Appl. Math. **28**, 323 (1975).
[53] For some recent more mathematical advances within the physics literature, see R. D. Benguria and M. C. Depassier, Phys. Rev. Lett. **77**, 1171 (1996); Phys. Rev. E **57**, 6493 (1998).
[54] For a recent extension to multidimensional cases, and for an entry into the mathematical literature, see, e.g., T. Ogiwara, and H. Matano, Discr. Cont. Dyn. Syst. **5**, 1 (1999).
[55] For a discussion of the few mathamatically precise results that are available for more complicated or higher order equations, we refer to the book by Collet and Eckmann, Ref. [51].
[56] A. N. Bers, in: *Handbook of Plasma Physics*, M. N. Rosenbluth and R. Z. Sagdeev, eds. (North-Holland, Amsterdam, 1983).
[57] P. Huerre, in: *Propagation in Systems far from Equilibrium*, J. E. Wesfreid, H. R. Brand, P. Manneville, G. Albinet, and N. Boccara, eds (Springer, New York, 1988).
[58] L.D. Landau and E.M. Lifshitz, *Course of Theoretical Physics*, vol 10 (Pergamon, New York, 1981).
[59] A. N. Stokes, Math. Biosciences **31**, 307 (1976).
[60] G. Dee and J. S. Langer Phys. Rev. Lett. **50**, 383 (1983).
[61] E. Ben-Jacob, H.R. Brand, G. Dee, L. Kramer, and J.S. Langer, Physica D **14**, 348 (1985).
[62] G. Dee, J. Stat. Phys. **39**, 705 (1985).
[63] W. van Saarloos, Phys. Rev. A **37**, 211 (1988).
[64] G. Dee and W. van Saarloos, Phys. Rev. Lett. **60**, 2641 (1988).
[65] W. van Saarloos, Phys. Rev. A **39**, 6367 (1989).
[66] W. van Saarloos and P. C. Hohenberg, Physica D **56** 303-367 (1992). Errata: **69** 209 (1993).
[67] J. A. Powell, A. C. Newell, and C. K. R. T. Jones, Phys. Rev. A **44**, 3636 (1991).
[68] G. C. Paquette, L.-Y. Chen, N. Goldenfeld, and Y. Oono, Phys. Rev. Lett. **72**, 76 (1994).
[69] G. C. Paquette and Y. Oono, Phys. Rev. E. **49**, 2368 (1994).
[70] L. A. Peletier and W. C. Troy, SIAM J. Math Anal. **28**, 1317 (1997).
[71] See also U. Ebert, W. van Saarloos and L. A. Peletier (unpublished).
[72] E. Brunet and B. Derrida, Phys. Rev. E **56**, 2597 (1997).
[73] J. Swift and P. C. Hohenberg, Phys. Rev. A **15**, 319 (1997).
[74] W. Spruijt, Master's thesis, Leiden University 1998 (unpublished).
[75] A new and simple proof that fronts in the Swift-Hohenberg equations are pulled, and a new mode expansion that leads to a generalization of (1.12) for pattern forming fronts which asympotically are periodic in the comoving frame, such as those arising in the Swif-Hohenberg equation, will be given in a future publication by W. Spruijt, U. Ebert, and W. van Saarloos.
[76] The convergence towards fronts whose dynamics remains nonperiodic in the comoving frame, such as those in the complex Ginzburg-Landau equation for some values of the parameters [12,62,66], will be discussed in a future publication together with C. Storm.
[77] M. Bramson, Mem. Am. Math. Soc. **44**, No. 285 (1983).
[78] D.A. Kessler, Z. Ner, and L.M. Sander, Phys. Rev. E **58**, 107 (1998).
[79] R. Durrett, Stoch. Proc. Appl. **9**, 117 (1979). We thank F. M. Hekking for bringing this reference to our attention.
[80] Th. Gallay and G. Raugel, http://xxx.lanl.gov/patt-sol/9809007 and 9812007.
[81] See, e.g., Fig. 6 of T. R. Powers, D. Zhang, R. E. Goldstein, and H. A. Stone, Phys. Fluids **10**, 1052 (1998), which is a full numerical study of the predictions of Ref. [9].
[82] J. S. Langer, in: *Directions in Condensed Matter Physics*, G. Grinstein and G. Mazenko, eds. (World Scientific, Singapore, 1986).
[83] An entry into the more mathematically oriented literature is the paper by P. W. Bates, P. C. Fife, R. A. Gardner, and C. K. R. T. Jones, Physica D **104**, 1 (1997).
[84] J. D. Buckmaster and G. S. S. Lundford, *Theory of Laminar Flames* (Cambridge University Press, Cambridge, 1982).
[85] U. Ebert and W. van Saarloos, Phys. Rev. Lett. **80**, 1650 (1998).
[86] W. van Saarloos, Phys. Rep. **301**, 9 (1998).

[87] G. I. Barenblatt, *Scaling, Self-Similarity and Intermediate Asymptotics* (Cambridge University Press, Cambridge, 1996).
[88] J. Canosa, IBM J. Res. Dev. **17**, 307 (1973).
[89] D. A. Larson, SIAM J. Appl. Math. **34**, 93 (1978).
[90] D. H. Sattinger, J. Diff. Eqn. **25**, 130 (1977).
[91] W. I. Newman, J. theor. Biol. **104**, 473 (1983).
[92] K. Kirchgässner, J. Diff. Eqn. **96**, 256 (1992).
[93] J.-P. Eckmann and C. E. Wayne, Commun. Math. Phys. **161**, 323 (1994).
[94] T. Kapitula, J. Diff. Eqns. **112**, 179 (1994).
[95] A brief overview of comparison type arguments can be found in the Appendix of Ref. [61].
[96] V. I. Arnold, *Ordinary differential equations* (MIT Press, Cambridge, 1978); *Geometrical Methods in the Theory of Ordinary Differential Equations* (Springer, New York, 1983).
[97] J. Guckenheimer and P. Holmes, *Nonlinear Oscillations, Dynamical Systems, and Bifurcations of Vector Fields* (Springer, New York, 1983).
[98] We stress that we claim no originality here. In the physics literature, this type of analysis has appeared in various places, quite often in relation to Ginzburg-Landau or mean-field type approaches. See, e.g., Refs. [99,101,82].
[99] J. D. Gunton, M. San Miguel, and P. S. Sahni, in: *Phase transitions and critical phenomena* vol. 8, C. Domb and J. L. Lebowitz, Wds. (Academic, New York, 1983).
[100] J. S. Langer, in *Solids far from Equilibrium*, C. Godreche, Ed. (Cambridge University Press, Cambridge, 1992).
[101] A. J. Bray, Adv. Phys. **43**, 357 (1994).
[102] A. Messiah, *Quantum Mechanics* (North-Holland, Amsterdam, 1974).
[103] M. Abramowitz and I. S. Stegun, Eds., *Handbook of Mathematical Functions* (Dover, New York, 1972).
[104] A. Goriely, Phys. Rev. Lett. **75**, 2047 (1995).
[105] See, e.g., C. M. Bender and S. A. Orszag, *Advanced Mathematical Methods for Scientists and Engineers* (McGraw-Hill, New York, 1978).
[106] We owe this argument to Willem Spruijt, Ref. [74].
[107] O. Diekmann, J. Diff. Eqs **33**, 58 (1979).
[108] S. Fedotov, cond-mat/9807352.
[109] D. Potter, *Computational Physics* (Wiley, New York, 1973). For the diffusion term, this method amounts to the *Crank-Nicholson* scheme, see, e.g., section 17.2 of W. H. Press, B. P. Flannery, S. A. Teukolsky and W. T. Vetterling, *Numerical Recipes* (Cambridge University Press, Cambridge, 1986).
[110] D. Carpentier [private communication]; and D. Carpentier and P. Le Doussal (unpublished).
[111] X. Y. Wang, S. Fan and T. Kyu, Phys. Rev. E **56**, R4931 (1997).
[112] P. Kaliappan, Physica D **11**, 368 (1984).
[113] M. Otwinowski, R. Paul, and W. G. Laidlaw, Phys. Lett. A **128**, 483 (1988).